Anal. Method Environ. Chem. J. 3 (1) (2020) 5-16

AMECJ

Research Article, Issue 1

Analytical Methods in Environmental Chemistry Journal

Journal home page: www.amecj.com/ir

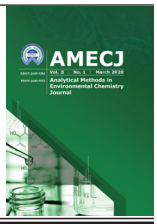

Nickel separation from human blood samples based on amine and amide functionalized magnetic graphene oxide nano structure by dispersive sonication micro solid phase extraction

Anne Trégouët[a], Masoud Khaleghi Abbasabadi[b] and Pooya Gholami[c,*]

[a] *Department of Chemistry, University Paris-Saclay, Saint-Aubin, Paris, France.*
[b] *Department of Chemistry, Iran University of Science and Technology, Tehran, Iran*
[c] *Nano Technology Center, Research Institute of Petroleum Industry (RIPI), P.O. Box 14665-1998, Tehran, Iran*

ARTICLE INFO:

Received 18 Dec 2019

Revised form 6 Feb 2020

Accepted 27 Feb 2020

Available online 25 Mar 2020

Keywords:
Nickel,
Human blood,
Fe_3O_4-supported Amine /Amide-functionalized graphene oxide,
Dispersive sonication micro solid phase extraction

ABSTRACT

Nickel (Ni) is toxic effect on human body and must be determined in human blood samples. In this study, Ni ions separated and preconcentrated from blood samples based on magnetic Fe_3O_4-supported amine/amide-functionalized graphene oxide (Fe_3O_4@A/A-GO) nanoparticles by dispersive sonication micro solid phase extraction (DS-µ-SPE). By procedure, 10 mg of Fe_3O_4@A/A-GO was dispersed in 10 mL of human blood samples with sonication for 5.0 min and then separated from liquid phase with magnetic accessory. The Ni ions was extracted based on amine/amide covalence bonding of Fe_3O_4@A/A-GO sorbent (Ni---: NH_2). Then, the Ni ions back-extracted from Fe_3O_4@A/A-GO in low pH with nitric acid (0.2 mL, 0.3 M) which was diluted with DW up to 0.5 mL and finally, was determined by ET-AAS (peak area). The LOD, linear range (LR), enrichment factor (EF) and absorption capacity (AC) were obtained 35 ng L^{-1}, 0.15 -7.2 µg L^{-1}, 19.8 and 131.6 mg g^{-1}, respectively. The method was validated by spiking samples.

1. Introduction

Nickel (Ni) is one of the toxic compounds in water contamination and caused to acute and chorionic effect in human bodies[1]. Ni(II) are released into environment from waste of different chemical factories such as battery manufacturing, mining and electroplating. The air of near factories contain the significant amount of heavy metals such as nickel and caused to adverse effects in environment and humans[2]. Nickel is known to bind to specific proteins and/or amino acids in the blood serum and the placenta. Orally absorbed nickel is distributed to the kidneys, followed by the liver, brain, and heart The harmful health effects of nickel lead to possible symptoms includes, chronic bronchitis, lung dysfunction, cancer in lung and nasal sinus[3]. Other target organs include the cardiovascular system, immune system, and the blood. In large doses (>0.5 g), some forms of nickel may be acutely toxic to humans when taken orally. Oral LD_{50} values for rats range from 67-9000 mg Ni per kg (ATSDR).

*Corresponding Author: Pooya Gholami
Email: pooya1989gh@gmail.com
https://doi.org/10.24200/amecj.v3.i01.96

Toxic effects of oral exposure to nickel usually involve the kidneys with some evidence from animal studies showing a possible developmental/ reproductive toxicity effect (ATSDR). Normal range for Ni in healthy peoples is 0.2 μgL^{-1} in serum and less than 3.0 μgL^{-1} in human urine. A national health and nutritional examination survey (NHNES) of hair found mean nickel levels of 0.39 mg L^{-1}, with 10% of the population having levels less than1.5 mg L^{-1} [4,5]. The vary techniques was used for measurement of nickel (Ni^{2+}) in human bodies such as serum and blood samples. Due to previous studies, the flame atomic absorption spectrometry (F-AAS) and electrothermal atomic absorption spectrometry (ET-AAS) were reported for analysis of heavy metals such nickel (Ni) which was suitable for the determination in biological matrixes [6-9] . Occasionally, the atom trapping flame atomic absorption spectrometry (AT-FAAS) and fluorescence spectrometry (XRF) also was used for heavy metal determaintion such as nickel in biological samples [10, 11]. Also, different methods such as, polarography [12], inductively coupled plasma-optical emission spectrometry (ICP OES, inductively coupled plasma-mass spectrometry (ICP-MS) [13, 14], and spectrophotometry [15] were used for nickel analysis in human samples [16]. But as difficulty matrixes in human biological samples such as blood or serum, the sample preparation is required to separation nickel ions from liquid phases. The different sample preparation technology exist for nickel extraction from blood samples such as liquid–liquid extraction (LLE) [17], solid-phase extraction (SPE) and functionalized magnetic-SPE [18], dispersive solvent by liquid–liquid microextraction method (DLLME) [19], phase extraction based on cloud point (CPE) [20], dispersive solid phase microextraction (D-SPME) [21], ultrasound-assisted solid phase extraction (USA-SPE) [22]. Recently, the dispersive sorbent in the liquid phase was presented as micro SPE (D-µ-SPE) for separation/determination of nickel in water and biological samples [23]. Some advantages such as high extraction efficiency, simple usability, fast and low time caused to select as a favorite technique for metal extraction. The sorbent characterizations are a main factor which was effected on heavy metal extraction by the D-µ-SPE procedure. The selective of favorite nanosturactures improved recovery. The different nanosorbent such as, carbon nanotubes (CNTs), graphene / graphene oxide sheets (NG, NGO) and silica (MSN) were used for extraction of Ni in blood samples [24-26]. Between them, the NGO was reported as efficient sorbents for metal extraction due to their surface properties. In this study, a novel sorbent based on Fe_3O_4-supported amine/amide-functionalized graphene oxide (Fe_3O_4@A/A-GO) was used for separation/ speciation Ni(II) from human blood samples by dispersive sonication micro solid phase extraction (DS-µ-SPE) at pH=8.0. The method was developed in blood samples by ET-AAS.

2. Experimental

2.1. Instrumental

The graphite furnace atomic absorption spectrophotometer (GF-AAS, 932 GBC, Aus) was used for nickel determination in blood samples with the Avanta software. The linear range of 3.0-150 µg L^{-1} (peak Area, Abs=1.91) was selected for Ni in optimized light. The current and wavelength of HCL lamp was adjusted 3.0 mA and 228.8 nm, respectively. The auto-sampler of spectrophotometer (Pal 3000) was used for micro injection (1µL) of sample volumes to furnace tube after adjusted injector. The pH of the sample was digitally calculated by Metrohm pH meter (Swiss). Fourier transform infrared (FT-IR) spectra were recorded from KBr pellets using a Perkin Elmer Spectrum 65 FT-IR spectrophotometer. Powder X-ray diffraction (XRD) was conducted on a Panalytical X'Pert PRO X-ray diffractometer. Scanning electron microscopy (SEM) images were obtained using a Tescan Mira-3 Field Emission Gun Scanning Electron Microscope (SEM). Magnetic

property of the catalyst sample was measured with a vibrating sample magnetometer (VSM) model LBKFB, Meghnatis Daghigh Kavir Co, Iran, at room temperature

2.2. Reagents

Chemicals including natural flake graphite (325 mesh, 99.95%), were purchased from Merck chemical company and used as received. The standard stock solutions (1000 mg L^{-1}) of Ni (II), acetone, acetate, HNO_3, NaOH, HCl and other reagents were purchased from Merck (Darmstadt, Germany). Ultra-pure deionized water (DW) purchased from Milli-Q plus water purification system (USA). The standard and experimental solutions of Ni^{2+} (0.1, 0.2.0.5, 1.0, 3, 5.9 and 7.0 µg L^{-1}) were prepared daily by appropriate dilution of the stock solutions with DW. The pH of samples were used with appropriate buffer solutions including sodium acetate for pH 3.5–5.6, sodium phosphate for pH of 5.8–8.0, and ammonium chloride for pH 8–10. All the laboratory glassware and plastic tubes were cleaned by 5% (v/v) HNO_3 for at least 12 h and then washed many times with DW and dried in oven prior to use. All reagents for synthesis of Fe_3O_4@A/A-GO prepared by RIPI Company.

2.3. Synthesis of graphene oxide (GO)

Graphite black powder was oxidized to GO following the modified Hummers method in the several steps [27-29]. Fore pre oxidation of graphite powder, 250 mL of H_2SO_4 was added to 5 g of graphite powder and the resulting mixture was stirred for 24 h. After 24 h, 30 g of $KMnO_4$ was added to the mixture stirring for 72 h at 50 °C. Next, a solution of 45 mL of H_2O_2 (30%) in 400 mL of deionized water was added to the mixture after which the brown color of the mixture turned into bright yellow. The GO dark solution was centrifuged and washed with deionized water and 10% HCl solution, and dried at 65 ˚C.

2.4. Preparation of nanomagnetic Fe_3O_4-supported Amine/Amide-functionalized graphene oxide (Fe_3O_4@A/A-GO)

2.4.1. Acyl-chlorination of graphene oxide

In the first step, thionyl chloride 60 mL was added GO (0.3 g) and stirred in at 70°C for 24 h. After acyl-chlorination reaction, the Acyl-chlorination of GO was washed with THF four times and the precipitated dried at 65°C [30].

2.4.1 Functionalization of graphene oxide with Ammonia

A total of 1 g of Ammonia was added to Acyl-chlorinated GO (0.3 g). Then, the mixture was refluxed for 72 h at 120°C under argon condition. Finally, the mixture reaction washed with DI water. A dark powder of Amine/Amide-functionalized graphene oxide was obtained [31].

2.4.2 Nano magnetization of Amine/Amide-functionalized graphene oxide

The Fe_3O_4-supported Amine/Amide-functionalized graphene oxide (Fe_3O_4@A/A-GO) nanoparticles were synthesized by co-precipitation of $FeCl_2 \cdot 4H_2O$ and $FeCl_3 \cdot 6H_2O$, in the presence of Amine/Amide-grafted graphene oxide. First, a solution of $FeCl_2 \cdot 4H_2O$ and $FeCl_3 \cdot 6H_2O$ was prepared with a molar ratio of 2:1. The weight ratio of GO to $FeCl_3$ in the nano composite was 1 per 20 (mGO: $mFeCl_3$ = 1:20). Afterward, 10 mg of Amine/Amide-grafted graphene oxide in 15 mL of DI water was ultrasonicated for 20 min. 12.5 mL solution of $FeCl_2 \cdot 4H_2O$ (125 mg) and $FeCl_3 \cdot 6H_2O$ (200 mg) in deionized water (10 mL) was added to the reaction mixture at room temperature. In order to raise pH value to 11, an aqua solution of 30% ammonia was added in the reaction mixture at 70 ˚C. Then, the reaction mixture was allowed to cool to room temperature and Fe_3O_4@A/A-GO washed five times with DI H_2O dried at 70 ˚C [32].

2.5 Analytical Procedure

In proposed procedure, 10 mL of blood and

standard solutions was prepared by buffer solution. The whole blood samples diluted with DW (1:1) before procedure. By DS-μ-SPE procedure, the pH of the standard solution containing 0.2 -7.0 μg L^{-1} of nickel was adjusted up to 8 and then 0.01 g of Fe_3O_4@A/A-GO as adsorbent was added to samples. The standard / blood samples was shaked for 5.0 min at room temperature and Ni ions physically adsorbed on surface of Fe_3O_4@A/A-GO and chemically extracted by amine and amide covalence bonding at pH=8. Then, the Fe_3O_4@A/A-GO separated from liquid phase by magnetic accessory. Finally, the Ni ions back-extraction with nitric acid (0.2 M) from Fe_3O_4@A/A-GO and after dilution up to 0.5 mL with DW was determined by ET-AAS. In optimized conditions, the recovery of physically and chemically adsorption by Fe_3O_4@A/A-GO was almost obtained 25.3% and 97.8%, respectively. The extraction efficiency of proposed method based on Fe_3O_4@A/A-GO was calculated by equation 1. The C_A is the stock concentrations of nickel and C_B is the remain concentration of Ni(II) after procedure (n=10, Eq. 1).

$$\text{Recovery of extraction}=(C_A-C_B)/C_A\times 100 \quad \text{(Eq.1)}$$

3. Results and Discussion

3.1. Characterization of the nano Fe_3O_4@A/A-GO

The Fe_3O_4-supported Amine/Amide-functionalized graphene oxide nanomagnetic (Fe_3O_4@A/A-GO) was synthesized according to the synthetic route shown in Figure 1. Firstly, graphite was oxidized to GO by the modified Hummers method [27-29]. Afterward, the GO was amination and amidation with Ammonia by according to our previously reported procedure [30, 31]. Finally, the resulted Amine/Amide-functionalized graphene oxide (Fe_3O_4@A/A-GO) was nano-magnetized by co-precipitation of ferrous (Fe^{2+}) and ferric (Fe^{3+}) ions in the presence of A/A-GO to afford the target adsorbent Fe_3O_4@A/A-GO [32].

Figure 2 shows the FT-IR spectra of GO and Fe_3O_4@A/A-GO. The broad peak in the range between 2600-3500 cm^{-1} in the IR spectra of these compounds is related to the (O-H stretching)

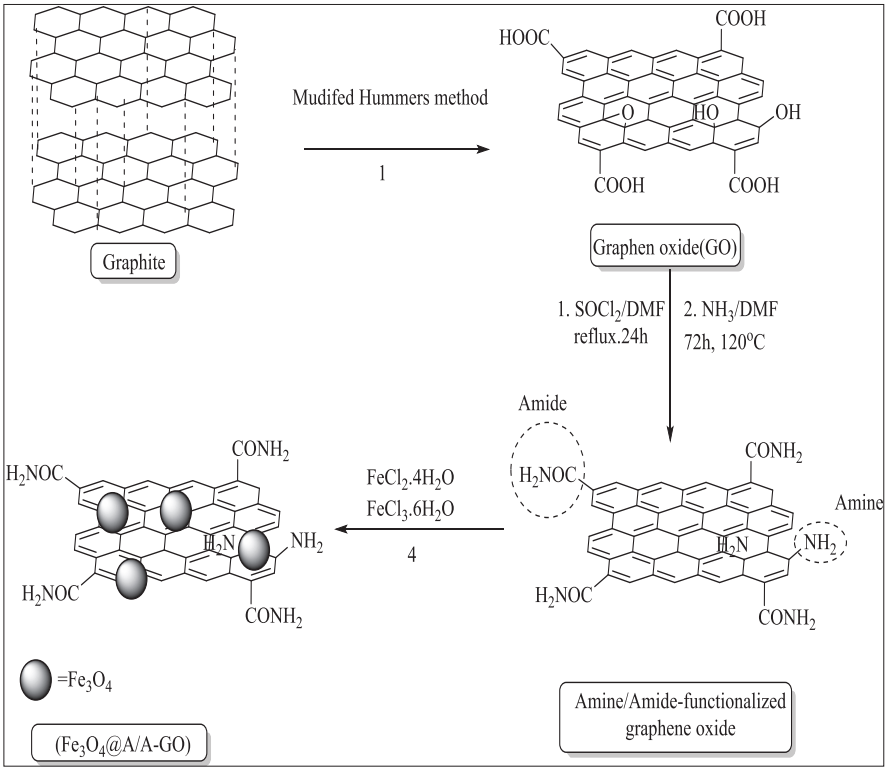

Fig 1. Synthetic route of Fe_3O_4@A/A-GO

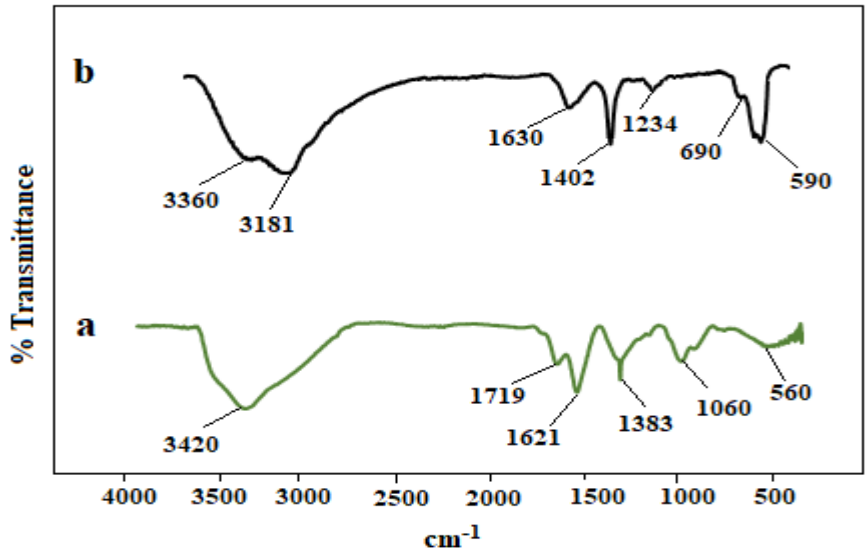

Fig. 2. FT-IR spectra of (a) GO, and (b) Fe_3O_4@A/A-GO

vibration of carboxylic and enolic functionalities [35]. The peaks at 3420, 1719, 1621, and 1060 cm^{-1} shown in the spectra of GO and Fe_3O_4@A/A-GO are ascribed to the (C-O stretching), (C=C stretching), (C=O stretching), and (O-H stretching) respectively [33, 34]. Also, The absorption bands at 3360, 3181, 1630, and 1234 cm^{-1} shown in the spectra of GO and amination GO are ascribed to the stretching bands ν(O-H), ν(N-H), ν(C=O), and ν(C-N) respectively. In the spectrum of Fe_3O_4@A/A-GO, the peaks observed at around 628 and 583 cm^{-1} are related to the Fe–O stretching vibration [37-39]. These results prove that the successful Amination and amidation of GO and synthesis of Fe_3O_4@A/A-GO.

The XRD patterns of GO, and Fe_3O_4@A/A-GO are demonstrated in Figure 3 (a,b). GO has the two main peak at 2θ = 11.5°, 42.58° are related to the diffraction planes of (002) and (100) respectively, which can be observed in the XRD patterns of both GO and Fe_3O_4@A/A-GO [40-42]. As shown in Figure 3 (b), the peaks at 2θ = 24° and 42.58° It is evident from the XRD pattern of Fe_3O_4@A/A-GO that was proved the presence of GO [42]. The main peaks at 2θ° = 30.12, 35.45, 43.07, 56.97, 62.47 in XRD pattern of Fe_3O_4@A/A-GO are in good accordance with the standard XRD data of magnetite Fe_3O_4. The main diffraction peaks at

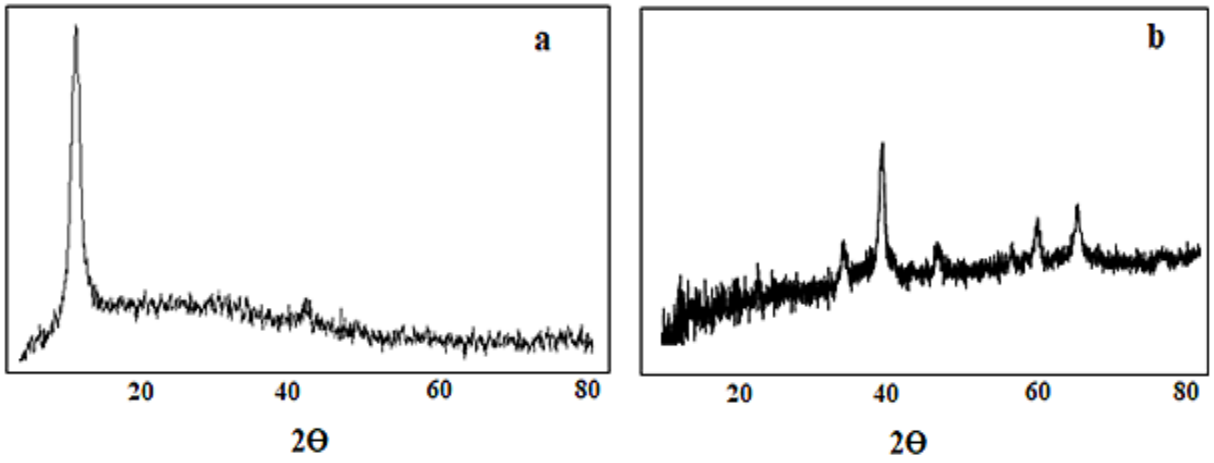

Fig. 3. XRD patterns of (a) GO, (b) Fe_3O_4@A/A-GO

20° = 62.47, 56.97, 43.07, 35.45, 30.12 are related to the reflection planes of cubic spinel crystal structure of Fe_3O_4 at (440), (511), (400), (311), (220) respectively [43-50].

The SEM image of GO shows that graphene oxide nano sheets consists of randomly accumulated and wrinkled thin sheets (Fig. 4a). Also, the SEM image of Fe_3O_4@A/A-GO shows in Figure 4(b) that the average diameter of Fe_3O_4 nanoparticles was about 35.43 nm and indicate a regularly spherical morphology on A/A-GO [51-52].

The Magnetic behavior of the Fe_3O_4@A/A-GO was recorded using a VSM. As shown in the Figure 5, the saturation magnetization of Fe_3O_4@A/A-GO was found to be 42 emu g^{-1}. This amount of a saturation magnetization value, the magnetized nanocomposite is expected to have considerable paramagnetism to make it magnetically separable from reaction mixture [32, 48].

3.2. Optimization of extraction procedure

For efficient extraction of nickel ions in human blood samples, the main parameters must be studied. The effective features such as, pH, sample volume, amount of Fe_3O_4@A/A-GO, shacking time and interferences ions must be optimized. Chemical bonding was strongly depended on the pH solutions. By procedure, the effect of pH on extraction of nickel through the amine functional group of Fe_3O_4@A/A-GO was evaluated. For this purpose, the different pH values from 1 to 11 with nickel concentration of 0.2-7 µg L^{-1} as LLOQ and ULOQ was examined according to DS-µ-SPE procedure. Obviously, the maximum of extraction

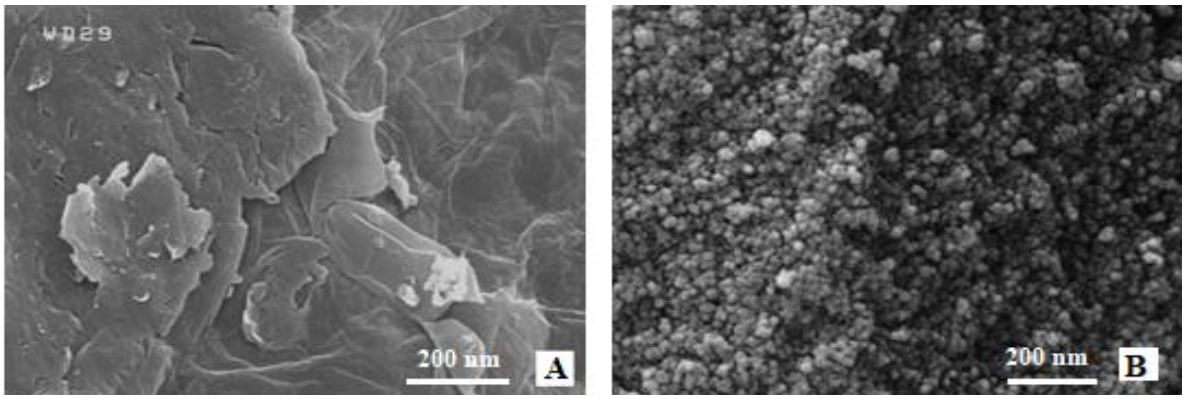

Fig. 4. SEM images of (a) GO, (b) Fe_3O_4@A/A-GO

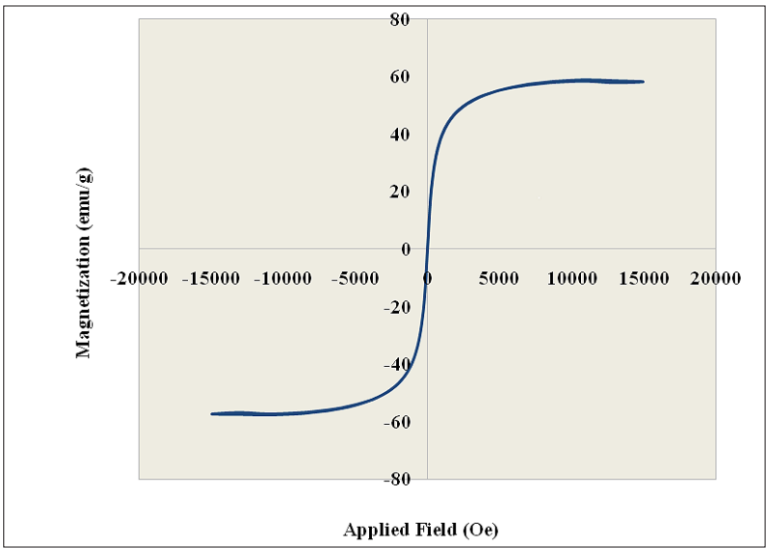

Fig. 5. VSM curve of Fe_3O_4@A/A-GO

efficiencies for Ni (II) ions based on Fe_3O_4@A/A-GO were obtained at pH range of 8.2, and then the recoveries were decreased by increasing or decreasing of pH (Fig. 6). In optimized conditions, the effect of sample volume of blood on nickel extraction was studied between 2-20 mL. The results showed, the optimum extraction was achieved for 12 mL of blood sample and 15 mL of standard samples, So, 10 mL of sample volume was used for further studies. Also, the amount of Fe_3O_4@A/A-GO for nickel extraction was evaluated by DS-µ-SPE procedure. Based on experimental results, 10 mg of Fe_3O_4@A/A-GO was selected as optimum point. The sonication time for extraction of Ni(II) was studied in optimized pH. Based on previous research, kind and size of adsorbents are the most important factors for extraction and sonication time. Therefore, the effect of sonication in blood samples was examined by DS-µ-SPE procedure. The results showed, the maximum efficiency was achieved at 5 min. The concentration of Interfering ions such as Na^+, K^+, Mg^{2+}, Ca^{2+}, Cu^{2+}, Zn^{2+}, Co^{2+}, Al^{3+}, Hg^{2+}, SO_3^{2-}, I^-, NO_3^-, Cl^- and F^- caused less than ± 5% deviation in the recovery of Ni(II) as the tolerance limit. So, the interfering ions has no effect on the recovery efficiencies of Ni(II) in blood samples.

3.3 . Validation methodology

Many methods was used for validation of methodology by SPE [53-55]. The analytical results of the developed DS-µ-SPE procedure were shown method at optimum conditions (Table 1). After sample preparation, Ni concentration in human blood and standard samples was determined by ET-AAS. The Human blood, serum and plasma as a real sample was used for determination of Ni by DS-µ-SPE procedure. The results was verified by analyzing the spiked samples with standard concentration of Ni (II) in human samples (Table 2). Based on results, a high and favorite recovery was obtained by spiking samples which confirms the accuracy of results in difficulty matrix. The

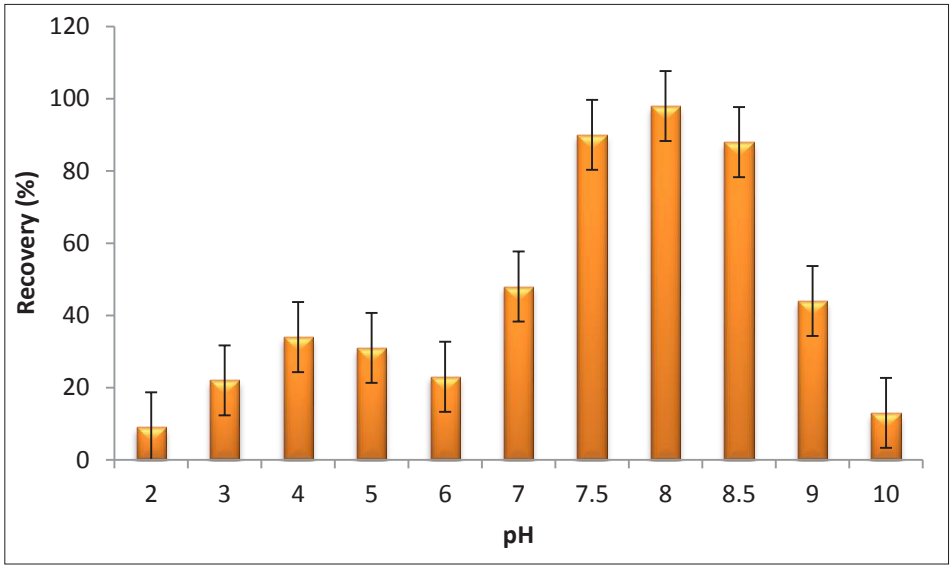

Fig. 6. The effect of pH on nickel extraction by DS-µ-SPE procedure

Table 1. Analytical results for Ni(II) extraction based on Fe_3O_4@A/A-GO by DS-µ-SPE

Element	[a]SV	[b]LR	R^2	[c]LOD (n = 10)	[d]RSD [b] (%)	[F]EF
Ni(II)	10	0.15- 7.2	0.9997	0.035	2.8%	19.8

[a] sample volume (mL), [b] Linear rang (µg L^{-1}) , [C]Limit of detection (µg L^{-1}) , [d] Relative standard deviation, [F] enrichment factor(EF),

Table 2. Determination of nickel in blood, serum and plasma solutions by DS- μ-SPE procedure (mean intra –day and inter day for 10 samples)

	Added(μg L^{-1})		* DS-μ-SPE (μg L^{-1})		
Sample	**Intra-day**	**Inter day**	**Intra-day**	**Inter day**	**Recovery (%)**
blood	------	------	3.65 ± 0.18	3.48 ± 0.15	------
	3.0	------	6.57± 0.28	------	97.3
	------	3.0	------	6.51± 0.32	101.0
Plasma	------	------	1.45 ± 0.06	1.57 ± 0.07	------
	1.5	------	2.88 ± 0.13	------	95.3
	------	1.5	------	2.99 ± 0.14	94.6
Serum	------	------	2.92 ± 0.14	2.86 ± 0.12	------
	3.0	------	6.02± 0.27	------	103.3
	------	3.0	------	5.82± 0.25	98.6

*Mean of three determinations of samples ± confidence interval (P = 0.95, n =10)

recoveries of spiked samples demonstrated that the results was satisfactory for Ni analysis by DS-μ-SPE. In order to validate the method, the extraction efficiency for intra-day and inter day analysis was evaluated by spiking samples (Table 3).

4. Conclusions

A fast and efficient method based on Fe_3O_4@A/A-GO as adsorbent was used for preconcentration, separation of trace Ni (II) in human blood samples by DS-μ-SPE procedure. The mechanism of extraction was achieved by interaction between negative charge (-) of amine group of Fe_3O_4@A/A-GO with positive charge (+) of nickel ions in favorite pH (Ni^{2+}….. NH_2). After extraction, the concentration of nickel was determined by ET-AAS technique. Finally, the developed method has low ion interference, simple usage with low LOD, favorite RSD(%) values and good LR with high recoveries for Ni extraction in blood samples (>95%). Therefore, the proposed method can be considered as applied techniques for Ni separation and determination in blood samples by DS- μ-SPE coupled to ET-AAS.

5. Acknowledgements

The authors wish to thank the Research Institute of Petroleum Industry (RIPI) for financial support to

Table 3. Validation of methodology for Ni(II) extraction from human samples based on Fe_3O_4@A/A-GO by DS-μ-SPE procedure

Sample*	**Added (μg L^{-1})**	***Found (μg L^{-1})**	**Recovery (%)**
Blood A	---	2.61 ± 0.13	---
	2.5	5.07 ± 0.24	98.4
Blood B	---	1.73 ± 0.08	---
	2.0	3.76 ± 0.18	101.5
Serum C	---	3.06 ± 0.15	---
	3.0	5.98 ± 0.33	97.3
Serum D	---	2.72 ± 0.14	---
	3.0	5.68 ± 0.28	98.6
Plasma E	---	1.46 ± 0.11	---
	1.5	3.02 ± 0.16	104.6
Plasma F	---	0.25 ± 0.02	---
	0.25	0.49 ± 0.03	96.0

*Mean of three determinations of samples ± confidence interval (P = 0.95, n =10)

carry out this research.

6. References

[1] A. Abbas, A.M. Al-Amer, T. Laoui, M.J. Al-Marri, M.S. Nasser, M. Khraisheh, Heavy metal removal from aqueous solution by advanced carbon nanotubes: critical review of adsorption applications, Sep. Purifi. Technol., 157 (2016) 141-61.

[2] S. Feng, X. Wang, G. Wei, P. Peng, Y. Yang, Z. Cao, Leachates of municipal solid waste incineration bottom ash from Macao: Heavy metal concentrations and genotoxicity, Chemosphere., 67 (2007) 1133-1137.

[3] S.K. Seilkop, A.R. Oller, Respiratory cancer risks associated with low-level nickel exposure: An integrated assessment based on animal, epidemiological, and mechanistic data, Regul. Toxicol. Pharm., 37 (2003) 173–190.

[4] Agency for Toxic Substances and Disease Registry, Division of Toxicology and Human Health Sciences, 1600 Clifton Road NE, Mailstop S102-1, Atlanta, GA 30333, revision 2019.

[5] Agency for Toxic Substances and Disease Registry (ATSDR), Toxicological profile for Nickel. Atlanta, GA: U.S. Department of Health and Human Services, Public Health Service, 2005.

[6] N. Altunay, A. Elik, R. Gürkan, Vortex assisted-ionic liquid based dispersive liquid liquid microextraction of low levels of nickel and cobalt in chocolate-based samples and their determination by F-AAS, Microchem. J., 147 (2019) 277-285.

[7] L. A. Escudero, A. J. Blanchet, L. L. Sombra, J. A. Salonia, J. A. Gasquez, Determination of the total and extractable fraction of Ni in lake sediments and natural waters of San Luis (Argentina) by F-AAS using a simple solid phase extraction system, Microchem. J., 116 (2014) 92-97.

[8] M. Felipe-Sotelo, A. Carlosena, J. M. Andrade, M. J. Cal-Prieto, D. Prada, Slurry-based procedures to determine chromium, nickel and vanadium in complex matrices by ET-AAS, Microchem. J., 81 (2005) 217-224

[9] A. Baysal, S. Akman, A rapid solid sampling method for determination of nickel and copper along human hair by ET-AAS, Microchem. J., 98 (2011) 291-296.

[10] G. Özzeybek, B. Alacakoç, Trace determination of nickel in water samples by slotted quartz tube-flame atomic absorption spectrometry after dispersive assisted simultaneous complexation and extraction strategy, Environ. Monit. Assess., 190 (2018) 498.

[11] J. Shan Qun, W. Xiang Yu, S. Jin Lyu, Analysis of nickel distribution by synchrotron radiation X-ray fluorescence in nickel-induced early- and late-phase allergic contact dermatitis in Hartley guinea pigs, Chinese Med. J., 132 (2019)1959-1964.

[12] S. Kanchi, B. Ayyappa , M. Sabela , K. Bisetty, N Venkatasubba Naidu, Polarographic Interaction of Nickel (II) with Ammonium Piperidine-1-Carbodithioate: Application to Environmental Samples, J. Environ. Anal. Chem., 1 (2014) 107.

[13] Y. Min Park, J. Yeon Choi, E. Yeong Nho, C. Mi Lee, Determination of macro and trace elements in canned marine products by inductively coupled plasma optical emission spectrometry (ICP-OES) and ICP-mass spectrometry (ICP-MS), J. Anal. Lett., 52 (2019) 1018-1030.

[14] S. C. Wilschefski, M. R. Baxter, Inductively coupled plasma mass spectrometry: introduction to analytical aspects, Clin. Biochem. Rev., 40 (2019) 115-133.

[15] A. Fadhil Khudhair, M. Khudhair Hassan , H. F. Alesary , A. S. Abbas, Simple pre-concentration method for the determination of nickel(II) in urine samples using UV-VIS spectrophotometry and flame atomic absorption spectrometry techniques, Indones. J. Chem., 19 (2019) 638 – 649.

[16] G. Saravanabhavan, K. Werry, M. Walker, D. Haines, M. Malowany, C. Khoury, Human biomonitoring reference values for metals and trace elements in blood and urine derived from the Canadian Health Measures Survey 2007–2013, Int. J. Hyg. Environ. Health, 220 (2017) 189–200.

[17] S. M. Sorouraddin, M. A. Farajzadeh H. Nasiri, Picoline based-homogeneous liquid–liquid microextraction of cobalt(ii) and nickel(ii) at trace levels from a high volume of an aqueous sample, Anal. Methods, 11 (2019) 1379-1386.

[18] S.Z. Mohammadi, H. Hamidian, L. Karimzadeh,

Z. Moeinadini, Simultaneous extraction of trace amounts of cobalt, nickel and copper ions using magnetic iron oxide nanoparticles without chelating agent, J. Anal. Chem., 68 (2013) 953–958.

[19] A. Hol, A. Akdogan, A.A. Kartal, U. Divrikli, L. Elci, Dispersive liquid-liquid microextraction of nickel prior to its determination by micro sample injection system-flame atomic absorption spectrometry, Anal. Lett., 47 (2014) 2195–2208.

[20] Q. Han, Y. Huo, L. Yang, X. Yang, Y. He, J. Wu, Determination of trace nickel in water samples by graphite furnace atomic absorption spectrometry after mixed micelle-mediated cloud point extraction, Molecul., 23 (2018) 2597.

[21] S. Davari, F. Hosseini, H. Shirkhanloo, Dispersive solid phase microextraction based on amine-functionalized bimodal mesoporous silica nanoparticles for separation and determination of calcium ions in chronic kidney disease, Anal. Methods Environ. Chem., J. 1 (2018) 57-66.

[22] H. Shirkhanloo, Z. Karamzadeh, J. Rakhtshah, N. Motakef Kazemi, A novel biostructure sorbent based on CysSB/MetSB@MWCNTs for separation of nickel and cobalt in biological samples by ultrasound assisted-dispersive ionic liquid-suspension solid phase micro extraction, J. Pharm. Biomed. Anal., 172 (2019) 285-294.

[23] M. Behbahani1, A. Veisi, F. Omidi, A. Noghrehabadi, A. Esrafili, M. Hossein Ebrahimi, Application of a dispersive micro-solid-phase extraction method for pre-concentration and ultra-trace determination of cadmium ions in water and biological samples, Appl. Organometal. Chem., (2017) e4134.

[24] M. A. Habila, Z. A. ALOthman, E. Yilmaz, M. Soylak, Activated carbon cloth filled pipette tip for solid phase extraction of nickel (II), lead (II), cadmium (II), copper(II) and cobalt (II) as 1,3,4-thiadiazole-2,5-dithiol chelates for ultra-trace detection by FAAS, Int. J. Environ. Anal. Chem., 98 (2018) 171-181.

[25] M.R. Pourjavid, M. Arabieh , A. A. Sehat, Study on column SPE with synthesized graphene oxide and FAAS for determination of trace amount of Co(II) and Ni(II) ions in real samples, Mater. Sci. Eng. C, 47 (2014) 114-122

[26] S. N. Nabavi, S. M. Sajjadi, Z. Lotfi, Novel magnetic nanoparticles ($CoO–Fe_2O_3@SiO_2@TiO_2$) as adsorbent in ultrasound-assisted micro-solid-phase extraction for rapid pre-concentration of some trace heavy metal ions in environmental water samples: desirability function, Chem. Papers, 74 (2019)1143–1159.

[27] W.S.J. Hummers, R.E. Offeman, Preparation of Graphitic Oxide, J. Am. Chem. Soc., 80 (1958) 1339-1339.

[28] M.K. Abbasabadi, A. Rashidi, S. Khodabakhshi, Benzenesulfonic acid-grafted graphene as a new and green nanoadsorbent in hydrogen sulfide removal, J. Nat. Gas Sci. Eng., 28 (2016) 87-94.

[29] M. Khaleghi-Abbasabadi, D. Azarifar, Magnetic Fe_3O_4-supported sulfonic acid-functionalized graphene oxide (Fe_3O_4@GO-naphthalene-SO_3H): a novel and recyclable nanocatalyst for green one-pot synthesis of 5-oxo-dihydropyrano[3,2-c] chromenes and 2-amino-3-cyano-1,4,5,6-tetrahydropyrano[3,2-c]quinolin-5-ones, Res. Chem. Intermed., 45 (2019) 2095–2118.

[30] M. Khaleghi Abbasabadi, A. Rashidi, J. Safaei-Ghomi, S. Khodabakhshi, R. Rahighi, J. A new strategy for hydrogen sulfide removal by amido-functionalized reduced graphene oxide as a novel metal-free and highly efficient nanoadsorbent, Sulfur Chem., 36 (2015) 660-671.

[31] K.S. Novoselov, Z. Jiang, Y. Zhang, S.V. Morozov, H.L. Stormer, U. Zeitler, J.C. Maan, .S. Boebinger, P. Kim, A.K. Geim, Room-temperature quantum hall effect in graphene, Sci., 315 (2007) 1379.

[32] M.Z. Kassaee, E. Motamedi, M. Majdi, Magnetic Fe_3O_4-graphene oxide/polystyrene: Fabrication and characterization of a promising nanocomposite, Chem. Eng. J., 172 (2011) 540-549.

[33] S. Khodabakhshi, F. Marahel, A. Rashidi, M. Khaleghi Abbasabadi, A Green Synthesis of Substituted Coumarins Using Nano Graphene Oxide as Recyclable Catalyst, J. Chin. Chem. Soc., 62 (2015) 389-392.

[34] D. Azarifar, M. Khaleghi-Abbasabadi, Fe_3O_4-supported N-pyridin-4-amine-grafted graphene oxide as efficient and magnetically separable novel nanocatalyst for green synthesis of 4H-chromenes

and dihydropyrano[2,3-c]pyrazole derivatives in water, Chem. Intermed., 45 (2019) 199–222.

[35] C. Nethravathi, M. Rajamathi, Chemically modified graphene sheets produced by the solvothermal reduction of colloidal dispersions of graphite oxide, Carbon, 46 (2008) 1994-1998.

[36] D. Chen, H. Zhang, K. Yang, H. Wang, Functionalization of 4-aminothiophenol and 3-aminopropyltriethoxysilane with graphene oxide for potential dye and copper removal, J. Hazard. Mater., 310 (2016) 179-187.

[37] J.S. Wang, R.T. Peng, J.H. Yang, Y.C. Liu, X.J. Hu, Preparation of ethylenediamine-modified magnetic chitosan complex for adsorption of uranyl ions Carbohydr. Polym., 84 (2011) 1169-1175.

[38] X.J. Hu, Y.G. Liu, H. Wang, A.W. Chen, G.M. Zeng, S.M. Liu, Removal of Cu(II) ions from aqueous solution using sulfonated magnetic graphene oxide composite, Sep. Purif. Technol., 108 (2013) 189-195.

[39] L.Z. Bai, D.L. Zhao, Y. Xu, J.M. Zhang, Y.L. Gao, L.Y. Zhao, J.T. Tang, Inductive heating property of graphene oxide–Fe_3O_4 nanoparticles hybrid in an AC magnetic field for localized hyperthermia, Mater. Lett., 68 (2012) 399-401.

[40] M. Khaleghi Abbasabadi, A. Rashidi, J. Safaei-Ghomi, S. Khodabakhshi, R. Rahighi, A new strategy for hydrogen sulfide removal by amido-functionalized reduced graphene oxide as a novel metal-free and highly efficient nanoadsorbent, J. Sulfur Chem., 36 (2015) 660-671.

[41] S. Khodabakhshi, B. Karami, Graphene oxide nanosheets as metal-free catalysts in the three-component reactions based on aryl glyoxals to generate novel pyranocoumarins, New J. Chem., 38 (2014) 3586-3590.

[42] H. Kim, K.Y. Park, J. Hong, K. Kang, All-graphene-battery: bridging the gap between supercapacitors and lithium ion batteries, Sci. Rep., 4 (2014) 5278.

[43] C. Hou, Q. Zhang, M. Zhu, Y. Li, H. Wang, One-step synthesis of magnetically-functionalized reduced graphite sheets and their use in hydrogels, Carbon, 49 (2011) 47-53.

[44] E. Rafiee, M. Khodayari, Two new magnetic nanocomposites of graphene and 12-tungestophosphoric acid: characterization and comparison of the catalytic properties in the green synthesis of 1,8-dioxo-octahydroxanthenes, RSC Adv., 16 (2016) 36433-36440.

[45] S. Khodabakhshi, M. Khaleghi Abbasabadi, S. Heydarianc, S Gharehzadeh Shirazi, F Marahel, Fe_3O_4 Nanoparticles as Highly Efficient and Recyclable Catalyst for the Synthesis of 4-Hydroxy-3-[aryloyl(benzamido)methyl]coumarin under Solvent-Free Conditions, Lett. Organ. Chem., 12 (2015) 465-470.

[46] J. Wang, Z. D. Han, The combustion behavior of polyacrylate ester/graphite oxide composites, Polym, Adv. Technol., 17 (2006) 335–340

[47] P. J. Yen and C. C. Ting, et al., Facile production of graphene nanosheets comprising nitrogen-doping through in situ cathodic plasma formation during electrochemical exfoliationJ. Mater. Chem. C, 5 (2017) 2597-2602

[48] C. C. Yang and M. H. Tsai, et al., Carbon Nanotube/Nitrogen-Doped Reduced Graphene Oxide Nanocomposites and Their Application in Supercapacitors, J. Nanosci. Nanotechnol., 17 (2017) 5366–5373.

[49] L. J. Li and C. W. Chu, et al., Plasma-assisted electrochemical exfoliation of graphite for rapid production of graphene sheets, RSC Adv., 4(2014)6946–6949.

[50] M. Rohaniyan, A. Davoodnia, A. Nakhaei, Another application of $(NH_4)_{42}[Mo^{VI}_{72}Mo^{V}_{60}O_{372}(CH_3COO)_{30}(H_2O)_{72}]$ as a highly efficient recyclable catalyst for the synthesis of dihydropyrano[3,2]chromenes, Appl. Organometal. Chem., 30 (2016) 626-629

[51] J. Wang and Z. D. Han, The combustion behavior of polyacrylate ester graphite oxide composites, Polym. Adv. Technol., 17(2006) 335–340.

[52] X. Wang and L. Zhang, Green and facile production of high-quality graphene from graphite by the combination of hydroxyl radicals and electrical exfoliation in different electrolyte systems, RSC Adv., 9 (2019) 3693-3703.

[53] ZH Mousavi, A Rouhollahi, Preconcentration and determination of heavy metals in water, sediment and biological samples, J. Serb. Chem. Soc., 76 (2011) 1583-1595

[54] HZ Mousavi, A Asghari, Determination of Hg in water and wastewater samples by CV-AAS following on-line preconcentration with silver trap, J. Anal. Chem., 65 (2010) 935-939.

[55] A Khaligh, F Golbabaei, Z Sadeghi, A Vahid, A Rashidi, On-line micro column preconcentration system based on amino bimodal mesoporous silica nanoparticles as a novel adsorbent for removal and speciation of chromium (III, VI) inenvironment samples, J. Environ.Health Sci. Eng., 13 (2015) 47.

Anal. Method Environ. Chem. J. 3 (1) (2020) 17-26

AMECJ

Research Article, Issue 1

Analytical Methods in Environmental Chemistry Journal

Journal home page: www.amecj.com/ir

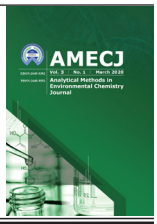

Extraction and determination of benzene from waters and wastewater samples based on functionalized carbon nanotubes by static head space gas chromatography mass spectrometry

Shahnaz Teimoori[a], Amir Hessam Hassani[b,*], Mostafaa Panaahie[b]

[a] *PhD student of environmental engineering, Faculty of Natural Resources and Environment, Science and Research Branch, Islamic Azad University, Tehran, Iran*

[b] *Department of environmental engineering, Faculty of Natural Resources and Environment, Science and Research Branch, Islamic Azad University, Tehran, Iran*

ARTICLE INFO:

Received 30 Nov 2019

Revised form 10 Jan 2020

Accepted 11 Feb 2020

Available online 26 Mar 2020

Keywords:

Benzene,
Water,
Dispersive micro solid phase extraction,
Phenyl sulfonic acid,
Carbon nanotubes,
Static head space gas chromatography mass spectrometry

ABSTRACT

Removal of benzene, as hazardous pollutants from waters and wastewater is a main problem of environment contamination due to high risk factor in human health. In this study, the phenyl sulfonic acid (PhSA) modified carbon nanotubes (CNTs) were used for benzene removal from waters by dispersive micro solid phase extraction method (D- μSPE). Due to adsorption mechanism, the polar–π and π–π electron donor–acceptor interactions was provided between the aromatic ring of benzene with the surface sulfonic acid groups (SO_3H) and phenyl ring (-C6H5) of CNTs, respectively. Therefore, 20-100 mg of sorbent, concentration of benzene (0.1–10 mg L^{-1}), pH (1-12) and contact time (5–120 min) were investigated and optimized for benzene removal from water samples in static system. The concentration of benzene in water was determined by static head space gas chromatography mass spectrometry (SHS-GC-MS). The results showed, the Langmuir-Freundlich (LF) isotherm provided the best fit for benzene sorption. By using the Langmuir model, the maximum adsorption capacity of 157.34 mg g^{-1} and 22.86 mg g^{-1} was achieved for benzene removal from waters with CNTs@PhSA and CNTs, respectively. The method was validated by certified reference material in waters.

1. Introduction

Benzene is a chemical aromatic and flammable compound which is a natural component of petroleum-derived products. It is one of the most highly used groups of raw materials and solvents in numerous chemical synthesis processes, and manufacturing industries [1-3] .The presence of benzene in groundwater is due to petroleum product's leakage into water sources and leaking underground storage tanks and pipelines [4, 5]. According to the US Environmental Protection Agency (EPA), benzene is one of the primary pollutants that adversely affects human health [6] .It is a serious health problem, causing several human diseases such as cancer, central nervous system disorders, leukemia, respiratory problems, skin and eye diseases [7-9]. Considering these health concerns and based on U.S.EPA announcement, the standard level of benzene in drinking water should not exceed 5 μg^{-1} [6]. Therefore, it is crucial to remove this pollutant from water supplies, especially surface water, and ground waters. Since their discovery by Iijima et al in 1991 [10], Carbon nanotubes (CNTs) have been in a major area of

* Corresponding Author: Amir Hessam Hassani
Email: ahh1346@gmail.com
https://doi.org/10.24200/amecj.v3.i01.91

interest within many contexts, especially in water treatment. CNTs are graphitic carbon sheets folded into hollow cylinders with diameters and lengths in nanometer and micrometer scales, respectively [11-13]. Unique properties of CNTs including hydrophobicity, high specific surface area, hollow and layered structure and existence of π-electrons on their surface make them superior adsorbents for removal of contaminants [14-16]. Some studies put further steps and investigated the effect of CNT's modification on their adsorption performance. Lu et al. showed that NaOCl-oxidized CNTs have significant adsorption capacity in comparison to other types of carbon adsorbents [17]. Su et al conducted a research in which multiwalled carbon nanotubes were oxidized by sodium hypochlorite solution and turned to a new adsorbent with enhanced adsorption performance [18]. These studies show high affinity of CNTs toward organic compounds, and open new avenue for developing carbon nanotube technologies to treat benzene and other organic chemicals in water. However, there is a high number of CNTs that can be used to remove benzene from water supplies and which subtype of CNTs family can have the most effective adsorption capacity, is still unknown. To our knowledge, so far, there is no data about the adsorption capacity of *phenyl* sulfonic acid (PhSA) modified hybrid carbon nanotubes (CNTs). Therefore, the main objective of this study is using *phenyl* sulfonic acid (PhSA) modified hybrid carbon nanotubes (CNTs) to remove benzene from water sources by dispersive solid phase extraction method.

2. Experimental

2.1. Material and methods

Gas chromatography based on mass detector (GC-MS) and air sample loop injection (ASL) was used for benzene determination by static head space accessory (SHS-GC-MS, Netherland). The headspace may be sampled using a gas tight syringe of appropriate volume. Gas-tight syringe (GTS) was used for determination VOCs[1] from water samples by shaking and heating samples. The auto-sampling of GTS units can retrofit to a standard GC with a split/split less injector. The GTS auto-sampler is beneficial for use with diverse samples. The Agilent 7890A GC can accommodate up to three detectors identified as front detector, back detector, and auxiliary detector. This model of GC design with three detectors in front, back, and auxiliary (FID, TCD, MS) and equipped with a split injector with poly di-methyl siloxane column (Table 1). The mass detector chosen was selected for benzene analysis in gas/liquid. Before injection, Slide the plunger carrier down until it is completely over the syringe plunger, and tighten the plunger thumb screw until finger- tight. The injector temperature was adjusted to 190°C and the detector temperature at 240°C. The GC oven temperature was programmed from 25°C to 250°C which was held for 12 min. Hydrogen(Cas number: 1333-74-0) as the carrier gas was used at a flow rate of 1.0 mL min^{-1}. The scanning electron microscopy (SEM) and Raman spectra were recorded by electron microscopy and spectrometer of CNTs@PhSA (Bruker). Fourier transformed infrared spectroscopy (FTIR, IR-200 Thermo-Nicolet 2.2) in KBr in the range 400–4000 cm^{-1} was used to confirm the covalently bound benzenesulfonic acid (CAS N: 98-11-3) group on the CNT surface. Transmission electron microscopy (TEM, Philips) with a conventional 15 kV electron microscope was used to analyze the surface morphology of CNTs@PhSA. X-ray diffraction (XRD; Panalytical) was used for XED patterns with wavelength 0.15405 nm for CNTs@PhSA. The intensity was measured by step scanning in a 2θ range of 5–80°. Benzene (CAS N: 71-43-2; C_6H_6) purchased from Sigma Aldrich. Five calibration solutions of benzene were prepared and the approximate concentrations of benzene were 0.1, 0.2, 0.5, 1.0, 5,0 and 10 mg L^{-1}. The other chemicals with high purity (99%) were purchased from Sigma (Germany). The analytical grade solvents such as benzene, chloroform, (CAS N: 67-66-3), 4-benzenediazoniumsulfonate (CAS: 305-80-6), acetone (CAS N: 67-64-1),, HNO_3 (CAS N:7697-37-2), HCl (CAS N: 7647-01-0), H_2SO_4(CAS N: 7664-93-9), acetic acid (CAS N:

1- Volatile organic compound

64-19-7) and NaOH (CAS N:1310-73-2) were also from Merck.CNTs@PhSA was synthesized in RIPI laboratory, Iran. Ultrapure water (18 MΩ·cm) was obtained from Millipore continental water system (Millipore, USA). Samples of water and wastewater collected in polyethylene bottles were filtered through Millipore cellulose membrane filter (0.45 µm porosity) to remove suspended particulate matter.

2.2. Synthesis of phenyl sulfonic acid modified hybrid carbon nanotubes

High-purity CNTs were synthesized by use of camphor, an environmentally friendly hydrocarbon as a carbon source using chemical vapor deposition method on Co–Mo/MgO nanocatalysts. The nanocatalyst was synthesized by sol-gel method. HCNTs were grown at temperatures of about 900–1000°C in 45–60 min. Concentration of active metals was 5–10%. The nanocatalyst (Co–Mo/MgO) was prepared by our special sol-gel method [19]. For functionalization of CNTs with phenyl-SO_3H (CAS N: 98-11-3) group, CNTs surface was activated by 50% HNO_3 (CAS N: 7697-37-2) for 1 h and washed with ultrapure water many times. The diazotization reaction was used for functionalization as follows; 0.03 mol of sulfanilic acid CAS N: 121-57-3) was dispersed in 300 mL of 1 M HCl (7647-01-0) in a three-necked ground flask [20]. The flask was kept in an ice water bath and the temperature controlled around 3ºC under stirring. Then, 33 mL of 1 M $NaNO_2$ (CAS N: 7632-00-0) was added dropwise into the mixture and stirred for 1 h at the same temperature. The resulting precipitate was filtered and washed with deionized water. In the following step, 5 g of 4-benzenediazonium sulfonate and 180 mg of activated CNTs were added into 120 mL of mixture of water and ethanol (1:1, v/v) at 3°C. Subsequently, 60 mL of H_3PO_2 aqueous solution (50 wt.%) was added to the mixture and stirred for 30 min. After this time, another 60 mL of H_3PO_2 (CAS N: 6303-21-5) was added and stirred for 1 h. The resulting mixture was washed with deionized water and dried overnight in an oven at 80°C (Fig. 1).

Table 1. The conditions of GC-MS for determination benzene

GC-MS	Conditions
Model	Agilent, 7890A
Sensitivity	0.1-20 ng
Injection Volume	1-5 µL; 10:1 split
Split ratio	2:1
Column	30 meter, 0.32mm x 0.25µm
Temperature Injector	220 °C
Detector FID	230 °C
Program , time= 5.0 min	25 to 100 °C at 25 °C per min
Carrier Gas	N_2, 1 mL min^{-1}
Column Oven Pressure Pulse	60°C
Column Flow	6 ml min^{-1}
Retention Time	8.153 (min)
Run Time (Min)	19.125 (min)
Flow Rate N_2	30 (mL min^{-1})
Flow Rate H^2	34(mL min^{-1})
Injection size	1-5µL
Flow Rate air	200-400(mL min^{-1})

2.3 Extraction Procedure

The CNTs@PhSA nanostructures based on D-µSPE method was used for extraction of benzene from waters (Fig. 2). First, 10 mg of CNTs@PhSA or

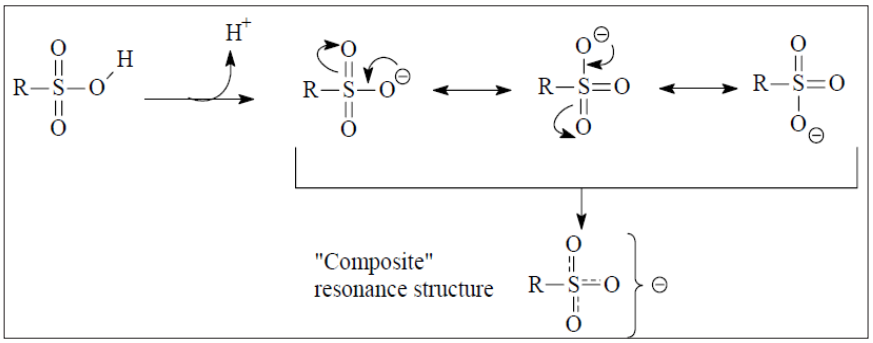

Fig. 1. Synthesis of composite with resonance structure

CNTs nanostructures was put on 5 mL of water samples with different benzene standard solution (0.1--10 mg L^{-1}) in GC vial. The mixture shacked for 10 min by magnetic shaker accessory (MSA) and after centrifuging for 3 min (3500rpm), the solid phase separated from liquid phase and finally the benzene concentration in water sample was determined by static head space gas chromatography mass spectrometry (SHS-GC-MS). After extraction, the recoveries were calculated with the ratio of initial/final concentration of benzene in vial GC by SHS-GC-MS (Eq. A). In addition, adsorption capacity and removal efficiency (RE) was calculated by equation Eq. B and Eq. C. X is the initial concentration of benzene in solution and Y is final concentration of benzene which determinate by SHS-GC-MS in water samples. The adsorption capacity (AC) of benzene (mg g^{-1}) and, the removal efficiency of benzene (%) was shown in Eq. B and Eq. C. The C_i (mg L^{-1}) and C_f (mg L^{-1}) are the concentration of benzene before and after extraction procedure, Vs (L) is the sample volume, and mass (g) is the amount of CNTs@PhSA.

– (Eq. A)

$(C \quad _f)\times$ (Eq. B)

(%) —— (Eq. C)

3. Results and discussion

Mechanism of extraction of benzene with CNTs@$PhSO_3H$ was achieved based on π–π stacking between aromatic chain and S=O bond of CNTs@$PhSO_3H$ and SO b and molecular of benzene in waters by sandwich or T shaped π–π bonding (Fig. 3).

3.1. Characterization

Figure 4 (a, b) showed the SEM and TEM images revealed the CNTs@$PhSO_3H$ consist of randomly aggregated and crumpled thin tubes which are closely associated with each other forming a disordered solid, and it can be inferred that the functionalization process does not change the general structure of HCNTs. The FTIR spectrum of the CNTs@$PhSO_3H$ sample showed the O=S=O, OH as a broad peak, C=C and C-S bond which was confirmed the SO_3 bond in CNTs (Fig. 5). Raman spectroscopy is a useful technique for the characterization of carbon nanotubes quality. Raman patterns of CNTs@$PhSO_3H$ confirm the presence of CNTs (Fig. 6) and XRD image showed the hexagonal structures in CNTs@$PhSO_3H$. After the attachment of SO_3H groups on the carbon wall of CNTs the three peaks which confirms the functionalization of SO_3H on CNTs@Ph have not any changes on the structure of CNTs (Fig. 7).

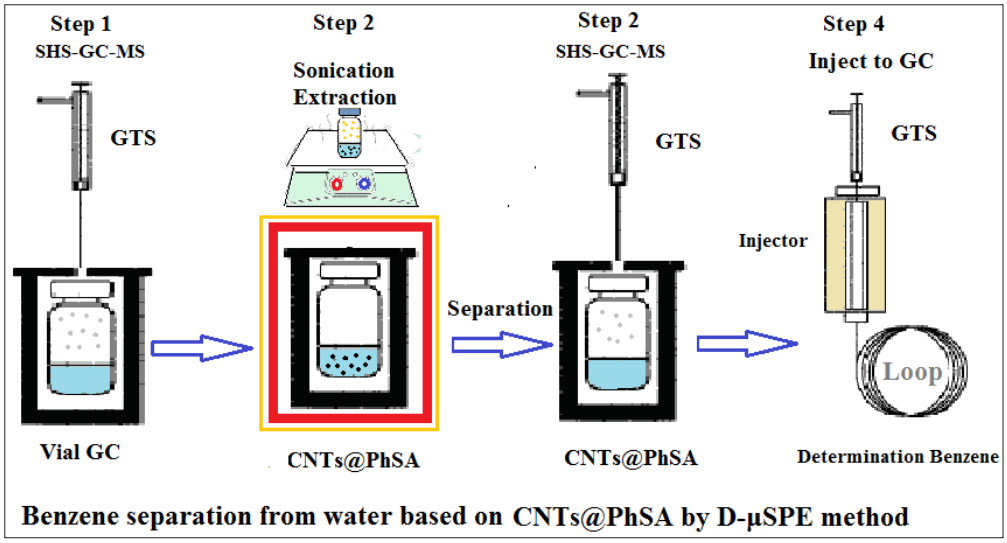

Fig. 2. Benzene extraction from waters based on CNTs@PhSA by D-µ-SPE method

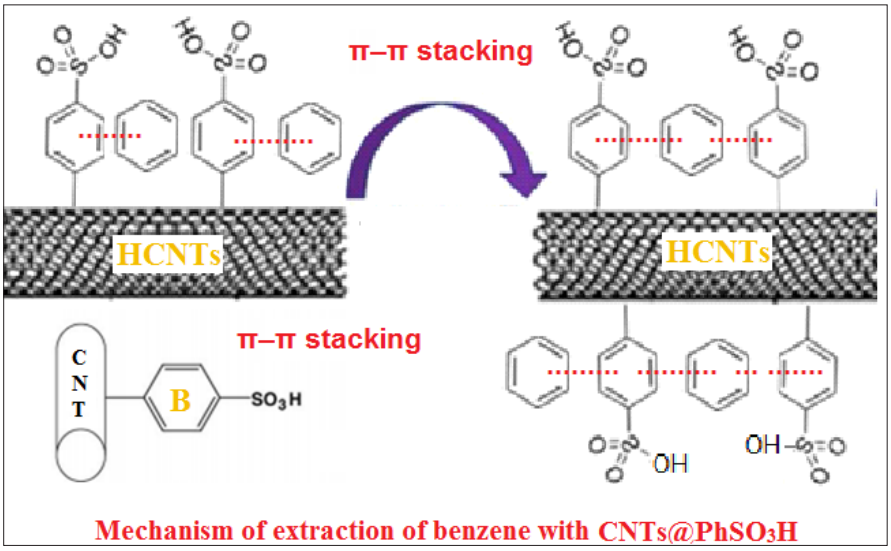

Fig. 3. Mechanism of extraction of benzene with CNTs@$PhSO_3H$

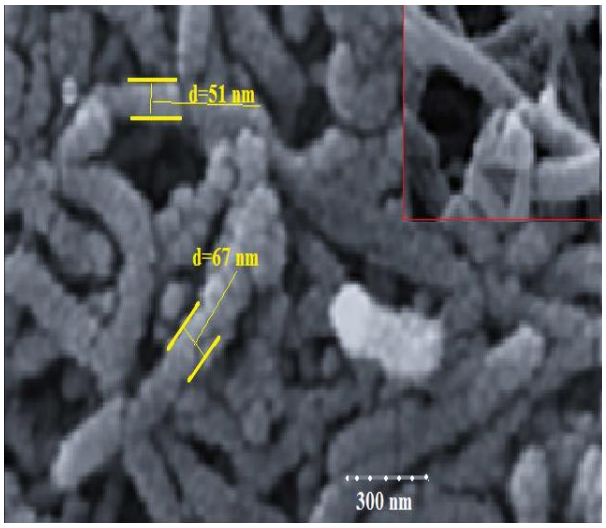

Fig. 4(a). SEM of CNTs@$PhSO_3H$

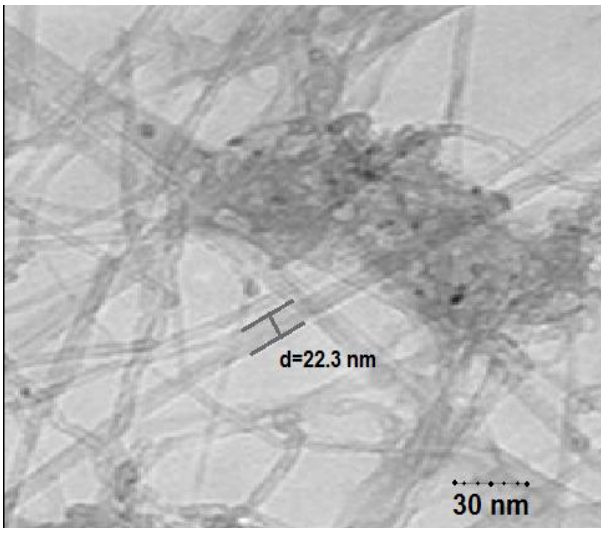

Fig. 4(b). TEM of CNTs@$PhSO_3H$

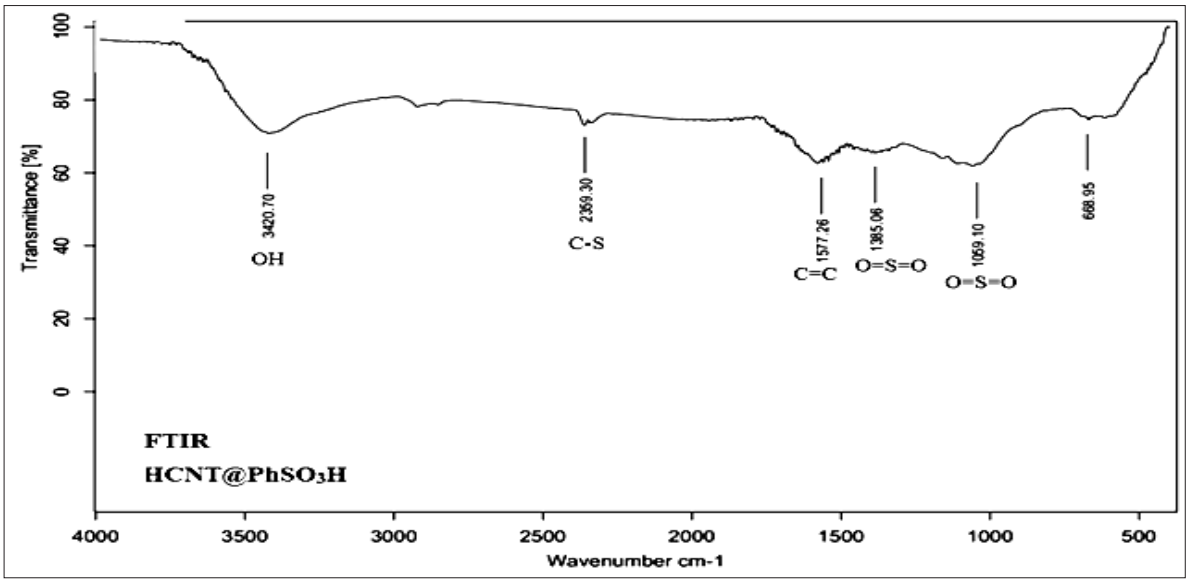

Fig. 5. FTIR spectrum of the CNTs@$PhSO_3H$

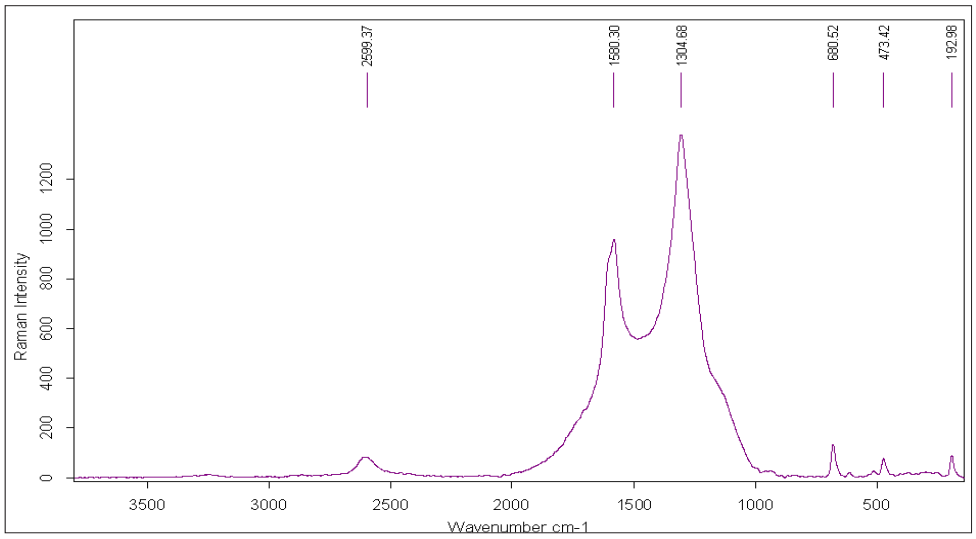

Fig. 6. Raman patterns of CNTs@$PhSO_3H$

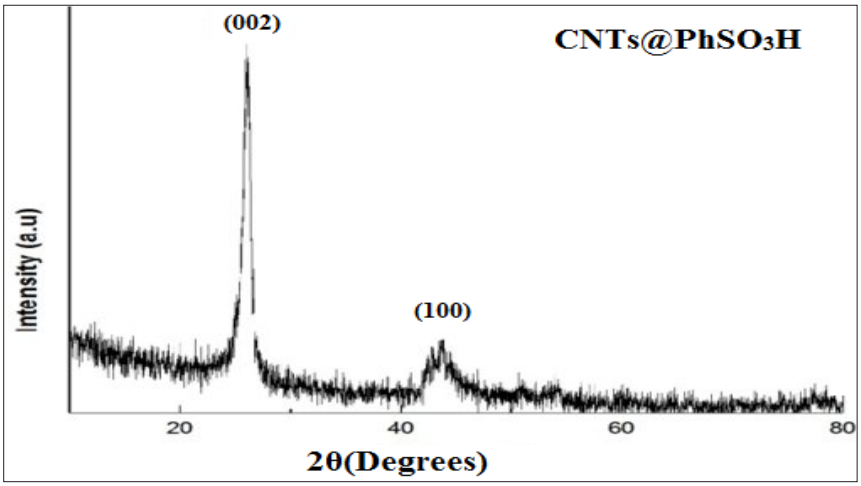

Fig. 7. XRD image of hexagonal structures in CNTs@$PhSO_3H$

3.2. Optimization parameters

The D-μ-SPE procedure based on CNTs@$PhSO_3H$ nanocomposite was used for extraction of benzene from well water and wastewater samples. The main effectiveness parameters such as, pH, amount of CNTs@$PhSO_3H$, volume of waters, adsorption capacity of sorbent were evaluated and studied. The pH sample is critical parameters and must be optimized. High adsorption of benzene from water samples based on CNTs@$PhSO_3H$ nanocomposite depended on pH solution which was extracted by D-μ-SPE methods. The pH range (1-12) was adjusted with buffer solution and the extraction efficiency of benzene in water samples was evaluated by benzene concentration (0.1-10 mg L^{-1}) and 10 mg of CNTs@$PhSO_3H$. The results showed, the recovery of extraction for benzene was decreased at acidic and basic pH ranges. Therefore, pH of 5.5-7.5 was selected as optimized pH for benzene extraction in waters (Fig. 8).

By D-μ-SPE method, the amount of on CNTs@$PhSO_3H$ nanocomposite was studied for 5 mL of water and wastewater samples. So, 1-20 mg of CNTs@$PhSO_3H$ and CNTs was examined by proposed procedure. The results showed us, benzene in water samples can be efficiently extracted with 8 mg CNTs@$PhSO_3H$ in optimized pH=7. So, 10 mg of CNTs@$PhSO_3H$ nanocomposite was used as optimum mass for benzene extraction in waters (Fig. 9).

The sample volume (SV) in important factor and must be studied. So, the effect of sample

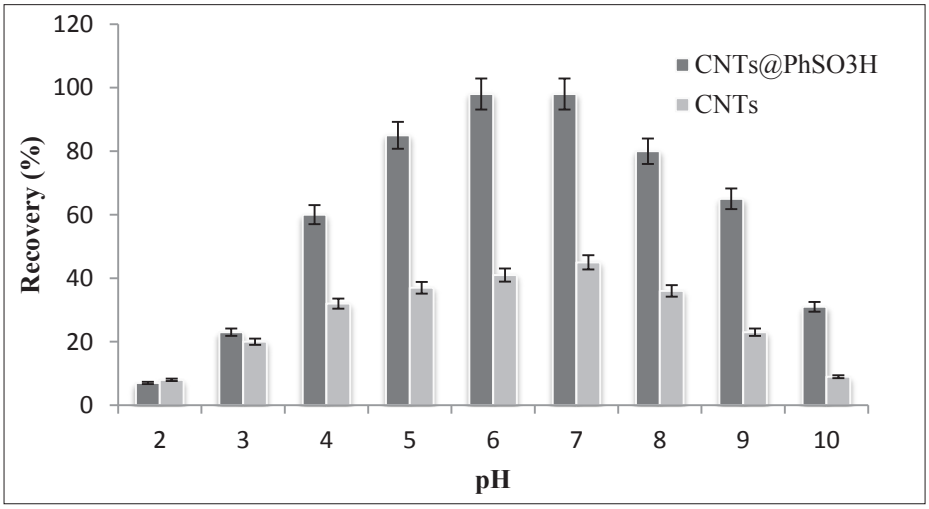

Fig. 8. The effect of pH on benzene extraction from water samples

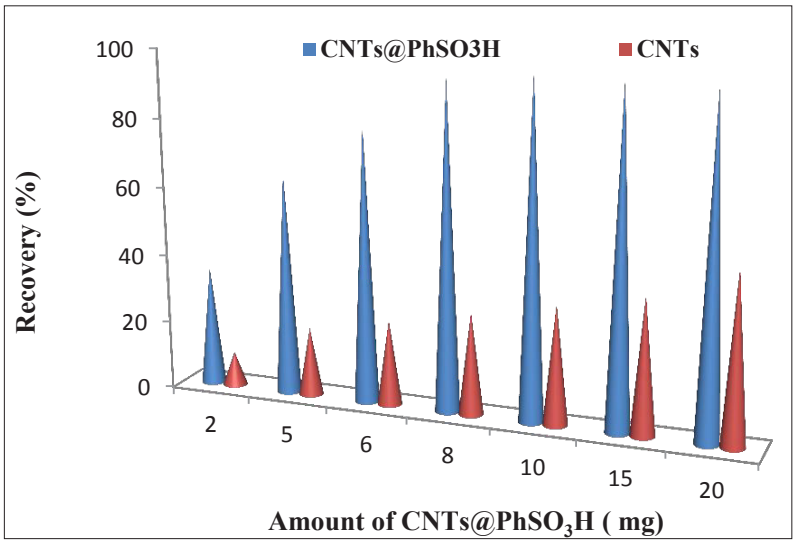

Fig. 9. The effect of amount of CNTs@$PhSO_3H$ on benzene extraction by D-μ-SPE method

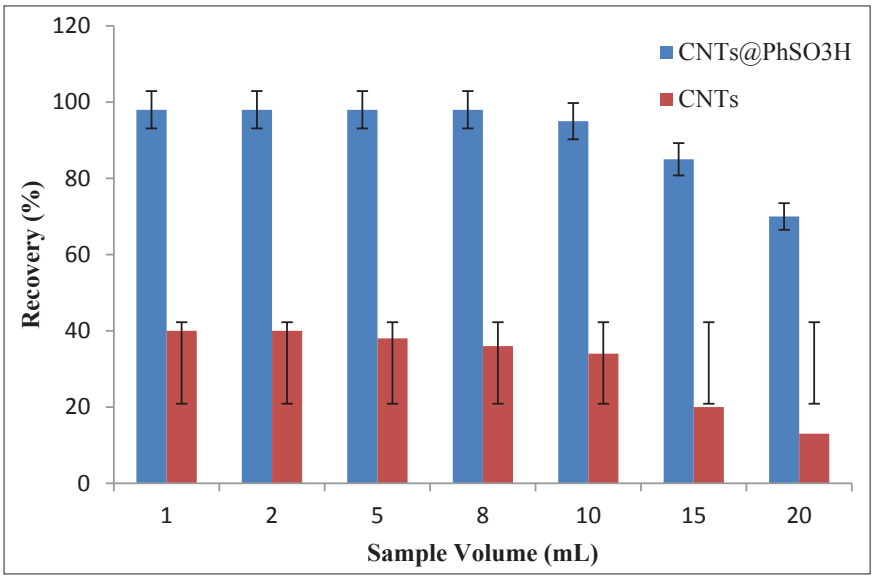

Fig 10. The effect of sample volume on benzene extraction by D-μ-SPE method

volume on benzene extraction in waters examined at optimized conditions. Due to procedure, the different water volumes between 1-10 mL with 10 mgL^{-1} of standard benzene solution were selected for benzene extraction by D-μ-SPE methodology. As magnetic shaking for 10 min, high recovery obtained for 10 mL of waters. Therefore, 5 mL of sample volume selected for further work (Fig. 10).

The validation methodology based on spiking well water and wastewater samples was achieved by concentration of standard benzene solution from LLOQ as 0.1 mgL^{-1} and ULOQ as 10 mgL^{-1} by optimized conditions (Table 2). All samples analyzed by static head space gas chromatography mass spectrometry (SHS-GC-MS).

3.3. Discussion

This study set out with the aim of assessing the modification of CNTs with phenyl sulfonic acid group and its effect on the extraction efficiency of benzene in water samples. According to our results, it is revealed that compared to CNTs, CNTs@PhSA significantly adsorbs benzene in water. As table 3, the results showed us the proposed method based on CNTs@PhSA had more efficient extraction of benzene from waters than CNTs sorbents which was presented by different authors [21-26]. Also the comparing of adsorption capacity(AC) of CNTs@PhSA (157.34 mg g^{-1}) with other sorbents such as CNTs (22.86 mg g^{-1}), CuO-NPs (100.24 mg g^{-1}), GO/MOF-5 (77 mg g^{-1}) , ZIF-8/GO(123 mg g^{-1}) and GO (158 mg g^{-1}) showed, the value of AC was near or more than others [27-30]. Osanloo at el was used graphene modified by ionic liquid (NG-IL) for toluene removal [31].

Table 2. The validation methodology based on CNTs@$PhSO_3H$ by SHS-GC-MS

samples	Added (mgL^{-1})	*Found (mgL^{-1})	Recovery (%)
Well Water	-------	0.43 ± 0.02	-------
	0.5	0.94 ± 0.03	102
Paint Wastewater	-------	14.16± 0.68	-------
	15	28.87± 1.26	98.1
Oil-Factory Wastewater	-------	38.12± 2.15	-------
	40	76.82± 3.75	96.8

* Mean of three determinations ± confidence interval (P = 0.95, n = 10)

Table 3. Comparing of dispersive micro solid phase extraction method based on CNTs@PhSA for benzene extraction from water samples with other published methods

This Study	Relevant Studies
In this study, phenyl sulfonic acid group was used for modification of CNTs in order to extract benzene from water samples.	CNTs have the capacity to be attached by functional groups. These functional groups can change physical and chemical properties of carbon nanotubes [21].
We prepared a range of benzene concentration including 0.1, 0.2, 0.5, 1.0, 5.0, 10 mg/L	Optimum benzene concentration for the investigation of CNTs adsorption efficiency in benzene removal procedure is 10 mg/L [22].
Contact time performed in this study was 10 min.	The mixture of CNTs and sample have been shaked for 10 minutes [22].
Extraction of benzene in waters by sandwich or T shaped π–π bonding.	Molecular torsion balance, developed by Wilcox et al. representing a closed model with a T-shaped π–π interaction [23, 24].
SEM and TEM images revealed that the CNTs@$PhSO_3H$ consists of randomly aggregated and crumpled thin tubes.	CNTs accumulation leads to pores formation which can create a bunch of adsorption sites on them [25].
Addition of SO_3H on CNTs@Ph had no change on the structure of CNTs.	According to SEM images of H_2SO_4-treated CNTs, there is no change in the morphology and structure of CNTs [21].
pH optimization in the range of 5.5-7.5 benzene extraction from water samples	When pH exceeds 6.2, the adsorption efficiency increases significantly [26].

4. Conclusions

The main goal of the current study was to determine the effect of phenyl sulfonic acid group functionalization on the adsorption efficiency of CNTs for benzene removal in water samples. The adsorption mechanism is referred to the polar-π and π-π interaction between aromatic ring of benzene and surface sulfonic acid group as well as phenyl ring. Surprisingly, hexagonal structure of CNTs@PhSA indicated no change in the basic structure of CNTs, after functionalization with SO_3H. However, the adsorption capacity of CNTs@PhSA for benzene removal was significant. These findings suggest that in general, CNTs are capable of being modified and therefore, they represent a critical role in the adsorption of benzene and other pollutants**.** All concentration benzene in waters determined based on D- μ-SPE procedure by SHS-GC-MS. Under optimal conditions, adsorption efficiency of CNTs@PhSA and CNTs was obtained 97.7% and 20.6 % for benzene removal from water samples, respectively.

5. References

[1] J.A. Kent, Riegel's handbook of industrial chemistry, Springer, 1992.

[2] C. Kent, Basics of toxicology, John Wiley & Sons, Vol. 3, 1998.

[3] J.R. McKetta, Encyclopedia of Chemical Processing and Design: Volume 64-Waste: Hazardous: Management Guide to Waste: Nuclear: Minimization During Decommissioning. CRC press, 1998.

[4] H. Shim, E. Shin, S. T. Yang, A continuous fibrous-bed bioreactor for BTEX biodegradation by a co-culture of Pseudomonas putida and Pseudomonas fluorescens, Adv. Environ. Res.,7 (2002) 203-216.

[5] L. Mohammadi, E. Bazrafshan, M. Noroozifar, A. Ansari-Moghaddam, F. Barahuie, D. Balarak, Adsorptive removal of benzene and toluene from aqueous environments by cupric oxide nanoparticles: kinetics and isotherm studies, J. Chem., 2017 (2017) 2069519.

[6] US environmental protection agency, Pollutants, Code of federal regulations, Title 40, Washington, DC, 1996.

[7] ATSDR, Toxicological profile for lead, US Department of Health and Human Services Atlanta, GA, 2007.

[8] N. Wibowo, Adsorption of benzene and toluene from aqueous solutions onto activated carbon and its acid and heat treated forms: influence of surface chemistry on adsorption. J. Hazard. Mater., 146 (2007) 237-242.

[9] M. Aivalioti, I. Vamvasakis, E. Gidarakos, BTEX and MTBE adsorption onto raw and thermally modified diatomite, J. Hazard. Mater., 178 (2010) 136-143.

[10] S. Iijima, Helical microtubules of graphitic carbon. Nnat., 354 (1991) 56-58.

[11] S. Zhang, T. Shao, S.S. Kaplan Bekaroglu, T. Karanfil, The impacts of aggregation and surface chemistry of carbon nanotubes on the adsorption of synthetic organic compounds, Environ. Sci. Technol., 43 (2009) 5719-5725.

[12] A. J. Brooks, H.N, Lim, J.E. Kilduff, Adsorption uptake of synthetic organic chemicals by carbon nanotubes and activated carbons, Nanotechnol., 23 (2012) 294008.

[13] K.Yang, W. Xilong, Z. Lizhong, X. Baoshan, Competitive sorption of pyrene, phenanthrene, and naphthalene on multiwalled carbon nanotubes, Environ. sci. Technol., 40 (2006) 5804-5810.

[14] L. Ji, Ch. Wei, D. Lin, Z. Dongqiang, Mechanisms for strong adsorption of tetracycline to carbon nanotubes: a comparative study using activated carbon and graphite as adsorbents, Environ. Sci. Technol., 43 (2009) 2322-2327.

[15] H. H. Cho, B.A. Smith, J.D. Wnuk, D.H. Fairbrother, W.P. Ball, Influence of surface oxides on the adsorption of naphthalene onto multiwalled carbon nanotubes, Environ. sci. Technol., 42 (2008) 2899-2905.

[16] O.G. Apul, T. Karanfil, Adsorption of synthetic organic contaminants by carbon nanotubes: a critical review, Water res., 68 (2015) 34-55.

[17] C. Lu, Su. Fengsheng, Hu. Suhkai, Surface modification of carbon nanotubes for enhancing BTEX adsorption from aqueous solutions, Appl. Surf. Sci., 254 (2008) 7035-7041.

[18] F. Su, Lu. Chungsying, Hu. Suhkai, Adsorption of benzene, toluene, ethylbenzene and p-xylene by NaOCl-oxidized carbon nanotubes, Colloids and Surfaces A: Physicochem. Eng. Aspects 353 (2010)

83-91.

[19] A. Rashidi, L. Roghayeh, F. Ehsaneh, Z. Masoud, Production of single-walled carbon nanotubes from methane over Co-Mo/MgO nanocatalyst: A comparative study of fixed and fluidized bed reactors, J. Nat. Gas chem., 20 (2011) 372-376.

[20] M.K. Abbasabadi, A. Rashidi, S. Khodabakhshi, Benzenesulfonic acid-grafted graphene as a new and green nanoadsorbent in hydrogen sulfide removal, J. Natural Gas Sci. Eng., 28 (2016) 87-94.

[21] F. Peng, Z. Lei, W. Hongjuan, Lv. Ping, Yu. Hao, Sulfonated carbon nanotubes as a strong protonic acid catalyst. carbon, 43 (2005) 2405-2408.

[22] B. Bina, M. Amin, A. Rashidi, H. Pourzamani, Benzene and toluene removal by carbon nanotubes from aqueous solution, Arch, Environ. Protect., 38 (2012) 3-25.

[23] S. Paliwal, S. Geib, C.S. Wilcox, Molecular torsion balance for weak molecular recognition forces. Effects of" tilted-T" edge-to-face aromatic interactions on conformational selection and solid-state structure. J. Am. Chem. Soc., 116 (1994) 4497-4498.

[24] E. I. Kim, S. Paliwal, C.S. Wilcox, Measurements of molecular electrostatic field effects in edge-to-face aromatic interactions and CH-π interactions with implications for protein folding and molecular recognition, J. Am. Chem. Soc., 120 (1998) 11192-11193.

[25] L. Zhang, F. Pan, X. Liu, L. Yang, X. Jiang, J. Yang, W. Shi, Multi-walled carbon nanotubes as sorbent for recovery of endocrine disrupting compound-bisphenol from wastewater, Chem. Eng. J., 218 (2013) 238-246.

[26] Y.H. Wang, S.H. Lin, and R.S. Juang, Removal of heavy metal ions from aqueous solutions using various low-cost adsorbents, J. Hazard. Mater., 102 (2003) 291-302.

[27] V. Kumar, Y. S. Lee, J. W. Shin, K. H. Kim, D. Kukkar, Y.F. Tsang, Potential applications of graphene-based nanomaterials as adsorbent for removal of volatile organic compounds, Environ. Int., 135 (2020) 105356.

[28] J. Cheng, L. Li, Y. Li, Q. Wang, C. He**,** Fabrication of pillar[5]arene-polymer-functionalized cotton fibers as adsorbents for adsorption of organic pollutants in water and volatile organic compounds in air, Cellulose, 26 (2019) 3299-3312.

[29] B.Y.Z. Hiew, L.Y. Lee, X.J. Lee, S. Thangalazhy-Gopakumar, S. Gan, S.S. Lim, G. T. Pan, T.C. K. Yang, W.S. Chiu, P.S. Khiew, Review on synthesis of 3D graphene-based configurations and their adsorption performance for hazardous water pollutants, Process Saf. Environ. Prot., 116 (2018) 262-286.

[30] H. Yan, H. Wu, K. Li, Y.W. Wang, X. Tao, H. Yang, A.M. Li, R.S. Cheng, Influence of the surface structure of graphene oxide on the adsorption of aromatic organic compounds from water, ACS Appl. Mater. Interfaces, 7 (2015) 6690-6697.

[31] M. Osanloo, O. Qurban Dadras, Nobel method for toluene removal from air based on ionic liquid modified nano-graphen, Int. J. Occup. Hyg., 6 (2014) 1-5.

Anal. Method Environ. Chem. J. 3 (1) (2020) 27-40

AMECJ

Research Article, Issue 1

Analytical Methods in Environmental Chemistry Journal

Journal home page: www.amecj.com/ir

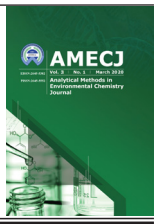

Combination of reduction with metallic sodium and adsorption with mesoporous materials for re-refining of used insulating oil via experimental design

Amir Vahid[a,*] and Masoud Sohrab[b]

[a,*] *Research Institute of Petroleum Industry (RIPI), West Entrance Blvd., Olympic Village, Tehran, 14857-33111, Iran*

ARTICLE INFO:

Received 21 Dec 2019

Revised form 19 Feb 2020

Accepted 10 Mar 2020

Available online 29 Mar 2020

Keywords:

Used oil,
Color reduction,
Total Acid Number,
Re-refining,
Mesoporous material,
Optimization.

ABSTRACT

In this study, re-refining of used insulating oil by mesoporous silicate material (MCM-41) and metallic sodium was investigated. Also, the effect of silicate absorbents which was synthesized and functionalized with aluminum (Al-MCM-41) was studied (18 wt% and 36 wt%). The physical and structural properties of Al-MCM-41 were characterized by FT-IR, BET, XRD, FESEM and the obtained results illustrated a successful synthesis of the mesoporous material. The refined oil was treated by MCM-41 adsorbent. After that, total acid number (TAN) of used insulating oil was effectively reduced by metallic sodium. The effect of some parameters such as contact time, temperature and the dosage (sodium and adsorbent to oil ratio) was designed and optimized by response surface method (RSM). The results showed that the acid number incredibly decreased at 150, 60 min and 2% of sodium to oil. The color of the re-refined oil was significantly reduced. The factors such as, time, temperature and dosage was statistically studied by ANOVA. The adsorption of MCM-41 was also studied by this way. Based on proposed procedure, the modeling was carried out. Treating of oil with MCM-41 after using metallic sodium causes lower color of oil.

1. Introduction

Used oils are the important contaminates of ecosystems which leads to water and soil pollution [1]. In other hands, the used oil is to provide a source of valuable base oil [2]. The oil has duties such as lubricating moving parts of engine, reducing friction, cooling agent, act as an anti-corrosion, protecting, against wear, act as an cleaning agent, conducting force and removing contaminates [3]. Some additives added to the oil to enhance its application for a specific task. These additives are almost hazardous materials for environment. The insulating (transformer) oil degradation under working condition of high voltage transformers occurs mainly due to oxidation and thermal decomposition at high temperatures after long period of using [4]. These oxidation products of used insulating oil contain carboxylic acids, ketones and alcohols, which then condense to from polymeric materials [5]. The oxidation of products caused to metal corrosion, viscosity increase, sludge and varnish formation [6]. The acidity of used oil is depended to oxidation of products [7]. Sodium

*Corresponding Author. Amir Vahid
E-mail: avahid753@gmail.com
https://doi.org/10.24200/amecj.v3.i01.74

is a reactive metal which is easily oxidized. It has a powerful affinity for certain oxidative organic species. The rate of reaction depends on the metal-oil interface. The rate of reaction between the solid metal and the oxidation of oil products depends on the extent of this interface. Sodium dispersions as resemble emulsions having a high metal surface area. The dispersion is used at a temperature which is above that of the melting point of the sodium (98°C). In this way a reasonable reaction rate can be achieved [8]. The reaction of sodium with oxidation products such as acid carbocyclic caused to obtain the solid and hydrogen as below equation 1. The reaction between sodium with ketones caused to reduce ketones and obtained tertiary alcohol. Also, the reaction of sodium with alcohols produced the solid and hydrogen (Eq. 2).

$$2CH_3COOH + 2Na \rightarrow 2CH_3COONa + H_2 \quad \text{(Eq. 1)}$$

$$2CH_3OH + 2Na \rightarrow 2CH_3ONa + H_2 \quad \text{(Eq. 2)}$$

Recycling of used oil is very important as less energy and cost compared to refining of crude oil.

Recycling of used oil helps to air, soil and water pollutions in the environment. Many sorbent were used for recycling of used oil as oxidation and refining of oil products. The various treatments were used for improving used oil by acid-clay process, solvent extraction, vacuum distillation and hydrogenation methods. These are high technology which combines a few generic methods in its process. Due to the hard recycling of used oil, the single method cannot be generated a standard emission controlled process. So, for specific processes of recycling waste oils, sophisticated equipment was used. KTI and STP methods combine the vacuum distillation and hydrofinishing together. By the STP method, dehydration, vacuum distillation, separation of the lubricating fraction and hydrofinishing were used [9-17]. In this paper, the MCM-41 was used for collecting product. By heating oil, the oxidation products and absorption of new oxidation products had created. For determination of constituent's acid number oil, the titration of alcoholic base method was used [18]. For determination of discoloration (reduce oxidation products) and new oxidation products, the spectrophotometer with wavelength of 419 nm and 312 nm was used.

2. Experimental

2.1. Reagent and Materials

The cetyltrimethyl ammonium bromide (CTAB), sodium silicate (Na_2SiO_3), polyethylene glycol 4000(PEG4000), ethanol, aluminum nitrate, acetic acid, sodium hydroxide (NaOH), TAN , 2-propanol, toluene, p-naphtholbenzein, potassium hydroxide, and deionized water (DW) was purchased from Merck, Germany and used for all synthesis and TAN method.

2.2. Synthesis of MCM-41

For synthesis of MCM-41, 180 g of DW and 3.7 g of CTAB mixed at room temperature and then 11.1 g of ethanol was added to suspension until receive colorless position and then, 11.1g sodium silicate as silicate source, 0.6g PEG4000 was used. The acid acetic 0.1 molar was used for fixing PH near 9.5. The mixture was stirrer at room temperature for 48h and then, put it awayfor1h. The precipitate product was filtered and washed by mixture of ethanol / DW (1:5 ratio) and dry at room temperature for 24h. Finally, the solid cavities put in electric furnace for 6h at high temperature up to 550°C (calcination process) [19].

2.3. Synthesis of Al-MCM-41

The synthesis of Al-MCM-41 method is similar to the synthesis of MCM-41method. For the synthesis of Al-MCM-41 method, the aluminum nitrate (Aluminum source) was added to suspension and then sodium silicate. For fixing PH, the NaOH (0.1molar) was used for reducing acidic PH [20].

2.4. Characterization Method

The X-ray diffraction (XRD) patterns recorded on seritef XRD 300 PTS. The X-ray diffractometer using cu kα radition (λ=1.54) and scan rate 0.02 2θ/S at room temperature was used. Nitrogen

adsorption-desorption isotherms for mesoporous (BET) recorded on BELSORP-miniII. Fourier transform infrared spectroscopy (FT-IR) recorded to 4000-400cm^{-1}area on a Thermo Nicolet Nexus 870. Scanning electron micros copy (SEM) images obtained on Tescan Mira3Xmu.

2.5. Total Acid Number (TAN)

For determining of acid, 2 g of sample added to 20-30 mL of solvent and then the sample dissolved completely in solvent (solvent: 100 mL toluene, 99 mL isopropanol and 1mL DW) and the resulting single-phases solution was titrated at room temperature with standard alcoholic base (solution Hydroxide potassium 0.1 molar). Finally, the end point indicated to changing color by adding 0.5 mL of p-naphtholbenzien solution (orange to green/ green-brown)[18].

2.6. Refining used oil by MCM-41 and silicate - Aluminums

The absorbent and acid (0.15) diluted with Heptane (1:9, 1 mL Oil + 9 mL Heptane) was added to used insulating oils and the refining was determined at 419 nm area. First, 20 mL of used insulating oils was poured in container 1 with amount of 0.2 g MCM-41, container 2 with amount of 0.2 AL-MCM-41 (18wt%) and container 3 with amount of 0.2 g of Al-MCM-41 (36wt%). In order to favorite contact between adsorbent and used insulating oils, the mixture was shacked for 15 min and then the sorbent separated t from used insulating oils by centrifuging process.

2.7. The experiment of sodium with used oil

The refining of used oil based on acid number 0.15 which was diluted with Heptane 1:9 (1:9, 1 mL Oil + 9 mL Heptane) and absorbent 2.436, was determined at 419 nm area.. 20 mL of used oil was poured in two containers. The amount of 0.2 g sodium metallic poured in container 1 and shacked based on magnet stirrer for interaction with used oil at room temperature (1 hour). In container 2, we increased temperature up to 100°C and then 0.2 g of sodium metallic was added to used insulating oils in present of magnet stirrer for 1h.

2.8. The experiment of sodium with used oil and refining by absorbents

The effect of sodium with used oil and refining by absorbents MCM-41, Al-MCM-41 were investigated before and after use of sodium metallic. The used oil contains acid number 0.26 that diluted with Heptane 1:9 (1mL Oil + 9 mL Heptane) that contain absorbent 2.794, 419 nm area. In first steps, each absorbent was used based on refining method at room temperature and then used sodium metallic added at 100°C. In second steps, we used sodium metallic at 100°C and next used absorbent at room temperature.

2.9. Optimized effective factors on acid number reduction

In this research, the effective parameters and their interaction (acid reduction and oil color reduction) were studied and optimized by RSM method. Finally, a model in which could explain influence effective parameters on reactions and interaction between them. Three parameters predict on influence factors on acid number reduction and color oil reduction were obtained by sodium metallic dosage, sodium metallic contact time and temperature. So, this design based on BBD method was used for experimental which could obtained more information about influence parameters of measurement. According to Design-Expert v7 software 17, the experimental was designed for metallic sodium and refining absorbent MCM-41 (Table 1). The experimental design of used insulating oils contained 0.09 acid numbers based on heptane diluted 1:9 ratios (1cc oil + 9cc heptane) and absorbent 4.818 in 3.12 nm to area.

3. Results and Discussions

3.1. FT-IR Spectrums

The spectrums of FT-IR were shown in figures of 1, 2 and 3. The Waveland of 816 cm^{-1} and 1050 cm^{-1} related to Si-O-Si bonds vibration in MCM-41 structure. The bands in 1050 cm^{-1} related to stretching vibration asymmetric Si-O-Si and related

Table 1. The design of experiment parameters

experiments	Contact time(min)	Tamperature(°C)	Dosege%
1	60	100	2
2	180	100	2
3	60	150	2
4	180	150	2
5	60	100	6
6	180	100	6
7	60	150	6
8	180	150	6
9	39	125	4
10	201	125	4
11	120	91	4
12	120	159	4
13	120	125	1.29
14	120	125	6.71
15	120	125	4
16	120	125	4
17	120	125	4

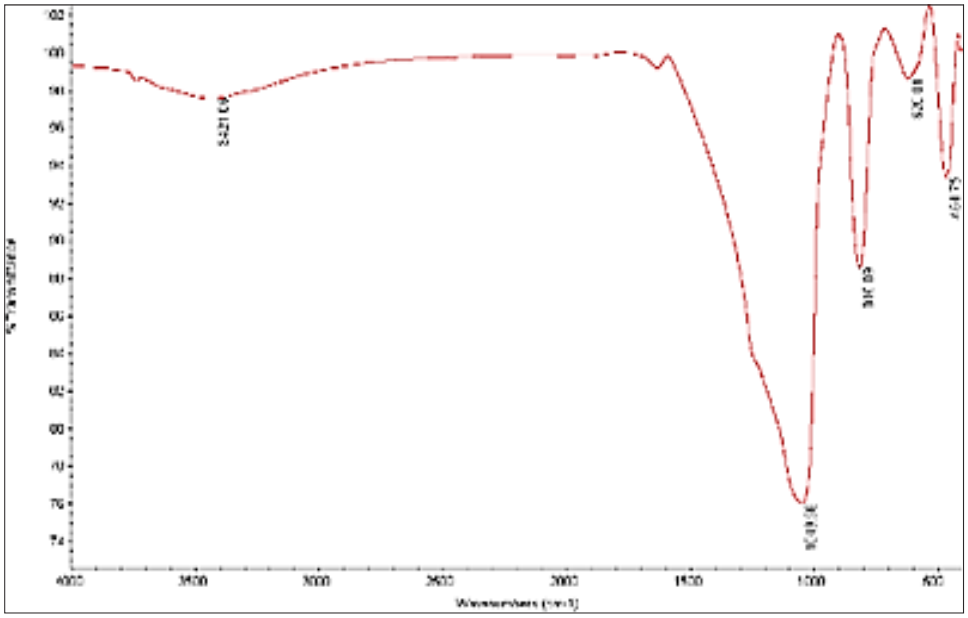

Fig. 1. The FT-IR of MCM-41

to stretching vibration symmetric
Si-O-Si and 465cm^{-1}is related to angular vibration Si-O-Si. The bands of 3421cm^{-1} and 1690 cm^{-1} related to vibration of sinanol hydroxide group that is the reason of adsorbent water molecules which was shown in figure 2, 3. Based on figures, the amount of metal and polarity structure was increased [21, 22].

3.2. XRD analysis

According to XRD pattern especially diffraction of XRD d_{100} spacing in low angele 2θ region, the confirm mesoporous structure and hexagonal lattice [23]. Well resolver sharp peaks at higher order diffractions imply that long range order present in this sample (Fig. 4).

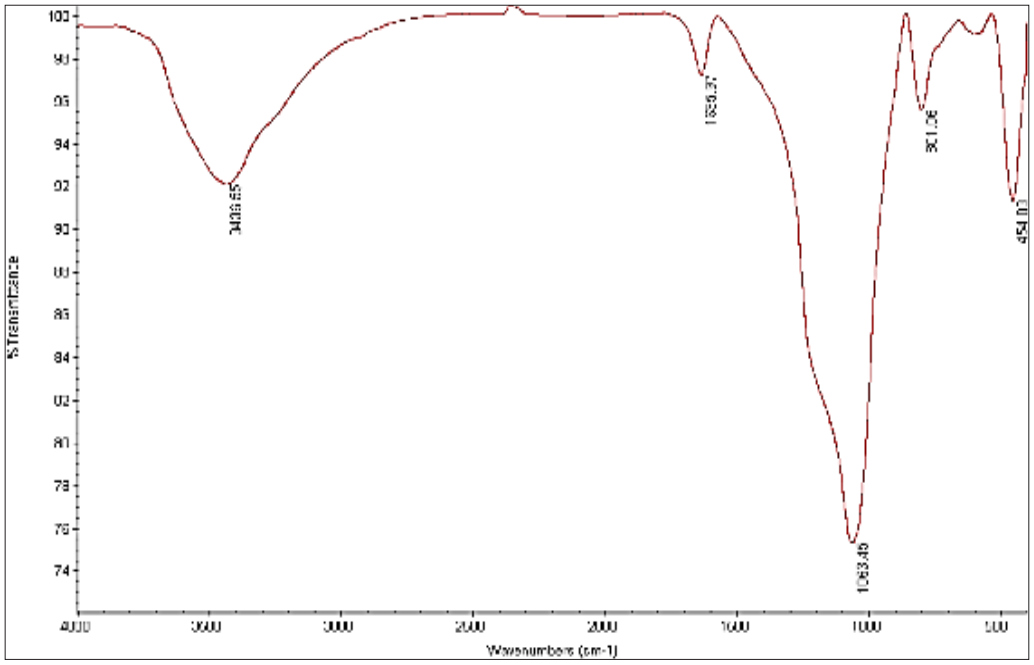

Fig. 2. The FT-IR of 18%wtAl-MCM-41

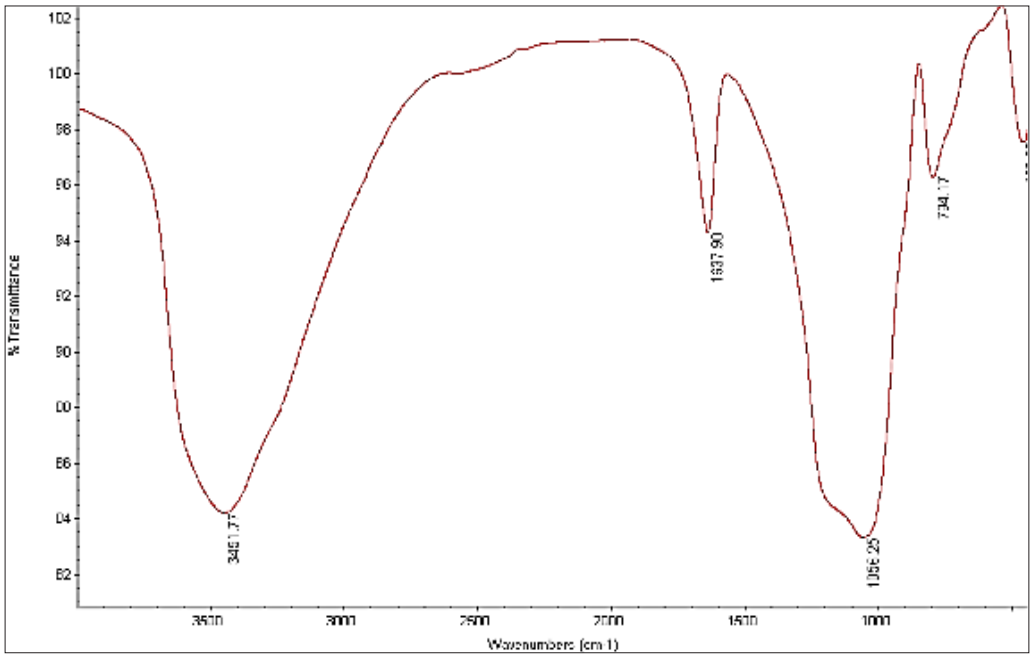

Fig. 3. The FT-IR of 36% wt Al-MCM-4

3.3. BET analysis

Nitrogen adsorption-desorption of MCM-41 and 36%wt Al-MCM-41 showed that the mesoporous MCM-41 had pore diameter more 3 nm and specific surface area about 919.65 m^2g^{-1}. Mesoporous functionlized with aluminium 36%wt(Al-MCM-41) have been pore diameter of aout 2.6 nm and specific surface area about 526.92 m^2g^{-1}. Decrease of surface area is due to the grafting of alluminom species

3.4. FESEM analysis

Figure 5 amd 6 showed the images of FESEM for MCM-41 and structure morphology with worm-

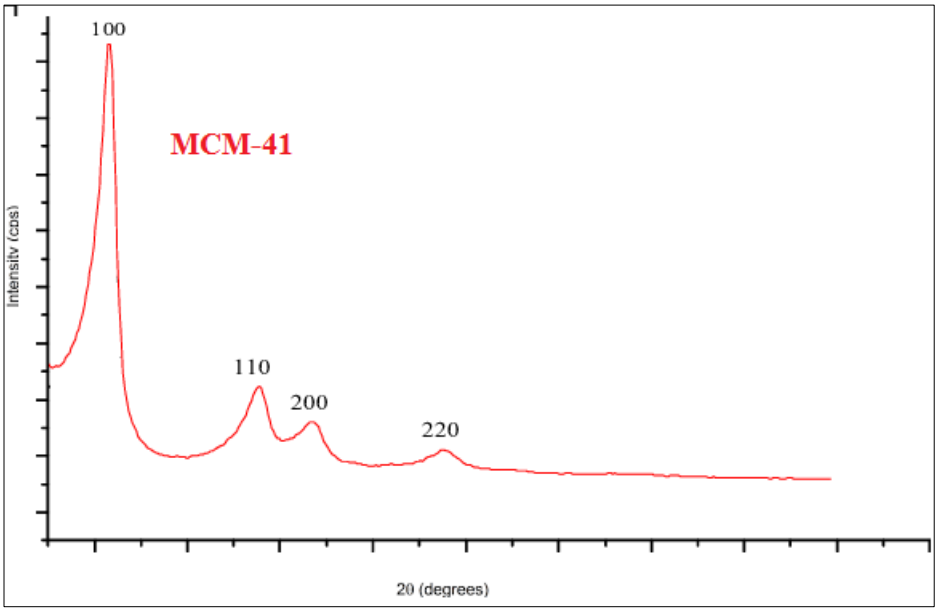

Fig. 4. The low angle of XRD patterns for MCM-41

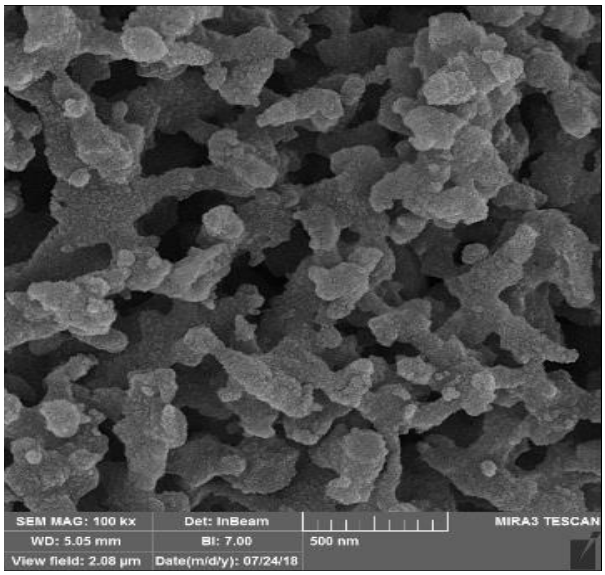

Fig. 5. The FESEM of MCM-41(200000)

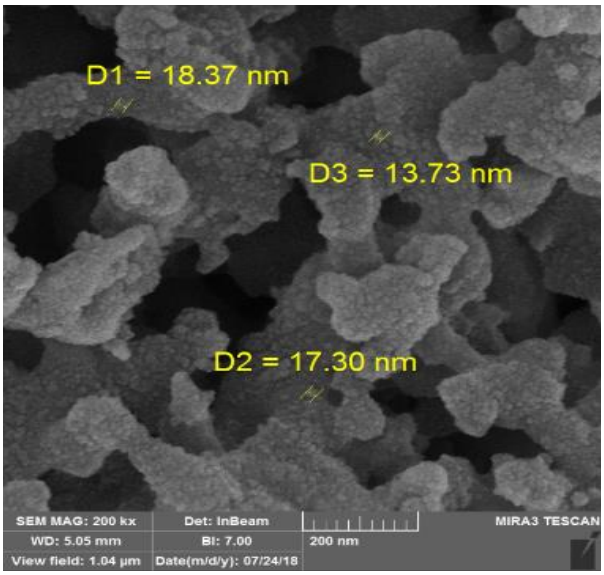

Fig. 6. The FESEM of MCM-41(100000)

like intera-particle structure. The FESEM with magnification 200000 and 100000 for MCM-41 was shown in Figure 5 and 6, respectively.

3.5. Analyzed refining used oil with MCM-41 absorbent

As comparing to BET analysis of Al-MCM-41(36wt%), the effective surface area was more than MCM-41. In Al-MCM-41, the reaction between aluminum metal and oxidation products occurred and therefore the acid number amount more than used oil color decreased. The Al-MCM-41(18 wt%) has less aluminum metal as compared to Al-MCM-41(36 wt%), therefore as low aluminum amount, the less reaction between aluminum and oxidation products occurred. In other words, according to aluminum amount reduction, the effective surface will increased and therefore the amount of acid number reduce (Table 2).

As lacking metal according to BET analysis, the MCM-41 has more effective surface than two other absorbent and adsorbent oxidation products

Table 2. .Results of refining analysis for used oil with MCM-41 and silicate rich Al

Type of absorbent	Absorbance(419nm)	Acid number
MCM-41	1.950	0.085
18wt%MCM-41	2.174	0.084
36wt%MCM-41	2.659	0.071

therefore acid number less reduce toward two other absorbent and so oil color reduce more.

3.6. Metallic sodium reaction

The reduction power of metallic sodium with oxidation products at 100°C was appreciably higher than that of 25°C. The melting point of metallic sodium is 98°C and therefore contact surface area with oil increase at 100°C and renewed continuously and amount of metallic sodium reaction with oxidation products increased. One of oxidation products was derivatives of carboxylic acids and carbonyl groups which reduced at this temperature. The sodium and TAN decreased by increasing sodium reaction time and temperature. The reaction between metallic sodium and oxidation products was increased and this products caused to increase the color of oil in this temperature (Table 3).

3.7. Analysis of metallic sodium and refining with MCM-41 and Al- MCM-41

The adsorbent addition and reduction based on metallic sodium is very important for re-refining process. Table 4 showed, the results of experiments at equal level of factors. The difference was depended to the order of treatment with adsorbent and reducing agent. The results showed, the first treating based on adsorbent in better quality of final re-refined insulating oil in terms of color. But the TAN process had a slightly higher.

3.8. Optimized of effective factors acid number reduction

According to DOE and temperature, dosage and contact time, different results were obtained and showed in Table 5. The ANOVA of he obtained results is shown in Table 6. Prob>F is a good measure of importance of each term in the first order model. Interaction terms are also importance although the BC has the lowest effect on the response of model.

The model can be mentioned in the following equation (Eq. 3) in terms of real factors. Adsorption of byproducts by mesoporous materials is investigated by DOE which was shown in Table 7.

Acidity calculating (A)

(Eq. 3)

$$A = -0.026272105 + (0.000324288 \times Time) + (0.000263706 \times Temperature) + (3.2824\times10^{-5} \times Dosage) - (0.00000225 \times Time \times Temprature) - (7.29167 \times 10^{-8} \times Time \times Dosage - (0.000000125 \times Temperature \times Dosage)$$

The quadratic equation (Eq. 4) has obtained after to

Table 3. Results of treatment of used insulating oil y metallic sodium.

Treatment	temperature	Absorbance(419nm)	Acid number
metallic sodium	25°C	2.575	0.11
metallic sodium	100°C	2.890	0.03

Table 4. Analysis of metallic sodium and refining with absorbent MCM-41 and Al- MCM-

Type of absorbent	Absorbance(419nm)	Acid number (TAN)
Metallic sodium+MCM-41	2.404	0.045
Metallic sodium+18 wt% Al-MCM-41	2.678	0.05
Metallic sodium+36 wt% Al-MCM-41	3.094	0.05
MCM-41+ Metallic sodium	2.300	0.056
18 wt% Al-MCM-41+ Metallic sodium	2.267	0.055
36 wt% Al-MCM-41+ Metallic sodium	2.480	0.056

Table 5. Experimental design data for metallic sodium and MCM-41

experiments	Acid number	Absorbance (312nm)	contact time (min)	Tamperatur e(°C)	Dosege (%)
1	0.009	4.597	60	100	200
2	0.019	4.655	180	100	200
3	0.014	4.675	60	150	200
4	0.011	4.400	180	150	200
5	0.016	4.647	60	100	600
6	0.023	4.659	180	100	600
7	0.019	4.723	60	150	600
8	0.014	4.562	180	150	600
9	0.014	4.743	39	125	400
10	0.014	4.760	201	125	400
11	0.018	4.679	120	91	400
12	0.019	4.735	120	159	400
13	00.15	4.614	120	125	129
14	0.014	4.477	120	125	671
15	0.014	4.659	120	125	400
16	0.014	4.667	120	125	400
17	0.014	4.625	120	125	400

Table 6. Results of metallic sodium

Source	Sum of squares	df	Mean square	F-Value	P-Value Prob>F
model	0.000165	6	2.75	22.50	<0.0001
A-Time	0.0000008	1	0.0000008	6.61	0.0278
B-Temp	0.0000023	1	0.0000023	18.92	0.0014
C-Dosage	0.0000033	1	0.0000033	27.27	0.0004
AB	0.0000911	1	0.0000911	74.64	<0.0001
AC	0.0000061	1	0.0000061	5.01	0.0490
BC	0.0000031	1	0.0000031	2.55	0.1407
Residual	0.0000012	10	0.00000012	-	-
Lack of fit	0.0000012	8	0.00000015	-	-
Pure Error	0	2	0	-	-
Cor Total	0.00017	16	-	-	-

Table 7. Results of adsorption of MCM-41.

source	Sum of squares	df	Mean square	F-Value	P-Value Prob>F
model	0.170	9	0.0189	30.8	<0.0001
A-Time	0.0114	1	0.0114	18.59	0.0035
B-Temp	0.0000042	1	0.0000042	0.069	0.8003
C-Dosage	0.0053	1	0.0053	8.68	0.0215
AB	0.045	1	0.045	74.8	<0.0001
AC	0.0035	1	0.0035	5.74	0.0476
BC	0.0081	1	0.0081	13.34	0.0081
A^2	0.0066	1	0.0066	10.83	0.0133
B^2	0.0067	1	0.0067	11.02	0.0128
C^2	0.082	1	0.082	134.7	<0.0001
Residual	0.0042	7	0.00061	-	-
Lack of fit	0.0033	5	0.0066	1.32	0.48
Pure Error	0.00099	2	0.00049	-	-
Cor Total	0.174	16	-	-	-

predict reduction of color of oil by MCM-41

Adsorption of predict reduction of color of oil by MCM-41(Ads) **(Eq. 4)**

$$Ads = 4.801224864 + (0.002992049 \times Time) - (0.009280222 \times Temprature) + (0.001318102 \times Dosage) - (0.0000505 \times Time \times Temprature) + (1.75 \times 10^{-6} \times Time \times Dosage) + (6.4 \times 10^{-6} \times Temprature \times Dosage) + (8.74636 \times 10^{-6} \times Time^2) + (5.0816 \times 10^{-5} \times Temprature^2) - (2.77655 \times 10^{-6} \times Dosage^2)$$

3.9. The effect of contact time

The graph of effect of time on acidity at dosage (400) and temperature (125°C) is linear with increasing of time, new oxidation products in oil was produced more and therefore, the acid number increased (Fig. 7).

3.10. The effect of temperature

The graph of temperature on acidity is linear which was shown in Figure 8. By increasing of temperature amount of acid number reduced and at 150°C the lowest acid number obtained. By increasing of temperature, the metallic sodium change to liquid an also viscosity of oil significantly reduced, because of its low viscosity index. As a result, the surface was expanded when the temperature, diffusion of oil and the surface of sodium particles increased. Therefore, the amount of metallic sodium with oxidation products as carboxylic acid has more reaction and caused to reduce TAN.

3.11. The effective of metallic sodium dosage

Figure 9 showed that the graph of dosage on acidity at temperature 125°C and contact time 120 min.

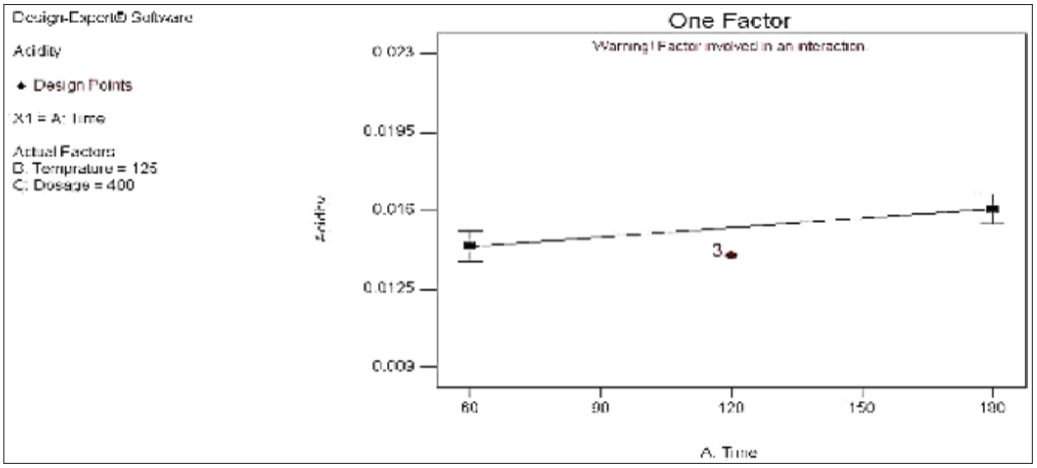

Fig. 7. The effect of metallic sodium contact time on TAN.

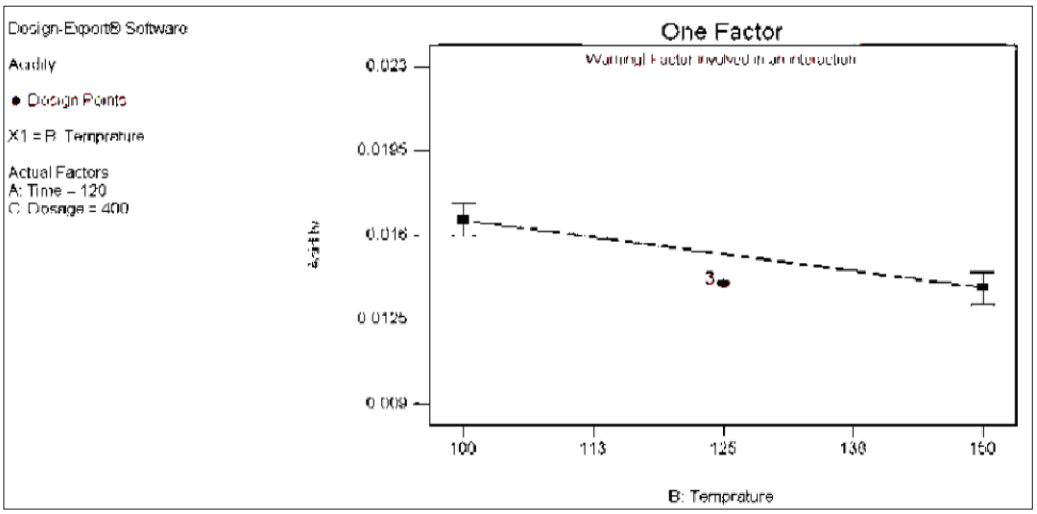

Fig. 8. The effect of metallic sodium reaction temperature on TAN

The linear graph is clear. By increasing of metallic sodium, the higher amount of acid number in dosage 600% was observed. Therefore, by increasing of metallic sodium, the more reaction between sodium and oxidation products as in carboxylic acid was happened.

3.12. The effect of contact time on color of oil by MCM-41

Based on Figure 10, the graph of time factor on oil color at temperature (125°C) and contact dosage (400) was constant. At 120 min, the color reduction was observed and after higher time, the color slightly increasing.

3.13. The effect of reaction temperature on oil color

As can be seen in the curvature in Figure 11 until temperature 125°C, discoloration was occurred. After 125°C, the color was increased with slow slop.

3.14. The effect of dosage on oil color by MCM-41

Figure 12 showed, the graph of dosage factor (metallic sodium ratio to oil) on color of oil in time (125 min) and temperature (125°C) was linear. Based on the curvature, the color increased up to 400 dosages and after it the color decreases.

The Figures 13, 14 and 15 displayed the interaction

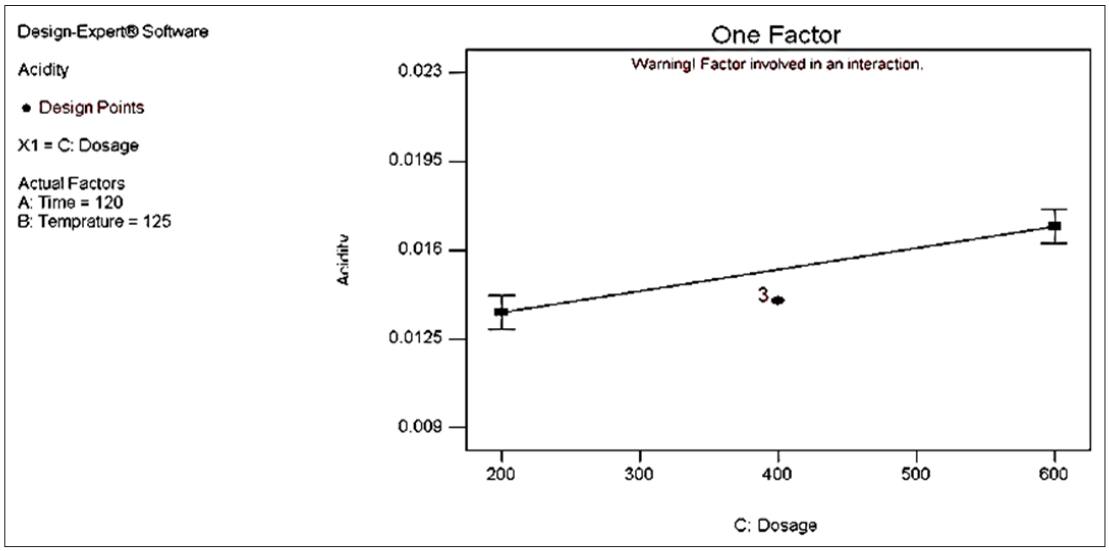

Fig. 9. The effect of metallic sodium dosage factor (sodium to oil ratio) on TAN

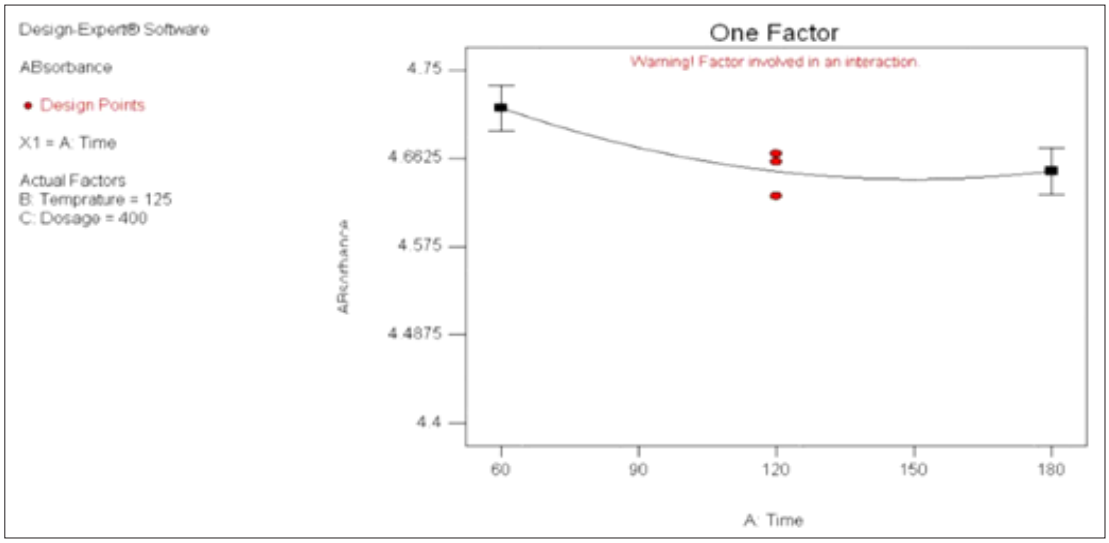

Fig. 10. The effect of contact time on oil color by MCM-41

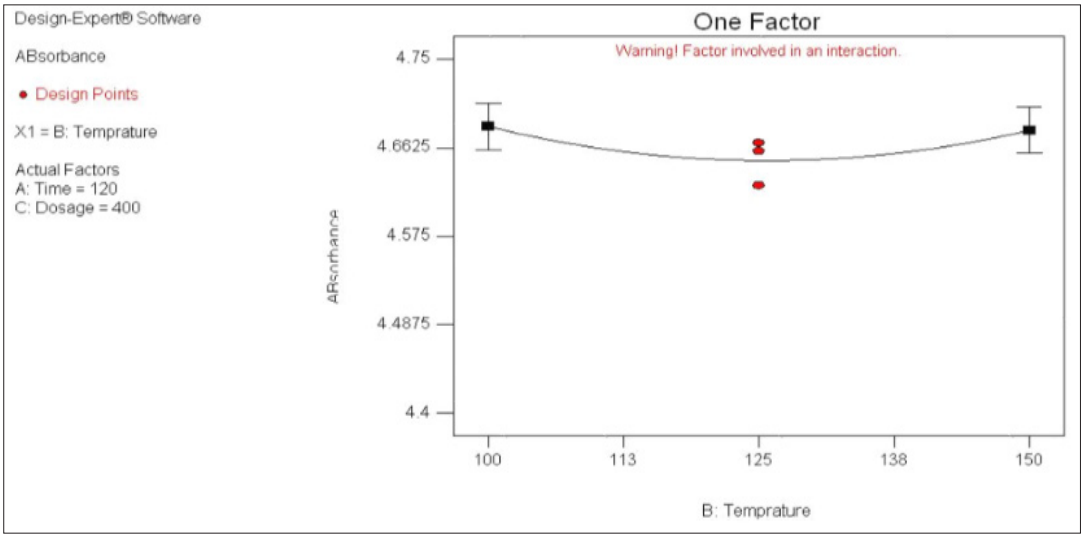

Fig. 11 .The effect of reaction temperature on oil color by MCM-41

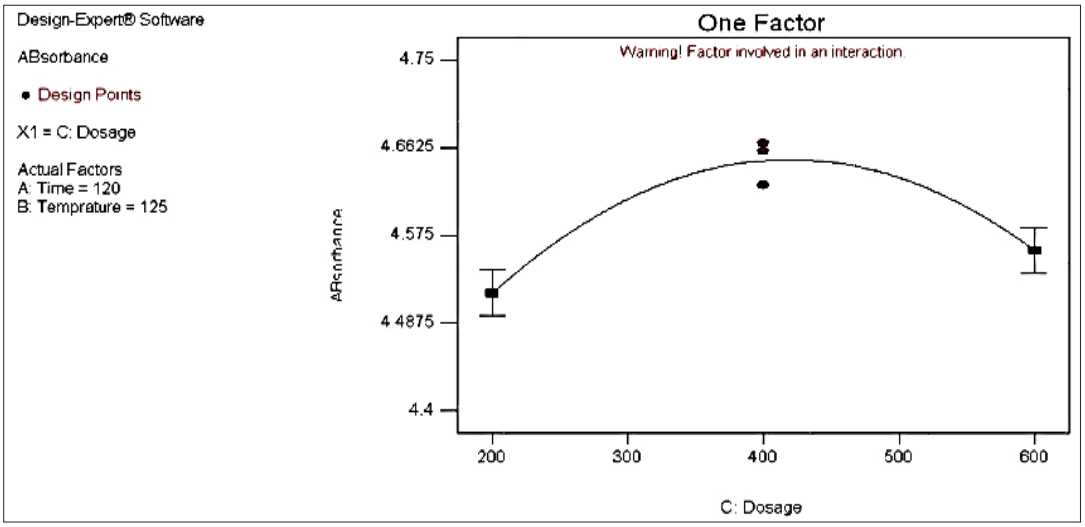

Fig. 12. The effect of dosage on oil color by MCM-41

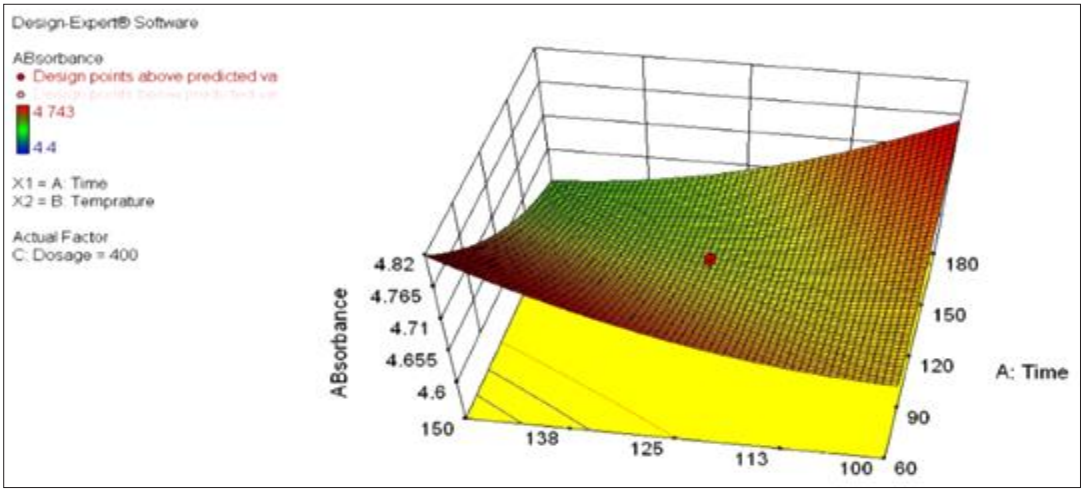

Fig. 13. The effect of interaction factors sodium metallic contact time and reaction temperature it on oil color by MCM-41

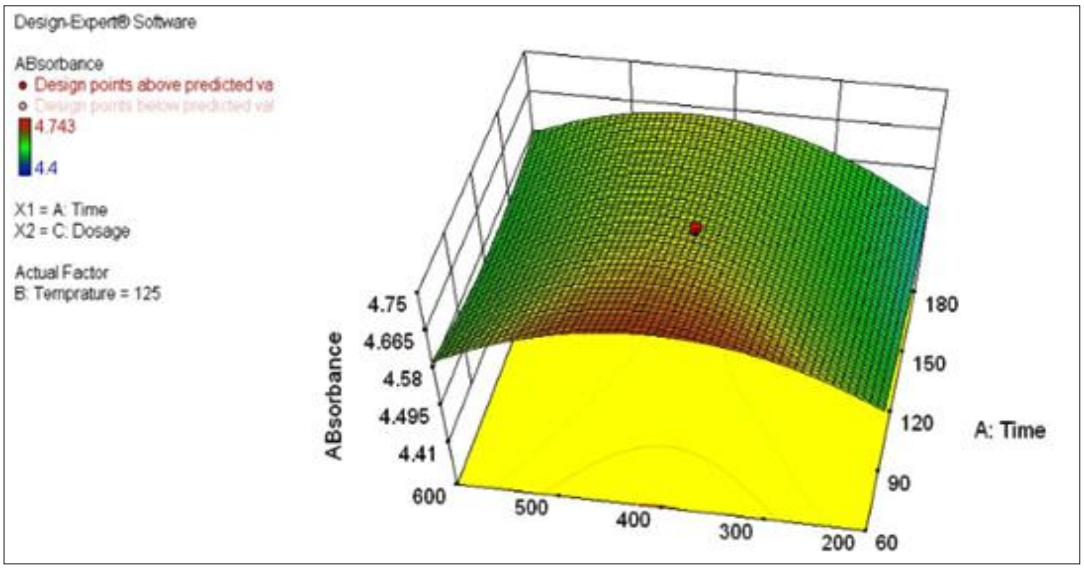

Fig. 14. The effect of interaction factors sodium metallic contact time and dosage(sodium to oil ratio) on color oil by MCM-41

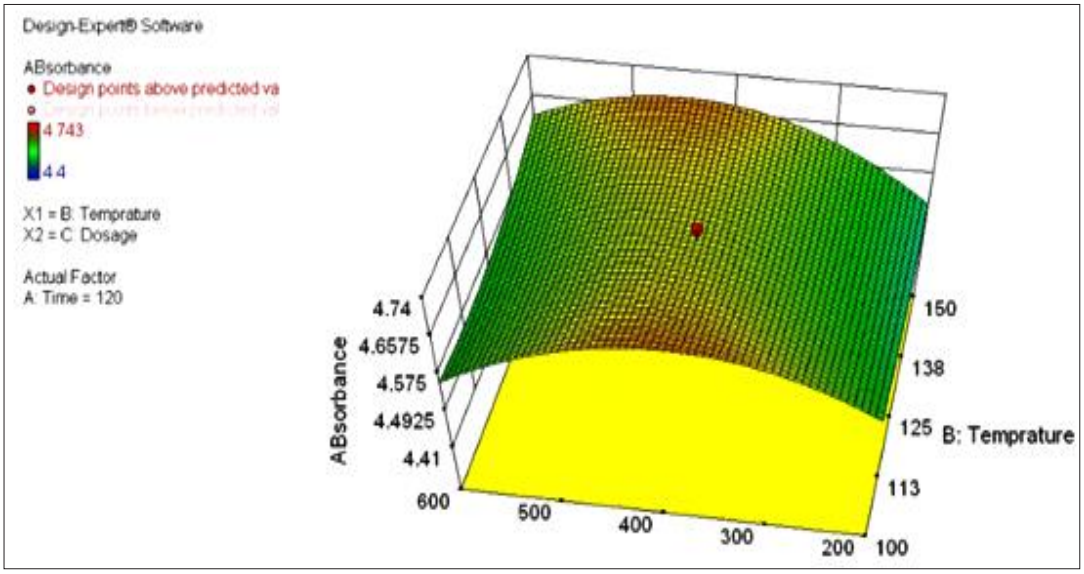

Fig. 15. The effect of interaction factors sodium metallic reaction temperature and dosage (sodium to oil ratio) on oil color by MCM-41

of AB, AC and BC. The curvature of the model was due to these terms. All main factors had interaction with each other.

4. Conclusions

In this research, we studied re-refining of used insulating oil by metallic sodium and mesoporous silicate containing aluminum. This method combines to adsorption and reduction of oxide species. The effective factors including time, temperature and dosage of sodium was statistically studied by ANOVA. The adsorption of mesoporous silica was also studied by this way. Based on proposed procedure, the modeling was carried out.

Treating of oil with mesoporous silicate after using metallic sodium causes lower color of oil. Treating of oil by adsorption using MCM-41 followed by reduction with metallic sodium is somehow better in final quality of oil. This method is very effective for re-refining of isolation oil which is very important in the industry. Higher temperature results in better quality of product because of higher activity of sodium and oxidant species and also better diffusion of these species to the surface of active sites of sodium and mesoporous silica. Aluminosilica is more polar than silica because of its higher aluminum. But due to the higher acidic nature of the surface of aluminosilica, it is weaker adsorbent for the removal of acidic species from the oil.

5. References

[1] A. Hamada, E. Alzubaidy, M. Fayed, Used lubricating oil recycling using hydrocarbon solvents, J. Evnviron. Manage., 74 (2005) 153-159.

[2] D. I. Osman, S. K. Attia, A. R.Taman, Recycling of used engine oil by different solvent, Egyptian J. Petrol., 27 (2018) 221-225.

[3] R. Abro, X. Chen, K. H. Harijan, Z.A. Dhakan, M. Ammar, A comparative study of recycling of used engine oil using extraction by composite solvent, single solvent, and acid treatment methods, Int. Sch. Res. Notices, 2013 (2013) 952589.

[4] J.A. Filho, L.G.M.M. Moura, A.C.S. Ramos, Liquid-liquid extraction and adsorption on solid surfaces applied to used lubricant oils recovery, Brazilian j. chem. Eng., 10 (2014) 687-697.

[5] T. Colclough, Role of additive and transition metalin lubricanting oil oxidation, Ind. Eng. Chem. Res., 26 (1987)1888-1895.

[6] K. Satish E. Klaus, L. Duda, Evaluation of liquid phase oxidation products of ester and minaral oil lubricants, Ind. Eng. Chem. Prod, Res. Dev., 23 (1984) 613-619.

[7] S. Bustamante, M. Manana, Dissolved gas analysis equipment for online monitoring of transformer oil: a review, Sensors, 19 (2019) 4057.

[8] Survey of currently available non-Incineration PCB destruction technologies, UNEP Chemical, 2000.

[9] R. Abu-Elella, M.E. Abu, R. Ossman, M. F. Abd-Elfatah, Used motor oil treatment: turning waste oil into valuable products, Int. J. Chem. Biochem. Sci., 7 (2015) 57-67.

[10] MO. Aremu, DO. Araromi, OO. Gbolahan, Regeneration of used lubricating engine oil by solvent extraction process, Int. J. Energy Environ. Res., 3 (2015) 1-12.

[11] M.E. Emetere, Investigations on aerosols transport over micro-and macro-scale settings of west Africa, Environ. Eng. Res., 22 (2017) 75-86.

[12] H. Mensah-Brown, Re-refining and recycling of used lubricating oil: an option for foreign exchange and natural resource conservation in Ghana, J. Eng. Appl. Sci., 10 (2015) 797-801

[13] S.S. Lam, K.K. Liewa, A.A. Jusoh C.T. Chong F.N. Ani, H.A. Chase, Progress in waste oil to sustainable energy, with emphasis on pyrolysis techniques, Renew. Sust. Energ. Rev., 53 (2016) 741–753.

[14] T.E. Oladimeji, J.A. Sonibare, J. A. Omoleye, A.A. Adegbola, H. Okagbue, Data on the treatment of used lubricating oil from two different sources using solvent extraction and adsorption, Data in Brief, 19 (2018) 2240–2252.

[15] R. Maceiras, V. Alfonsín, F.J. Morales, Recycling of waste engine oil for diesel production, Waste Manage., 60 (2016) 351-356.

[16] S. Shiung Lam, R. Keey Liewa, A. Jusoh, C.T. Chong, F. Nasir Ani, H.A. Chase, Progress in waste oil to sustainable energy, with emphasis on pyrolysis techniques, Renew. Sust. Energ. Rev., 53 (2016)741–753.

[17] S. Salem, A. Salem, A. A. Babaei. Application of Iranian nano-porous Ca-bentonite for recovery of waste lubricant oil by distillation and adsorption techniques, J. Ind. Eng. Chem., 23 (2015)154–162.

[18] Standard Test Method for Acid and Base Number by color –Indicator Titratian-D947-04.

[19] J.M. Morales, A. Moragues, J.E.l. Haskouri, C. Guillem, J. Latorre, S. Murcia-Mascarós, A. Beltrán, D. Beltrán, P. Amorós, Low-Cost synthesis of bimodal mesoporous silica-based materials by pseudomorphic transformation, Chem. Plus chem., 80 (2015)1014-1028.

[20] R.J. With, R. Luque, V.L. Budarin, J.H. Clark, J.D. Macquarrie, Supported metal nanoparticles on porous materials nethods and applications, Chem. Soc. Rev., 38 (2009) 481-494.

[21] Y.D. Chiang, H.Y. Lian, S.Y. Leo, S.G. Wang, Y. Yamauchi, Controlling particle size and structural properties of mesoporous silica nanoparticles using the Taguchi method, J. Phys. Chem. C, 115 (2011) 13158-65.

[22] P. Swan , R. Walker , B. Wopenka, J. Freeman, Absorption in interplanetary dust particles: evidence for indigenous hydrocarbons and a further link to comet halley, Meteoritics, 22 (1987) 510-511.

[23] A. Zhang , Z. Li ,Y. Shen ,Y. Zhu , Effects of different Ti-doping methods on the structure of pure silica MCM-41 mesoporous materials, Appl. Surf. Sci., 254 (2008) 6298-304.

Anal. Method Environ. Chem. J. 3 (1) (2020) 41-48

AMECJ

Research Article, Issue 1

Analytical Methods in Environmental Chemistry Journal

Journal home page: www.amecj.com/ir

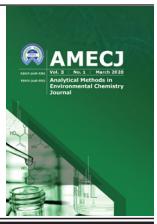

Speciation of arsenic in wastewater samples based on pyributicarbamate /ionic liquids by dispersive liquid-liquid microextraction

Nafiseh Esmaeili[a], Nadia Kokabi[a], and Eskandar Kolvari[a,*]

[a]*Department of chemistry, Faculty of Science, Semnan University, Semnan, Iran*

ARTICLE INFO:

Received 6 Dec 2019

Revised form 30 Jan 2020

Accepted 15 Feb 2020

Available online 28 Mar 2020

Keywords:

Arsenic, Speciation,
Wastewater,
Pyributicarbamate,
Task specific Ionic liquid,
Dispersive liquid-liquid microextraction

ABSTRACT

A simple and applied method based on O-3-Tert-butylphenyl N-(6-methoxy-2-pyridyl)-N-methylthiocarbamate (Pyributicarbamate; TBMPMTC) was used for arsenic speciation (As_{III} and As_{V}) in urine and water samples by dispersive liquid-liquid microextraction (DLLME) procedure. The concentrations of arsenic in the liquid phase were determined by hydride generation atomic absorption spectrometry in the presence of flame accessory (HG-AAS). By procedure, a mixture of ionic liquid (0.1 g, [APMIM][PF6]@[HMIM][PF_6]), acetone (0.2 mL) and pyributicarbamate was injected into wastewater sample containing arsenic (As_{III} and As_{V}) ions, which were already extracted by pyributicarbamate at the optimized pH. The task-specific ionic liquid (TSIL) of 1-3-aminopropyl)-3-methyl-imidazoliumhexafluorophosphate [APMIM][PF6] was chemically synthesized and used for increasing of As(V) extraction in the liquid phase. As(III) was extracted based on the sulfur bond of pyributicarbamate at pH=5.3. As (V) can be extracted by amine group of TBMPMTC and [APMIM][PF6] at pH=3.0 (As(V)---:NH2). The influence of parameters such as, pH, amount of ionic liquid, and ligand was studied. Based on results, the LOD, enhancement factor (EF) and linear range (LR) were obtained 3.2 ngL^{-1}, 9.85 and 0.01-1.2 $\mu g\ L^{-1}$, respectively. The procedure validated by certified reference material (CRM).

1. Introduction

The toxicities of heavy metals in waters cause to main problem in humans and environment and cannot be biodegraded as VOCs. The factories and chemical activity are real source of heavy metals such arsenic which can entrance to environment and caused different disease in humans such as, renal, liver and brain [1]. The most of arsenic in waters has two forms As(III) and AS(V). The arsenic concentration in waters has generally ranged between 1 and 2 $\mu g\ L^{-1}$. Water in volcanic rock and sulfide mineral has high levels about 12 $mg\ L^{-1}$. Mean arsenic concentrations in sediment the mean of As has ranges from 5 to 3000 $mg\ kg^{-1}$ [2, 3]. The occupational exposure and oral intake (food and water) of arsenic are the most important route in humans. The mean daily intake of arsenic from drinking water to human body must be less than 10 µg. By increasing of arsenic concentration in waters, dangerous diseases created in human body after drink waters for many times. Many changes in CNS and peripheral nervous system (PNS) such as, tenderness and vomiting headaches occurred for arsenic exposure. Liver and renal may moved to cancer problem as different toxicity and

* Corresponding author: Eskandar Kolvari
Email: kolvari@semnan.ac.ir
https://doi.org/10.24200/amecj.v3.i01.93

oxidation state of arsenic [4-7]. Different analytical procedure used for arsenic determination of speciation/determination in water samples. A few of them only determination without speciation such as graphite furnace atomic absorption spectrometry (GF-AAS) [8], Flame atomic absorption spectrometry (F-AAS) [9], hydride generation atomic absorption spectrometry (HG-AAS) [10], capillary electrophoresis with inductively coupled plasma-mass spectrometry (CE-ICP)[11] and arsenic species can be determined with ion chromatography coupled to inductively coupled plasma mass spectrometry (IC-ICP-MS)[12]. As low concentration of arsenic species in waters (sub ppb), sample preparation must be used before instrumental analysis. Recently, solid-phase extraction (SPE) based on nanomaterials was used to improve the extraction procedure. For this purpose, many carbon structure such as, modified activated carbon [13], carbon nanotubes [14], and alumina supported on graphene oxide [15], were reported by researchers. In addition, the liquid-liquid extraction technique (LLE) and dispersive liquid-liquid microextraction (DLLME) was used for extraction analyte from liquid phase based on ligand by immiscible solvents or ionic liquid which was directly immersed in water samples and dispersed by acetone [16-22]. The organic solvents such as tetrachloride carbon are toxic. Therefore, the ionic liquids (ILs) as green solvents have used as extracting solvent. ILs has many advantages as compared to organic solvents, such as favorite vapor pressure, viscosity and density. Therefore, ILs have used as benign solvent in DLLME procedure.

In this study, a new procedure based on TBMPMTC -DLLME coupled to HG-AAS for the speciation and determination of trace amount of As (III) and As (V) in wastewater samples at pH of 5.3 and 3.0, respectively. Flame conditions with 1.2 $Lmin^{-1}$ fuel and minimum flow air have used.

2. Experimental

2.1. Apparatus

The experiments were performed using a GBC-932 atomic absorption spectrometer equipped with a hydride generation module (HG3000-AAS -AUS). A hollow cathode lamp operated at a current of 8 mA and a wavelength of 193.7 nm with a spectral band width of 1 nm and deuterium background corrector was applied. The deuterium-lamp background corrector, As hollow-cathode lamp, and a circulating reaction loop was used for arsenic determination.

The instrument conditions of HG-AAS have showed in Table 1. The pH values of the solutions have adjusted by a digital pH meter (Metrohm 744, Herisau, Switzerland). A Hettich centrifuge (model EBA 20, Germany) and an ultrasonic bath with heating system (Tecno-GAZ SPA, Italy) have used.

Table 1. The instrumental parameters for analysis of arsenic

Features	Value
Precision (%RSD, N=10)	1.4
LOD	3.5 µg L^{-1}
Linear range, PA	0.1 – 10.3 µg L^{-1}
Wavelength	193.7 nm
Spectral band width	1 nm
Lamp current	8 mA
Correlation coefficient	R = 0.9997

PA = Peak Area, PH = Peak Height

2.2. Reagents and Materials

All the reagents were of analytical grade. Arsenic standard solutions were prepared from a stock solution of 1000 mg L^{-1} as ultra trace in 2% nitric acid from Fluka Switzerland (CAS N: 39436). Arsenic (V) oxide prepared from Sigma, Germany (As_2O_5; CAS N: 1303-28-2). The powder of O-3-Tert-butylphenyl N-(6-methoxy-2-pyridyl)-N-methylthiocarbamate (pyributicarbamate; TBMPMTC) purchased from Sigma which was prepared daily by DW ($C_{18}H_{22}N_2O_2S$; CAS N: 88678-67-5, Germany). 1-Hexyl-3-methylimidazolium hexafluorophosphate ($C_{10}H_{19}F_6N_2P$; CID 2734175; [HMIM][PF_6]) was purchased from Sigma, Germany. The ionic liquid of 1-(3-aminopropyl)-3-methyl-imidazoliumhexafluorophosphate [APMIM][PF6] synthesis in center of organic chemistry in Semnan University, Iran. Sodium acetate /acetic as buffer solutions for pH 3–6 was

prepared from Sigma, Germany (1.5 mol L^{-1}). Ultrapure water has obtained from a water system of RIPI. The plastic, vials and glasses equipments were cleaned by soaking in HNO_3 (1 M) and were rinsed with deionized water for 10 times prior to use.

2.3. Sampling

Drinking and river water samples were collected paint and chemical wastewaters from Iran. These samples were immediately acidified with 0.1% of concentrated HCl which provided a pH lower than 2. The samples have then filtered in the laboratory using a pore membrane filter (0.45 µm, Macherey-Nagel, PTFE) to remove suspended solids.

2.4. Synthesis of [APMIM][PF6]

As reported by Hu and Yeon, the procedure of synthesis of [APMIM][PF6], was done by center of organic chemistry, Semnan. For this purposed methylimidazole and bromopropylammonium bromide ($C_3H_9Br_2N$) dissolved in acetonitrile in boiling flasks with magnetic stirrer and refluxed at 90°C. Finally, the solution of [APMIM][Br] was obtained. After cooling, the KPF6 (10 g) added to 20 mL of DW) and after 24 h, the solvents were separated and the ionic liquid was removed by extraction in methanol/chloroform. The suspension was then filtered and washed with diethyl ether (10 times) to remove impurities [23, 24].

2.5. Procedure

After synthesis of [APMIM][PF6], the procedure followed by 0.5 mL of TBMPMTC solution (2%, w/w), 0.1 g of 1-Hexyl-3-methylimidazolium hexafluorophosphate in acetone solution (0.2 mL) which was mixed and injected to 10 mL of sample solution containing As(III)/As(V). The cloudy solution has shaken with a vortex for 5 min and pH adjusted up to 5.3 based on favorite buffer solutions. Then, the arsenic (III) was efficiently extracted (As-:SR) in [APMIM][PF6] @ [HMIM]

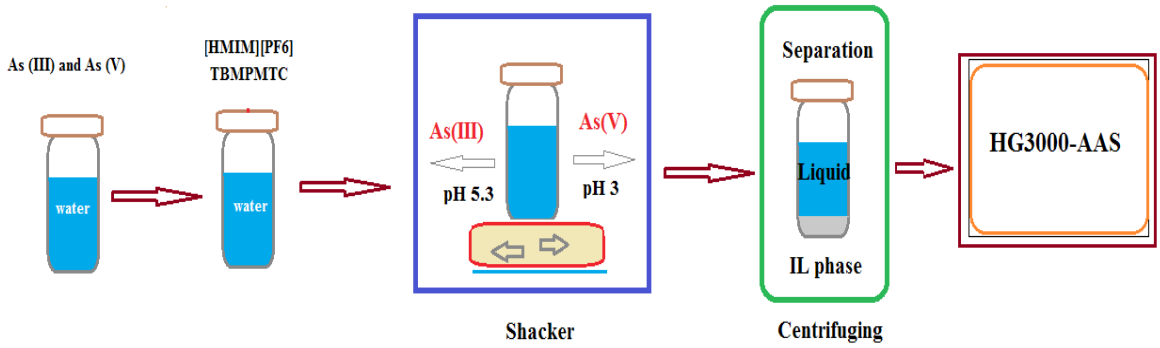

Fig. 1. The procedure for speciation of arsenic in wastewater samples based on pyributicarbamate /ionic liquids

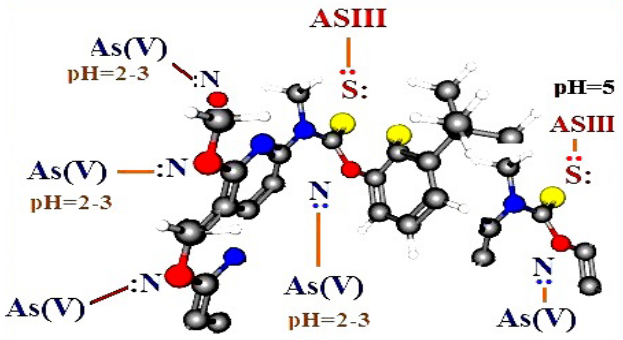

Fig. 2. The mechanism of extraction of As(III) and As(V) based on TBMPMTC by DLLME procedure

[PF_6]. Finally, the IL separated in conical tube by centrifuging accessory for 7 min at 4000 rpm. The water sample removed from upper phase, arsenic (III) back extracted from IL with 0.25 mL of nitric acid solution (0.5M) in lower phase, dilution with DW up to 1 mL and determined by HG-AAS. As(V) was also extracted with same procedure in pH=3.0 by mixture of TBMPMTC/[APMIM][PF6]@[HMIM][PF_6]. Total As was calculated by summarizing of As(III) and As(V) which was shown in Figure 1. In addition, the mechanism of proposed procedure has presented in Figure 2.

3. Results and Discussion

Analytical conditions for HG-AAS determination have optimized in this work. Absorption (S/N) and repeatability that were investigated for speciation and determination As(III) and As(V) in wastewater samples in paint factories and chemical industries by HG-AAS. In view of the possibility of As extraction with TBMPMTC, this ligand was used to chelated of arsenic in ionic liquids phase. All conditions such as pH, amount of Il, amount of TBMPMTC, sample volume and shaking time were optimized by DLLME procedure.

3.1 Effect of pH

The complexation phenomenon has strongly conditioned by the pH of solutions and subsequently affects on the extraction efficiency of the As_{III}-SR and As_V-SR. For this reason, the pH between 2-10 was examined for As (III) and As(V) in water samples by DLLME method. Two groups of ligands include N and S bonding have important role in speciation arsenic in liquid phase when pH optimized. Based on solubility and charge of ions, they can be extracted by bonding group of TBMPMTC. The results showed, As (III) extracted with sulfur group of TBMPMTC at pH=4.8-5.5 and As (V) captured by amine group of TBMPMTC/[APMIM][PF6] at pH=2.5-3.2. S0, pH of 3.0 and 5.0 was selected as optimum pH in this study (Fig.3). The pH adjustments of samples were made using nitric acid (0.1 mol L^{-1}) for pH 1-2, and appropriate buffer solutions including sodium acetate (CH_3COONa/CH_3COOH, 1-2 mol L^{-1}) for pH 3.75-5.75, sodium phosphate (Na_2HPO_4/NaH_2PO_4, 0.2 mol L^{-1}) for pH of 5.8-8.0, and ammonium chloride (NH_3/NH_4Cl, 0.2 mol L^{-1}) for pH 8-10.

3.2. Effect of amount of TBMPMTC

It is important to establish the favorite concentration of ligand for arsenic extraction with high recovery as shown in Figure 4. The different concentration of TBMPMTC was used for optimization of arsenic extraction from 0.5 -50 micro molar. The results showed that the 17 micro molar has

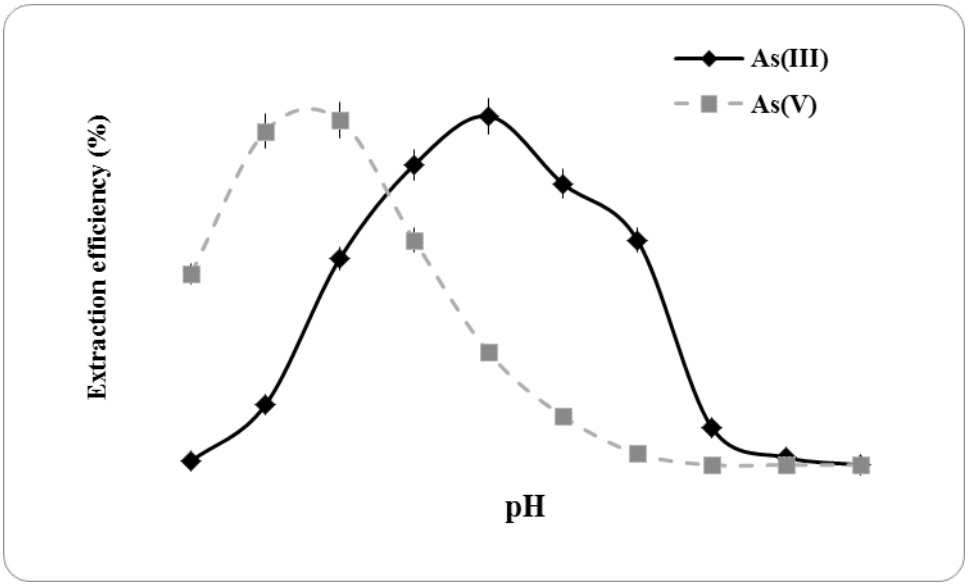

Fig. 3. The effect of pH on arsenic speciation based on TBMPMTC by DLLME procedure

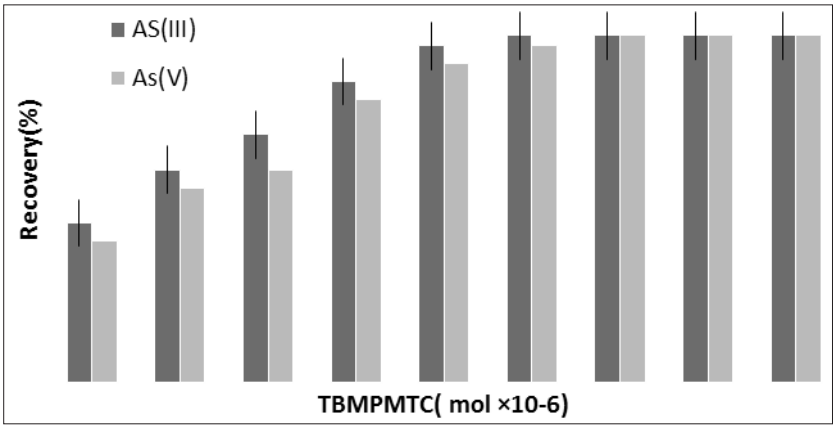

Fig. 4. The effect of amount of TBMPMTC on arsenic speciation by DLLME procedure

maximum recovery for arsenic (III, V) extraction from wastewater samples by DLLME. Based on statistical report in analytical chemistry the minimum ligand concentration was necessary to use with maximum extraction efficiency. So, the 20 micro molar selected as optimum concentration by proposed procedure.

3.3. Effect of amount of ionic liquid

The amount of ionic liquid as green organic solvent for extraction of arsenic in wastewaters must be optimized by DLLME. For this purpose, the different mass and kind of ionic liquid was studied. The results showed [HMIM][PF_6] have more extraction as compared to others ([BMIM][PF_6], [EMIM][PF_6], [MMIM][PF_6]). So, the 0.05-0.2 g of [HMIM][PF_6] examined by procedure. The quantitative extraction was observed for more than 0.08 g of [HMIM][PF_6] and therefore, 0.1 g of [HMIM][PF_6] was chosen as optimum IL for further works (Fig. 5). The [APMIM][PF6] had no effect on separation process but helped to increase efficiency extraction of As(V) from liquid phase.

3.4. Effect of sample volume and elution

The effect of sample volume was examined in a range of 1-20 mL for µg L^{-1} As (III) and As(V). The quantitative extraction has observed less than15 mL wastewaters. So, 10 mL of sample volume was selected in optimum conditions. The acid concentrations were used in order to obtain the maximum extraction with the minimal concentration and volume of the acid solution. The presented DLLME method based on the elution of arsenic species from IL phase with a mineral acidic solution achieved. Low pH leads to dissociation and releasing of As (III) and As(V) into the aqueous phase. So, 100-500 µL of different mineral

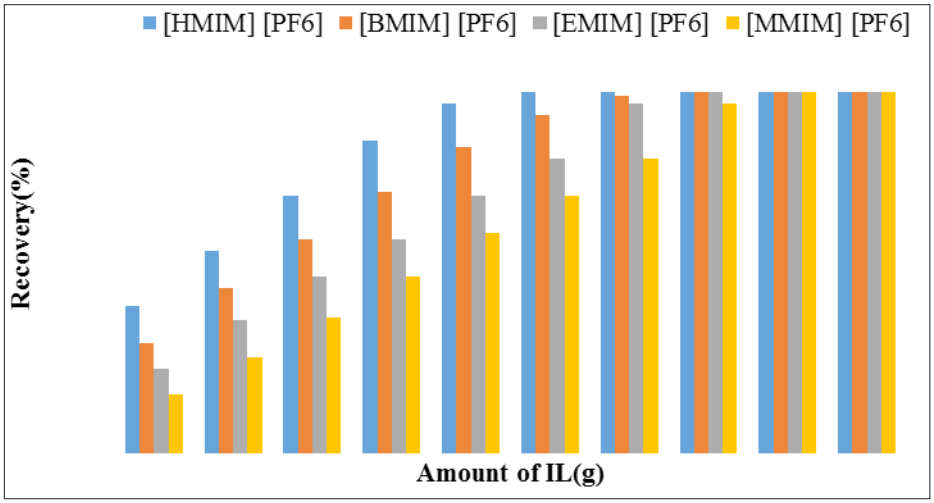

Fig. 5. The effect of amount of ionic liquid on arsenic speciation based on TBMPMTC by DLLME procedure

acids such as HCl, HNO_3, H_2SO_4 and H_3PO_4 (0.1-1 mol L^{-1}) were examined. The results showed that 0.5 mol L^{-1} HNO_3 (250 µL) quantitatively back-extracted arsenic from IL.

3.5. Effect of dispersion time

Dispersion is the main factor in arsenic extraction by DLLME method and so, allows the direct contact of the analytes with TBMPMTC ligand and then extracted. Due to the dispersion of TBMPMTC/ILs into the aqueous phase, the mass-transference phenomenon was obtained with high efficiency in short time. The influence of the shaking time was studied within the 1–5 min. The results showed that the relative response increased at 4 min and then remained constant. So, 5 min was chosen as favorite time as shaking. By centrifuging, the extraction was accelerated for phase separation between IL and liquid phase. The different times for centrifuging were tested from 2 to 10 min at 4000 rpm. The result showed that 5 min centrifugation time was sufficient to get a satisfactory biphasic system.

Table 2. The effect of interferences ions on extraction of As (III) and As (V) in water samples by DLLME procedure

Interfering Ions (M)	Mean ratio (C_M /$C_{As(III)}$)	Recovery (%)
Ni^{2+}, Co^{2+}, Cd^{2+}	600	96.9
Mn^{2+}, Cu^{2+}, Zn^{2+}	900	98.7
I^- , Br^-, F^-, Cl^-	1100	99.2
Na^+, K^+, Ca^{2+}, Mg^{2+}	900	98.2
NO_3^-, Cl^-, F^-, CO_3^{2-}	1200	97.4
Hg^{2+}	100	95.5
NH_4^+, SO_4^{2-}	400	96.8
Pb^{2+}	250	97.3
Interfering Ions (M)	**Mean ratio (C_M /$C_{As(V)}$)**	**Recovery (%)**
Ni^{2+}, Co^{2+}, Cd^{2+}	500	96.9
Mn^{2+}, Cu^{2+}, Zn^{2+}	800	98.7
I^- , Br^-, F^-, Cl^-	900	99.2
Na^+, K^+, Ca^{2+}, Mg^{2+}	900	98.2
NO_3^-, Cl^-, F^-, CO_3^{2-}	1200	97.4
Hg^{2+}	200	95.5
NH_4^+, SO_4^{2-}	500	96.8
Pb^{2+}	300	97.3

3.6. Interference of coexisting ions

As efficient analytical procedure in water samples, the interference of some coexisting ions was investigated in optimized condition. By DLLME procedure, the different concentration of the interfering ions added to 10 mL of standard sample solution containing 1.0 µg L^{-1} of As (III) and As (V). The results showed that most of concomitant ions have no effect on the extraction efficiencies of As (III) and As (V) at the optimized pH. The tolerable concentration ratio of metals per As (III) and As (V) for Ni^{2+}, Co^{2+}, Cd^{2+}, Mn^{2+}, Cu^{2+}, Zn^{2+}, K^+, Na^+, Pb^{2+}, Hg^{2+}, NO_3^-, Cl^-, F^-, CO_3^{2-} and SO_4^{2-} was obtained in water samples (Table 2).

3.7. Validation

The DLLME method based on TBMPMTC as a ligand was used for determination of As (III) and As (V) in 10 mL of wastewater and water samples by HG-AAS. The results were verified by spiking water samples with nickel standard solution. Based on results, the acceptable recovery was achieved by adding standard solution (As (III) and As (V) to real samples as a found analyte amount. The recoveries of spiked samples were 95-103% by DLLME methods (Table 3). Wastewaters of a chemical factory (A), a paint factory (B), well water (C), and drinking water (D) were selected as real samples which were used by procedure. The results demonstrated that TBMPMTC-DLLME can used for speciation of As (III) and As (V) in wastewater, and water samples which were determined by HG-AAS. In addition, the certified reference material (CRM, NIST 2670) was used for validation As (III) and As (V) in urine samples by TBMPMTC-DLLME (Table 4).

4. Conclusions

The procedure has many advantage such as simplicity, reliability and high extraction efficiency in short time for arsenic speciation based on TBMPMTC-DLLME by sensitive HG-AAS technique. By improving the procedure, the favorite and acceptable preconcentration/separation/speciation of the trivalent and pentavalent inorganic

Table 3. Speciation and determination of As (III) and As (V) in spiked water samples by TBMPMTC-DLLME method

	[a]Added (µg L^{-1})		[a]Found (µg L^{-1})			Recovery (%)	
Sample	As (III)	As (V)	As (III)	As (V)	Total	As (III)	As (V)
A	------	------	0.432 ± 0.023	0.266 ± 0.014	0.698 ± 0.037	------	------
	0.4	------	0.827 ± 0.043	0.262 ± 0.015	1.089 ± 0.052	98.8	------
	------	0.3	0.435 ± 0.022	0.568 ± 0.028	1.003 ± 0.049	------	100.6
B	------	------	0.501 ± 0.023	0.197 ± 0.011	0.698 ± 0.034	------	------
	0.5	-----	0.993 ± 0.048	0.195 ± 0.009	1.188 ± 0.057	98.4	------
	-----	0.3	0.498 ± 0.024	0.504 ± 0.026	1.002 ± 0.055	------	102.3
C	------	------	0.102 ± 0.006	0.068 ± 0.003	0.170 ± 0.009	------	------
	0.1	-----	0.203 ± 0.009	0.064 ± 0.003	0.267 ± 0.012	101.0	------
	-----	0.1	0.098 ± 0.005	0.165 ± 0.013	0.263 ± 0.018	------	97
D	------	------	0.032 ± 0.001	ND	0.032 ± 0.001	------	------
	0.05	------	0.081 ± 0.004	ND	0.081 ± 0.004	98	------
	------	0.05	0.030 ± 0.001	0.002 ± 0.048	0.078 ± 0.003	------	96

[a]Mean of three determinations ± Confidence interval (P = 0.95)

Table 4. Method validation for speciation of arsenic based on TBMPMTC-DLLME by standard reference material (ng L^{-1})

	Certified value	Certified value	*Found	*Found	Recovery	Recovery
sample	As (III)	As (V)	As (III)	As (V)	As (III) (%)	As (V) (%)
CRM	833.3	500.0	827.4 ± 45.6	488.7 ± 24.6	99.3	97.7
Added	400.0	------	1209.8 ± 58.5	482.3 ± 26.3	95.6	------
Added	------	500.0	831.2 ± 51.2	990.2 ± 47.7	------	100.3

[a]NIST CRM 2670, Arsenic in frozen dried urine, pH 4.0, - 20°C, diluted with DW(1:3)
[b]Mean of three determinations ± confidence interval (P = 0.95)

forms of arsenic was achieved as alternative to HPLC-ICP-MS. The results showed the quantitative recovery more than 96% and EF of 9.85 as curve fitting analysis for As(III) /As(V) were obtained at pH of 5.0 and 3.0, respectively. If the ionic liquid of [APMIM][PF6] as TSIL wasn't used, the recovery obtained up to 73% for As(V) in optimized conditions. The certified reference material and spiking real samples showed the high accuracy and precisions results which were agreement with the certified values. In DLLME procedures, the satisfactory results based on TBMPMTC ligand was achieved for arsenic species in wastewater samples.

5. References

[1] R. Dixit, D. Malaviya, K. Pandiyan, U.B. Singh, A. Sahu, R. Shukla, B.P. Singh, J.P. Rai, P.K. Sharma, H. Lade, Bioremediation of heavy metals from soil and aquatic environment: an overview of principles and criteria of fundamental processes, Sustainability, 7 (2015) 2189-2212.

[2] R. Nickson, J. McArthur, W. Burgess, K.M. Ahmed, P. Ravenscroft, M. Rahmanñ, Arsenic poisoning of Bangladesh groundwater, Nat., 395 (1998) 338-338.

[3] M. Tuzen, K.O. Saygi, I. Karaman, M. Soylak, Selective speciation and determination of inorganic arsenic in water, food and biological samples, Food Chem. Toxicol., 48 (2010) 41-46.

[4] V.M. Nurchi, A.B. Djordjevic, G. Crisponi, J. Alexander, G. Bjørklund, J. Aaseth, Arsenic toxicity: Molecular targets and therapeutic agents, Biomolecul., 10 (2020) 235.

[5] M. Molin, S.M. Ulven, H.M. Meltzer, J. Alexander, Arsenic in the human food chain, biotransformation and toxicology–Review focusing on seafood arsenic, J. Trace Elem. Med. Biol., 31 (2015) 249-259.

[6] A. Emadi, S.D. Gore, Arsenic trioxide—an old drug rediscovered, Blood Rev., 24 (2010) 191-199.

[7] C.M. George, L. Sima, M. Arias, J. Mihalic, L.Z. Cabrera, D. Danz, W. Checkley, R.H.

Gilman, Arsenic exposure in drinking water: an unrecognized health threat in Peru, Bull. World Health Org., 92 (2014) 565-572.

[8] A.Q. Shah, T.G. Kazi, J.A. Baig, M.B. Arain, H.I. Afridi, G.A. Kandhro, S.K. Wadhwa, N.F. Kolachi, Determination of inorganic arsenic species (As3+ and As5+) in muscle tissues of fish species by electrothermal atomic absorption spectrometry (ETAAS), Food chem., 119 (2010) 840-844.

[9] C. Zeng, Y. Yan, J. Tang, Y. Wu, S. Zhong, Speciation of Arsenic (III) and Arsenic (V) based on Triton X-100 hollow fiber liquid phase microextraction coupled with flame atomic absorption spectrometry, Spect. Lett., 50 (2017) 220-226.

[10] M. Welna, P. Pohl, Potential of the hydride generation technique coupled to inductively coupled plasma optical emission spectrometry for non-chromatographic As speciation, J. Anal. Atomic Spect., 32 (2017) 1766-1779.

[11] L. Liu, Z. Yun, B. He, G. Jiang, Efficient interface for online coupling of capillary electrophoresis with inductively coupled plasma–mass spectrometry and its application in simultaneous speciation analysis of arsenic and selenium, Anal. Chem., 86 (2014) 8167-8175.

[12] S.H. Son, W.B. Lee, D. Kim, Y. Lee, S.H. Nam, An alternative analytical method for determining arsenic species in rice by using ion chromatography and inductively coupled plasma-mass spectrometry, Food Chem., 270 (2019) 353-358.

[13] R. Sawana, Y. Somasundar, V.S. Iyer, B. Baruwati, Ceria modified activated carbon: an efficient arsenic removal adsorbent for drinking water purification, Appl. Water Sci., 7 (2017) 1223-1230.

[14] A. Naghizadeh, A.R. Yari, H.R. Tashauoei, M. Mahdavi, E. Derakhshani, R. Rahimi, P. Bahmani, H. Daraei, E. Ghahremani, Carbon nanotubes technology for removal of arsenic from water, Arch. Hyg. Sci., 1 (2012) 6-11.

[15] A. Baranik, A. Gagor, I. Queralt, E. Marguí, R. Sitko, B. Zawisza, Determination and speciation of ultratrace arsenic and chromium species using aluminium oxide supported on graphene oxide, Talanta, 185 (2018) 264-274.

[16] J. Ali, M. Tuzen, T.G. Kazi, Determination of Total Arsenic in Water and Food Samples by Pressure-induced Ionic Liquid-based Dispersive Liquid-Liquid Microextraction Method Prior to Analysis by Hydride Generation Atomic Absorption Spectrometry, Atomic Spect., 38 (2017) 57-64.

[17] X. Wang, G. Xu, P. Chen, Y. Sun, X. Yao, Y. Lv, W. Guo, G. Wang, Fully-automated magnetic stirring-assisted lab-in-syringe dispersive liquid–liquid microextraction for the determination of arsenic species in rice samples, RSC Adv., 8 (2018) 16858-16865.

[18] E.F. Fiorentini, B.V. Canizo, R.G. Wuilloud, Determination of As in honey samples by magnetic ionic liquid-based dispersive liquid-liquid microextraction and electrothermal atomic absorption spectrometry, Talanta, 198 (2019) 146-153.

[19] H Shirkhanloo, M Ghazaghi, MM Eskandari, Cloud point assisted dispersive ionic liquid-liquid microextraction for chromium speciation in human blood samples based on isopropyl 2-[(isopropoxycarbothiolyl) disulfanyl, Anal. Chem. Res., 10 (2016)18-27.

[20] H Shirkhanloo, A Khaligh, HZ Mousavi, MM Eskandari, AA Miran-Beigi, Ultra-trace arsenic and mercury speciation and determination in blood samples by ionic liquid-based dispersive liquid-liquid microextraction combined with flow injection, Chem. Papers, 69 (2015) 779-790.

[21] H Shirkhanloo, ZH Mousavi, A Rouhollahi, Preconcentration and determination of heavy metals in water, sediment and biological samples, J. Serb. Chem. Soc., 76 (2011) 1583-1595.

[22] H Shirkhanloo, AAM Beigi, MM Eskandari, B Kalantari, Dispersive liquid-liquid microextraction based on task-specific ionic liquids for determination and speciation of chromium in human blood, J. Anal. Chem., 70 (2015) 1448-1455

[23] Q. Hu, J. Zhao, F. Wang, F. Huo, H. Liu, Selective extraction of vanadium from chromium by pure [C8mim][PF6]: An anion exchange process, Sep. Purif. Technol., 131 (2014) 94-101.

[24] S.-H. Yeon, K.-S. Kim, S. Choi, H. Lee, H.S. Kim, H. Kim, Physical and electrochemical properties of 1-(2-hydroxyethyl)-3-methyl imidazolium and N-(2-hydroxyethyl)-N-methyl morpholinium ionic liquids, Electrochim. Acta, 50 (2005) 5399-5407.

Anal. Method Environ. Chem. J. 3 (1) (2020) 49-54

AMECJ

Research Article, Issue 1

Analytical Methods in Environmental Chemistry Journal

Journal home page: www.amecj.com/ir

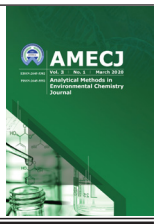

Fabrication of electrochemical sensor biosystems through hexagonal boron nitride Nanosheets for extraction lead in human serum

Alisha Saanvi [a], Ringo Krishnan [a], Amoli Hassan [a], Rmesh K. Gupta[a,*]

[a] *Department of Chemistry, Indian Institute for Advanced Materials, India*

ARTICLE INFO:

Received 27 Nov 2019

Revised from 26 Jan 2020

Accepted 20 Feb 2020

Available online 29 Mar 2020

Keywords:

Boron nitride nanosheets,
Triazine azide,
Lead,
L-cysteine,
Electrochemical Sensor,
Solid phase extraction

ABSTRACT

Lately a flood of expanded enthusiasm for the peeling of boron nitride (h-BN) has seen because of its energizing electrical, warm, photonics mechanical properties and detecting. A few ways to deal with have risen depicting the peeling, functionalized and solubilization of h-BN. In this investigation, we report on a direct way to deal with alter the surface and its application as another sort of biomedical applications. The readied item is basically described by FTIR spectroscopy, field outflow (FESEM), TGA strategy, XPS range, and BET surface zone estimations. Nano-composites were immobilized on terminals to distinguish the glucose, L-cysteine in cushion medium by cyclic voltammetry (CV), square wave voltammetry (SWV), and electrochemical impedance spectroscopic (EIS). Potential utilization of the covalent functionalization, modest forerunners, biodegradability and multifunctionality of superior composites boron nitride, they could be utilized for a wide scope of things to come biomedical applications. Also, the composites boron nitride was used for extraction lead (Pb^{2+}) ions in human serum by micro solid phase extraction coupled with atom trap atomic absorption spectrometry (AT-AAS) by researchers. The LOD and enrichment factor was obtained 2.96 and 9.82, respectively for 10 mL of human serum sample (RSD < 2%). The validation was confirmed by CRM, NIST solution.

1. Introduction

Recently, more consideration has seen a flood of enthusiasm for the shedding of graphene, other layered mixes, particularly hexagonal boron nitride (h-BN) [1-4]. The h-BNNs significantly higher compound security and protection from oxidation contrasted with that of graphene. Boron nitride (BN) is the isoelectric and isostructural simple to graphite with rotating boron and nitrogen iotas in the structure [5,6]. Following these underlying reports, a few different techniques, for example, mechanical shedding by means of drawing, Lithium particle intercalation and low vitality ball processing were utilized to create little amounts of top-notch h-BN nanosheets [7-11]. Substance shedding of h-BN was later proceeded as an option in contrast to the mechanical courses, driving a basic and practical path for the mass peeling of h-BN nanosheets. These were performed by treating the mass h-BN powder in different natural solvents, N,N Di-methylformamide (DMF), methane sulfonic corrosive (MSA), and liquid metal hydroxides. These methodologies yield low-convergence

* Corresponding Author: Rmesh K. Gupta
E-mail: r.gupta.k1983@gmail.com
https://doi.org/10.24200/amecj.v3.i01.89

of h-BN nanosheets significantly after broad sonication [12-18]. With the expansion of practical gatherings triazine azide an improved scattering and strength of h-BN exists in an assortment of solvents. In this, we report the covalent compound functionalization of h-BN nanosheets utilizing receptive nitrene radicals. Point by point portrayal of the functionalized h-BN was performed to check the covalent idea of the connection [6, 18-22]. Many method was used for triazine determination in liquid phases. The functionalization technique was reached out to covalently unite triazine azide to the outside of h-BN nanosheets by nitrene addition and utilize these nano composites-functionalized BN nanosheets for cooperations with biosystems and improve detecting properties [22-26]. Electrochemical impedance spectroscopy (EIS) has as of late developed as a device to analyze forms that happen at various timescales. The idea of "impedance" is comparable to opposition yet takes into account depiction of complex circuits which have nonlinear current–voltage connections, for example, those which show capacitance, inductance, or mass dispersion. EIS exploits this idea by relating hypothetical circuit components to real electrochemical procedures happening in a material and permitting fitting of current, voltage, and recurrence information to equal circuit models. EIS information is produced by applying an AC potential to an electronic gadget, estimating the AC current reaction, and recording stage move and adequacy changes over a scope of applied frequencies. By analyzing the present reaction over a scope of frequencies permits partition of procedures which happen on various timescales, making it perfect for isolating electronic and ionic procedures in blended conductors [27-30]. This is a key favorable position of EIS making it a well-suited instrument to consider particle dispersion in HOIPs and resolve the substance personality of the particle [3]. In addition h-BN nanosheets was used for separation Pb ions in human biological samples by covalence bonding of BN to Pb (BN:----Pb) by μ-SPE coupled to AT-AAS. The absorption capacity was achieved 141.4 mg g-1 at pH=8.2.

2. Experimental

2.1. Materials and Instruments

All general materials such as KCl, $Fe(CN)_6$, triazine azide, and azine were provided by Merck. h-BNN were purchased from Sigma-Aldrich company. The graphene was provided by Indian Institute for Technology. Other chemicals with analytical grad such as HNO_3, HCl and NaOH were purchased from Merck, Germany. The pH was adjusted based on 0.32 mol L^{-1} of buffer solution (HPO_4/H_2PO_4) from pH of 5.0 to 8.4. The polyoxyethylene octyl phenyl ether as the anti-sticking material was used in human samples (Merck). GBC906 Flame atomic absorption spectrophotometer based on atom trap (AT-FAAS, AUS) measured Pb in serum samples. The air-acetylene based on background correction (LD_2) tuned by the software of AVANTA of AT-FAAS. The AT-FAAS can be determined Pb with micro liter of the sample with LOD of 0.04 mg L^{-1}.

2.2 Preparation of h-BNNs

h-BNNs were modified with triazine azide at room temperature with a ratio of 1:2 weight from h-BN nanosheets: triazine azide for giving TN_3-functionalized BNNSs (TN_3-h-BNNs). After stirring for 24 h, the final product was centrifuged at 5500 rpm per minute. The obtained Tr-h-BNNs sediment was purified by dialysis against DMF for 2 days and dried at 100˚C. So., a white powder was obtained for characterization.

2.3 Electrochemical characterization of BN-TrAz modified electrode

The electrochemical properties of BN-TrAz/GCE were examined using EIS and CV. The EIS method can be used to study the kinetics of electron transfer between electrolyte and electrode surface. According to Fig. 1, the effect of the modified electrode on the electrochemical response, the EIS spectrum (A) and the cyclic voltammonogram (B) of the 7 mM [$Fe(CN)_6$] solution containing 0.1 M KCl for bare glass carbon electrodes (a) BN/GCE (c) and TriAz/BN/GCE (b) was investigated [1-8].

2.4. SPE procedure

By µ-SPE method, 10 mL of serum were used for speciation and determination of lead ions at pH 8.2. First, 20 mg of *h-BNNs* added to 1-octyl-3-methylimidazolium hexafluorophosphate [OMIM] [PF_6] in ethanol and the suspension of *h-BNNs* in IL were injected to serum sample with concentration of 100 µg L^{-1} at pH=8.2. After shaking with an ultrasound bath for 6.0 min, the Pb (II) ions were efficiently extracted with the nitrate of *h-BNNs* (N:---Pb) as dative bond in pH=8.2. The *h-BNNs* trapped in [OMIM][PF_6] and separated from the liquid phase in the bottom of the conical tube after centrifuging (3500 rpm). Then, the pb^{2+} ions back-extracted from *h-BNNs* by 0.5 mL of nitric acidic (0.2M, up to 1mL) and after diluted determined by AT-FAAS.

3. Results and Discussion

3.1. Characterization

As appeared in Figure 1, the IR range of perfect h-BN uncovers a deviated bond at 1384 cm-1 which compares to B-N stretch and the bond at 818 cm-1 doled out to B-N-B extending vibration. The IR range of Triazine shows groups at 1701 cm−1 which were appointed to C=N extending vibration. The morphology and structure of h-BNNs and Tr h-BNNs was explored by SEM. The shedding procedure brings about not many layer h-BNNs sheets with smooth surfaces and edges and sidelong size in the scope of 1-2 µm (Fig. 1). The Tr -h-BNNs sample showed a morphology different from that for h-BNNs. Due to the grafted Triazine-azide groups, surface of Nitrene -h-BNNs become relatively smooth and compact with porous features with the structure of h-BNNPs crystalline produced is preserved [9-11].

According to Figure 2, the effect of the modified electrode on the electrochemical response, the EIS spectrum (A) and the cyclic voltammonogram (B) of the 7 mM $[Fe(CN)6]^{3-/4-}$ solution containing 0.1 M KCl for bare glass carbon electrodes (a) BN/GCE (c) and TriAz/BN/GCE (b). The electrochemical behavior of the electrode was investigated after interaction with 200 µM L-cysteine by DPV method was investigated and the results were shown in (Fig.3).

3.2. Optimization and Validation

All parameters such as pH, sample volume, mass of sorbent, shaking time for extraction Pb from serum samples was optimized, Based on procedure sample volume from 5-15 mL have good efficiency for lead extraction so 10 mL of sample was used for further study. Also, pH of sample was evaluated between 2-10 and results showed us the pH 7.5-8.2 have high recovery for lead extraction, So, pH of 8 was used as optimum pH (Fig. 4). The amount of

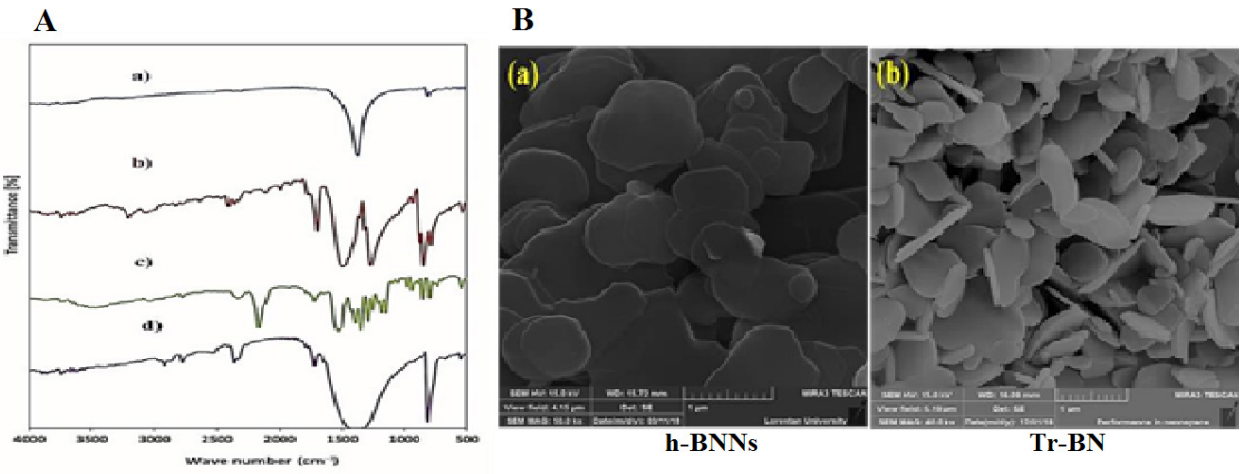

Fig. 1. A) FTIR spectra of (a) h-BNNs, (b) Triazine, (c) Triazine-azide, (d) Tr- BN. B) Different magnification of SEM images of the a) h-BNNs and b) Tr-BN.

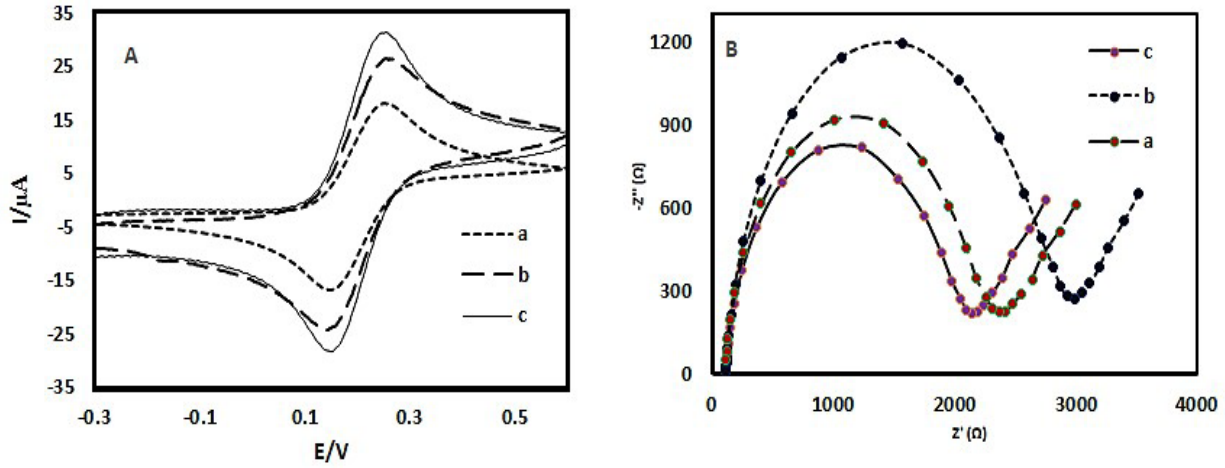

Fig. 2. The impedance spectra (A) and CV voltammograms (B) of for bare glass carbon electrodes (a) BN/GCE (c) and TriAz/BN/GCE (b) in 7 mM $[Fe(CN)6]^{3-/4-}$ solution containing 0.1 M KCl

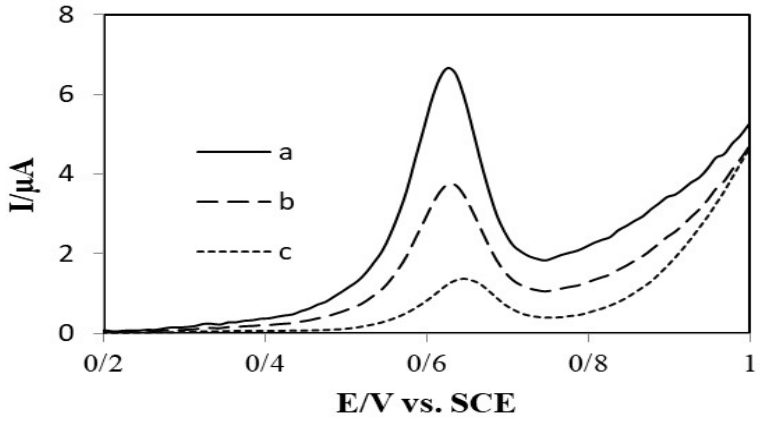

Fig. 3. Difference pulse voltammogram of 200 µML- cysteine for different electrodes at pH =7. DPV Voltammograms at the bare glass carbon (b), BN/GCE (a) and TriAz/BN/GCE (c).

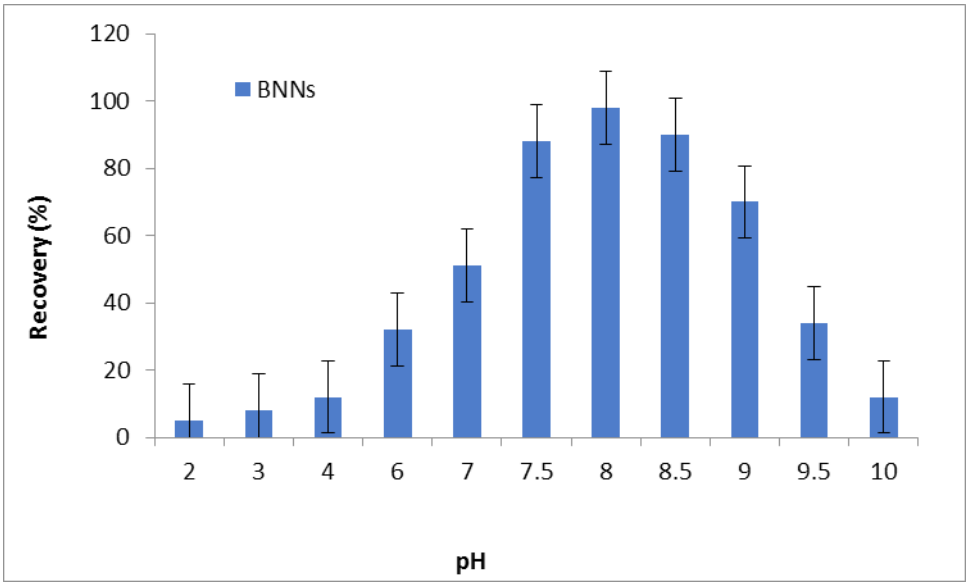

Fig. 4. The effect of pH on lead extraction by BNNs

Table 1. Validation of µ-SPE method based on BNNs for lead extraction by certified reference material (CRM, NIST)

Sample	Reference (µg L^{-1})	Added	Found*(µg L^{-1})	Recovery (%)
[a]CRM	139.5 ± 0.8	-----	135.8 ± 8.2	-----
		100.0	231.2± 10.5	95.4
[b]CRM	277.6 ± 1.6	-----	271.5 ± 14.4	-----
		200.0	466.4± 22.7	97.3

CRM955c, caprine blood, level 2
[b]CRM955c, caprine blood, level 3

h-BNNs for extraction was optimized and 20 mg of sorbent was selected as optimum mass. The CRM was used for validation samples as Table 1.

4. Conclusions

In present study, nitrene molecules were successfully grafted on the surface of h-BNNs and the resulted compound was used as an L-cysteine sensor of two sulfur of L-cysteine through the formation of Substitution reaction to Chlorine triazine azide. The most important achievement of this study is that L-cysteine is diagnosed in a straightforward manner. In summary, this synthesized modified electrode, could be used as a biosensing interface in the fields of biomedical and clinical diagnostics of Sulfur Protein Amino Acid such as L-cysteine. The modified electrochemical sensor was characterized by SWV, CV, and EIS. Based on results lead (Pb) can be extracted by h-BNNs in pH=8 by µ-SPE method at optimized conditions

5. References

[1] P. Moon, M. Koshino, Electronic properties of graphene/hexagonal-boron-nitride moiré superlattice, Phys. Rev., 90 (2014) 155406.

[2] M. Onodera, K. Watanabe, M. Isayama, M. Arai, S. Masubuchi, R. Moriya, T. Taniguchi, T. Machida, Carbon-rich domain in hexagonal boron nitride: carrier mobility degradation and anomalous bending of the landau fan diagram in adjacent grapheme, Nano Lett., (2019) 7282–7286.

[3] S. M. Mostafavi A. Rouhollahi, M. Adibi, F. Pashaee, M. Piryaei, Electrochemical investigation of thiophene on glassy carbon electrode and quantitative determination of it in simulated oil solution by differential pulse voltammetry and amperometry techniques, Asian J. Chem., 23 (2011) 5356-60.

[4] O. Zabihi, A. Khodabandeh, S. M. Mostafavi, Preparation, optimization and thermal characterization of a novel conductive thermoset nanocomposite containing polythiophene nanoparticles using dynamic thermal analysis, Polymer degra. stability, 97(2012) 3-13.

[5] Y. Kubota, K. Watanabe, O. Tsuda, T. Taniguchi, Deep ultraviolet light-Emitting hexagonal boron nitride synthesized at atmospheric pressure, Sci., 317 (2007) 932–934.

[6] M. Yankowitz, J. Xue, D. Cormode, J. D. Sanchez-Yamagishi, K. Watanabe, T. Taniguchi, P. Jarillo-Herrero, P. Jacquod, B.J. LeRoy, Emergence of superlattice dirac points in graphene on hexagonal boron nitride, Nat. Phys., 8 (2012) 382–386.

[7] T.B. Hoffman, B. Clubine, Y. Zhang, K. Snow, J.H. Edgar, JOptimization of Ni–Cr flux growth for hexagonal boron nitride single crystals, J. Cryst. Growth, 393 (2014) 114–118.

[8] S. Liu, R. He, Z. Ye, X. Du, J. Lin, H. Jiang, B. Liu, J.H. Edgar, Large-scale growth of high-quality hexagonal boron nitride crystals at atmospheric pressure from an Fe– Cr flux, Cryst. Growth Des., 17 (2017) 4932–4935.

[9] S. M. Mostafavi, 3D graphene biocatalysts for development of enzymatic biofuel cells: a short review, J. Nanoanal., 2 (2015) 57-62.

[10] S. Liu, R. He, L. Xue, J. Li, B. Liu, J.H. Edgar, Single crystal growth of millimeterSized monoisotopic hexagonal boron nitride, Chem. Mater., 30 (2018) 6222–6225.

[11] A.M. Al'Abri, S. Mohamad,S.N. Abdul Halim, N.K. Abu Bakar, Development of magnetic porous coordination polymer adsorbent for the removal and preconcentration of Pb(II) from environmental water samples, Environ. Sci. Pollut. Res. Int., 26 (2019) 11410-11426.

[12] A. Davoudiroknabadi, S. S. Sajadikhah, An introduction to nanotechnology, Mikima Book,

2016. ISBN 978-0994498014
[13] A. Davodiroknabadi, A. A. Pasban, Fundamentals of nanostructure and nanomaterial. Mikima Book, 2016. ISBN 978-0994498223
[14] Y.P. Wang, Y. Sun, B. Xu, X.P. Li, X.H. Wang, H.Q. Zhang, D.Q. Song, Matrix solidphase dispersion coupled with magnetic ionic liquid dispersive liquid–liquid microextraction for the determination of triazine herbicides in oilseeds, Anal. Chim. Acta 888 (2015) 67–74.
[15] M.G. Silly, P. Jaffrennou, J. Barjon, J.S. Lauret, F. Ducastelle, A. Loiseau, E. Obraztsova, B. Attal-Tretout, E. Rosencher, Luminescence properties of hexagonal boron nitride: cathodoluminescence and photoluminescence spectroscopy measurements, Phys. Rev., 75 (2007) 085205.
[16] T.Y. Zhou, J. Ding, L. Ni, J. Yu, H.Y. Li, H. Ding, Y.H. Chen, L. Ding, Preparation of magnetic superhydrophilic molecularly imprinted resins for detection of triazines in aqueous samples, J. Chromatogr. A 1497 (2017) 38–46.
[17] L. Museur, D. Anglos, J.P. Petitet, J.P. Michel, A.V. Kanaev, Photoluminescence of hexagonal boron nitride: effect of surface oxidation under UV-laser irradiation, J. Lumin., 127 (2007), 595–600.
[18] M. Yankowitz, J. Xue, D. Cormode, J.D. Sanchez-Yamagishi, K. Watanabe, T. Taniguchi, P. Jarillo-Herrero, P. Jacquod, B.J. LeRoy, Emergence of superlattice dirac points in graphene on hexagonal boron nitride, Nat. Phys., 8 (2012) 382–386.
[19] M. Roldán-Pijuán, R. Lucena, M.C. Alcudia-León, S. Cárdenas, M. Valcárcel, Stir octadecyl-modified borosilicate disk for the liquid phase microextraction of triazine herbicides from environmental waters, J. Chromatogr. A 1307 (2013) 58–65.
[20] Y.P. Wang, Y. Sun, B. Xu, X.P. Li, R. Jin, H.Q. Zhang, D.Q. Song, Magnetic ionic liquid-based dispersive liquid–liquid microextraction for the determination of triazine herbicides in vegetable oils by liquid chromatography, J. Chromatogr. A 1373 (2014) 9–16.
[21] X. Yang, R. Yu, S.H. Zhang, B.C. Cao, Z.L. Liu, L. Lei, N. Li, Z.B. Wang, L.Y. Zhang, H.Q. Zhang, Aqueous two-phase extraction for determination of triazine herbicides in milk by high-performance liquid chromatography, J. Chromatogr. B 972 (2014) 111–116.
[22] G. Cassabois, P. Valvin, B. Gil, Hexagonal boron nitride is an indirect bandgap semiconductor, Nat. Photonics, 10 (2016) 262–266.
[23] D. Rhodes, S.H. Chae, R. Ribeiro-Palau, J. Hone, Disorder in van der waals heterostructures of 2D materials, Nat. Mater., 18 (2019) 541–549.
[24] K. Watanabe, T. Taniguchi, H. Kanda, Direct-bandgap properties and evidence for ultraviolet lasing of hexagonal boron nitride single crystal. Nat. Mater., 3 (2004) 404–409.
[25] T. Yamaguchi, Y. Inoue, S. Masubuchi, S. Morikawa, M. Onuki, K. Watanabe, T. Taniguchi, R. Moriya, T. Machida, Electrical spin injection into graphene through monolayer hexagonal boron nitride, Appl. Phys. Express, 6 (2013) 073001.
[26] L. Britnell, R.V. Gorbachev, R. Jalil, B.D. Belle, F. Schedin, M.I. Katsnelson, L. Eaves, S.V. Morozov, A.S. Mayorov, N.M.R Peres, A.H. Castro Neto, J. Leist, A.K. Geim, L.A. Ponomarenko, K.S. Novoselov, Electron tunneling through ultrathin, boron nitride crystalline barriers, Nano Lett., 12 (2012) 1707–1710.
[27] S. Jafari, S. A. Mostafavi, Investigation of nitrogen contamination of important subterranean water in the plain, Med. Biotech. J., 3 (2019) 10-12.
[28] S.J. Grenadier, A. Maity, J. Li, J.Y. Lin, H.X. Jiang, Origin and roles of oxygen impurities in hexagonal boron nitride epilayers, Appl. Phys. Lett., 112 (2018) 162103.
[29] S. M. Mostafavi, H. Malekzadeh, M. S. Taskhiri, In silico prediction of gas chromatographic retention time of some organic compounds on the modified carbon nanotube capillary column, J. Com. Theor. Nanosci., 16 (2019) 151-156.
[30] S. Nekouei, F. Nekouei, I. Tyagi, S. Agarwal, V. K. Gupta, Mixed cloud point/solid phase extraction of lead(II) andcadmium(II) in water samples using modified-ZnO nano-powders, Process Saf. Environ. Protection, 99 (2016)175–185 .

Anal. Method Environ. Chem. J. 3 (1) (2020) 55-62

AMECJ

Research Article, Issue 1

Analytical Methods in Environmental Chemistry Journal

Journal home page: www.amecj.com/ir

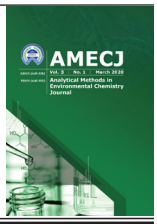

In-vitro extraction and separation of copper ions from human blood samples based on amoxicillin/clavulanic acid by ultrasound assisted-dispersive centrifuge liquid-liquid micro extraction

Jamileh Esmaeili[a,b], Samira Shirooei[c] and Azam Bakhtiarian[d,*]

[a] *Ph.D Student in Department of Biology, School of Basic Science, Science and Research Branch, Islamic Azad University, Tehran , Iran*
[b] *Department of Pharmacology, Tehran University of Medical Sciences*
[C] *Sciences Research center, Health Institute, Kermanshah University of Medical Sciences, Kermanshah, Iran*
[*,d] *Department of Pharmacology Tehran University of medical Sciences*

ARTICLE INFO:

Received 18 Nov 2019
Revised form 9 Jan 2020
Accepted 12 Feb 2020
Available online 30 Mar 2020

Keywords:
Copper,
Separation,
Human blood,
Amoxicillin/clavulanic acid,
Ultrasound assisted-dispersive centrifuge liquid-liquid micro extraction

ABSTRACT

The low concentration of copper (Cu^{2+}) can be effected on the central nervous system (CNS) and caused to multiple sclerosis (MS). Although many *antibiotics* can treat the bacterial infections but some of *antibiotics* decrease essential metal concentrations in human body and must be controlled by determining. In this study, in-vitro extraction of copper (Cu^{2+}) with amoxicillin/clavulanic acid (AMOXC) has been studied due to interacting with metals. By procedure, Cu^{2+} ions were separated from blood samples by *ultrasound assisted-dispersive* centrifuge liquid-liquid micro extraction (USA-DC-LLME). The mixture of AMOXC (0.01 g), ionic liquid ([BMIM][PF6]) and acetone injected to 10 ml of serum blood sample at human pH=7.2. After extraction, the concentration of Cu^{2+} ions was determined by flame atomic absorption spectrometry (F-AAS). The LOD, enrichment factor (EF), linear range (LR) and working range (WR) were obtained 6 µg L^{-1}, 9.92, 0.018-0.5 mg L^{-1} and 0.02-2.58 mg L^{-1}, respectively (RSD<1.1%). The validation of technology was confirmed by ICP and spiking samples.

1. Introduction

Copper (Cu) acts as a main co-factor in humans and enter into cuproenzymes that catalyze electron transfer reactions (ETR) required for cellular respiration, iron oxidation, neurotransmitter biosynthesis, antioxidant, peptide amylation. The Cu intake has been associated with toxic effects in humans include influenza-like syndrome , hemolysis and kidney failure due to Cu sulfate intake [1]. Cu exists in blood plasma in Cu bound to caeruloplasmin (65–71%) and convert the iron Fe^{2+} into Fe^{3+}which was bonded to transferrin [2]. Copper enter to biochemical reactions and human physiology. In biological matrix such as plasma, copper complex to proteinsas caeruloplasmin and albumin or amino acids [3]. The defect of central nervous system caused to multiple sclerosis (MS) disease in human due to demyelination of nerve fibers of the brain and spinal cord. Based on previous studies, the genetic, immunological and environment factors have main source for creating MS in humans with disability. But, the environment factors such as heavy metals such as copper, zinc, cadmium and lead has significant role in MS [5, 6]. The deadline of time exposure of heavy metals in

*Corresponding Author: Azam Bakhtiarian
Email: bakhtiar12@yahoo.com
https://doi.org/10.24200/amecj.v3.i01.94

human blood samples depended to kind of heavy metals and chorionic/acute exposure (cadmium was seen in blood up to 1 hour as acute exposure). In chorionic exposure the concentration of heavy metals can be followed in nail or hair. Copper used for many products as an essential element in nature and copper has concentration between 80-180 μg dL^{-1} in blood of human adults (Mean= 1.5 mg L^{-1}). Copper exposure in industry occurs primarily through inhaled particulates and according to studies, copper can be a cause of the pathogenesis of MS [6]. The value of copper (Cu^{2+}) effect on the central nervous system (CNS) and reducing of their concentration caused to numerous CNS disorders such as multiple sclerosis (MS), Wilson disease, Alzheimer and Parkinson's diseases [7-9]. Also, some of antibiotics caused to decrease essential metals such as Zn^{2+} and Cu^{2+} in human body. So, in present of antibiotics, determination of Zn^{2+} and Cu^{2+} in human matrixes is very important. Some receptors such as β-ketoenol-bipyridine and ketoenol–pyrazole were functioned on silica hybrid adsorbent and other sorbents [10, 11]. For determination of copper the different analytical techniques such as, ET-AAS [12, 13], ion selective electrode, Square wave□adsorptive anodic stripping voltammetric (SW□ASV) [14] and flame atomic absorption spectrometry (F-AAS) [15] were used in different samples such as blood, waters and tissues(fish)[16]. High interferences in human blood are main problems for determination copper by instruments. So, sample preparation must be used before analysis by instruments. The different procedures such as, cloud point extraction (CPE)[9], liquid-liquid extraction (LLE) [15],solid-phase extraction (SPE) in human biological fluid (blood, serum and urine) [17,18-22] and dispersive liquid-liquid microextraction (D-LLME) based on ionic liquids (IL) [23,24,15] were used before Cu analysis. Recently, a applied dispersive liquid-liquid microextraction was used for separation/extraction of ions from liquid samples. In this study, USA-DC-LLME based on AMOXC was used for efficient extraction of Cu ions in human biological samples before determination by F-AAS. The hydrophobic ionic liquid was used for simple separating of Cu-AMOXC from blood samples.

2. Experimental

2.1. Instrumental

The spectra GBC 906 double beam atomic absorption spectrophotometer was used for copper determination (FAAS, GBC, Model; Plus 906, Australia). The air-acetylene as fuel gas based on background correction was selected for F-AAS. The light of HCL adjusted on burner by vertical and horizontal positions. The Avanta software of spectra was used for collecting data. The copper hollow cathode lamp (HCL, slit=0.7) with wavelength of 327.4 nm and current of 4.0 mA was adjusted in vertical and horizontal position. For copper analysis, the limit of detection, working range was obtained 0.06 mg L^{-1} and 0.2-24.0 mgL^{-1}, respectively by F-AAS. All samples as minimum volume were used by auto-sampler injector (0.5-5 mL). The pH values of the solutions were measured by a digital pH meter (Metrohm 744), especially in human samples. All samples were shaken with Thermo accessory as mixer (250 rpm, USA) and centrifuged with Thermo fisher (1000-4500 rpm, USA).

2.2. Reagents

The ultra-trace reagents with analytical grade such as; HNO3, HCl, NaOH, copper salt and acetone solutions were purchased from Merck (Darmstadt, Germany). The pure AMOXC as amoxicillin trihydrate: potassium clavulanate (4:1) was purchased from sigma, Germany (Product N: SMB00607, Batch N: 128M4800V, 75% AMOX and less than 15% clavulanic acid and less than 15% water) (Fig.1). The Cu(II) stock standard solution was prepared as nitrate salt of 1000 mg L^{-1} (ppm) solution in 1 % HNO_3. The standard solutions were prepared daily by dilution of the standard solution of Cu(II) by ultra-pure water(UPW). High purity distilled water had already prepared from Millipore (Bedford, USA). 1-Ethyl-3-methylimidazolium acetate (CAS N: 143314-17-4), 1-Ethyl-3-methylimidazolium tetrafluoroborate (CAS N: 143314-16-3), 1-Ethyl-3-methylimidazolium hexafluorophosphate (CAS N: 155371-19-0), and 1-butyl-2,3-dimethylimidazolium

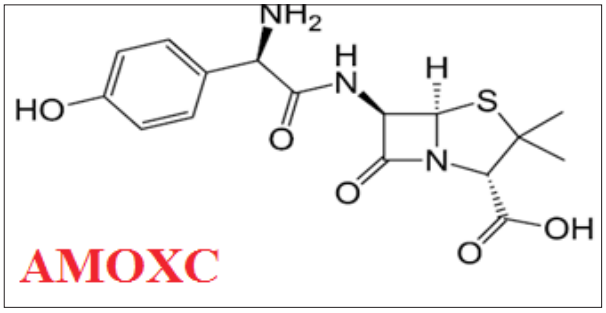

Fig. 1. Schema of amoxicillin trihydrate: potassium clavulanate

hexafluorophosphate ([BDMIM] [PF_6]) as a hydrophobic ionic liquids were was selected for separation AMOXC from blood sample. The T-X100 with analytical grade were purchased from Merck Co., Darmstadt, Germany. The pH was adjusted with buffer solutions (Merck, Germany). Sodium phosphate and citric acid was used for phosphate citrate buffer for PH=2.0–7.5.

2.3. Sample preparation

The glasses were washed with a HNO_3 solution (0.5M) for at least 24 h and thoroughly rinsed 10 times with ultra-pure water. For sampling, 20 ml of samples of blood were collected from subjects and control peoples (N=30, men, 30-55 age). 10 mL of blood sample mixed with heparin (pure, 20 micro liter) and storage in low temperature. Then, 10 mL of blood samples were stay at the room temperature for 30 minutes to coagulate and then centrifuged at 3000 rpm for 5 minutes. Next, serums were separated by a sampler. Plasma was also prepared by procedure by centrifuging process. The human blood/serum samples were maintained at –20 °C up to 72 h. In humans with low sample volume of blood, it diluted up to 20 mL and then was used. The Ethical Committee of Azad University confirmed the human sample method (SN.IAU.SRB.940522664.

2.4. Procedure

By USA-DC-LLME procedure, the 10 mg of pure AMOXC powder (15 micro molar conc.) mixed with ionic liquid ([BMIM][PF6], IL, 0.1 g) in present of 500 micro liter of acetone/ethanol, then, the mixture was injected to 10 ml of serum blood sample at human pH=7.2 (Fig.2). After 5 min shaking time, the hydrophobic ionic liquid BMIM][PF6] was separated by centrifuging at 3500 rpm for 4 min in conical glass tube. The upper liquid phase separated by auto-sampler accessory (1-100 mL) and remained phase (IL-AMOXC/Cu^{2+}) were back-extracted from IL phase by decreasing pH up to 1 (HNO_3, 0.5 M, 0.5 mL). Finally the concentration of Cu^{2+} ions was simply determined by F-AAS after dilution with DW up to 1 mL.

3. Results and discussion

For extraction copper from blood samples all parameters (pH, sample volume, amount of AMOXC and IL) must be optimized. The serum, blood, urine samples was prepared from patients with copper disease such as multiple sclerosis. After tuning pH with favorite buffers, the sample determines by ultrasound assisted-dispersive centrifuge liquid-liquid micro extraction (USA-DC-LLME) coupled to F-AAS.

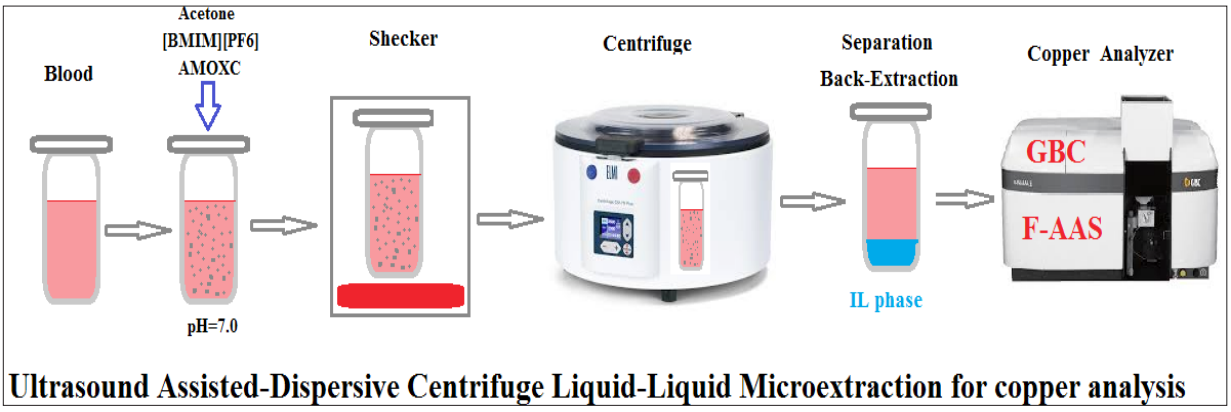

Fig. 2. The copper extraction from blood samples based on AMOXC by USA-DC-LLME

3.1. PH effect

The effect of sample pH on complexation of Cu(II) ions on AMOXC was studied for 0.2 mg L^{-1} and 2.0 mg L^{-1} of Cu(II) (lower limit of quantification; LLOQ and upper limit of quantification; ULOQ) from different pH 1-12. The complexation of AMOXC-Cu was depended on the pH of solutions and function group of ligand. The results showed, the maximum extraction of Cu(II) was achieved in human pH (7.0), and the recovery values for Cu(II) were below 5% in acidic or basic pH. The extraction mechanism of Cu(II) ions with AMOXC was highly referred to pH and complex formation between Cu(II) ions and dative sulfur bonding of AMOXC (Fig. 3). The sulfur groups can be deprotonated (:S-R) at wide range of pH from 6 to 9. The extraction efficiency of Cu(II) at pH values below 6 and upper of 8 cannot occurred due to similarity charge or precipitation of hydroxyl copper ($Cu(OH)_2$).

3.2. Sample volume effect

The sample volume in one of the important factors which must be optimized for Cu extraction from blood samples by AMOXC. As evaluation extraction efficiency, different volumes between 1.0-30 mL of blood and serum samples was examined and optimizes in pH=7. The results showed us that the maximum recovery for copper extraction based on AMOXC was achieved for less than 12 mL for human blood samples and less than 17 mL of standard solutions. Therefore, 10 mL and 15 mL of sample volume was selected as optimum point for copper extraction for blood and water samples, respectively by USA-DC-LLME procedure (Fig.4).

3.3. AMOXC effect

The amount of ligand is very important for copper extraction in blood samples, so, the concentration of AMOXC in human samples must be studied for high extraction. For this purpose, the vary concentration between 1-50 micro molar concentration of AMOXC was prepared and used for evaluation of copper extraction in blood/standard samples by USA-DC-LLME procedure. The experimental results showed, the high extraction of copper was obtained with more than 15 micro molar of AMOXC in 10 mL of samples (~ 10 mg pure powder) by USA-DC-LLME procedure (Fig. 5). Also, the extraction efficiency more than 97% was made by 12 micro molar of AMOXC concentration in 10 mL of water samples. First, 10 mg of pure AMOXC powder mixed with ethanol/acetone (0.5 mL) and then added to 0.1 g of IL in 2 mL syringe. After shacking, the mixture injected to 10 mL of blood samples. The extraction efficacy was decreased about 74.6% when the mixture added step by step without shacking.

3.4. Ionic liquid effect

Separation process for AMOXC-Cu from liquid samples (blood, standard solution) is very difficult.

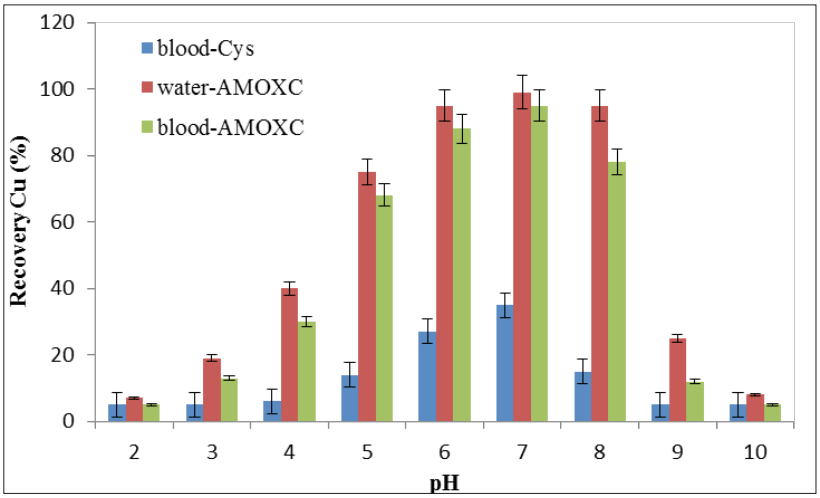

Fig. 3. The effect of pH on copper extraction based on AMOXC by USA-DC-LLME procedure

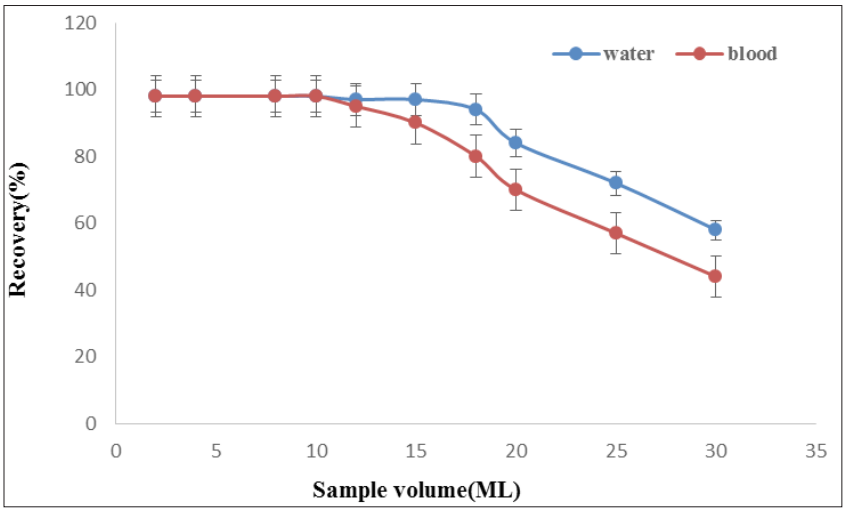

Fig. 4. The effect of sample volume on copper extraction based on AMOXC by USA-DC-LLME procedure

The different techniques with filter, centrifuging and organic solvents was used for separation ligands from liquid phase. Recently, the benign solvents as green solvents (IL) was introduced in many papers. In this study we used different hydrophobic ionic liquids for separation processes in blood samples. The different volumes or gram (0.05-0.3 g) of 1-Ethyl-3-methylimidazolium acetate, 1-Ethyl-3-methylimidazolium tetrafluoroborate, 1-Ethyl-3-methylimidazoliumhexafluorophosphate,and1-butyl-2,3-dimethylimidazolium hexafluorophosphate [BDMIM][PF_6] as a hydrophobic ionic liquids were was selected for separation AMOXC from blood sample. Based on results, 0.1 g of [BDMIM][PF_6] has more extraction efficiency as compared to others (Fig. 6). The 1-Ethyl-3-methylimidazolium acetate and 1-Ethyl-3-methylimidazolium tetrafluoroborate had lower recovery because of solubility in liquid phase and missed of IL. The1-Ethyl-3-methylimidazolium hexafluorophosphate as hydrophobic IL can be separated copper-AMOXC from blood samples but has lower recovery (85%) as compared to [BDMIM][PF_6] with (97.8%).

3.5. Interference ions study

Many ions such as Zn^{2+}, Mn^{2+}, Na^{+}, K^{+}, HCO_3^{-}, SO_3^{-}, Fe^{2+}, Co^{2+}, exist in water or blood samples and can be effected on complexations of copper with AMOXC in presence of interference ions. The complexation copper depended on power of ligand and competition

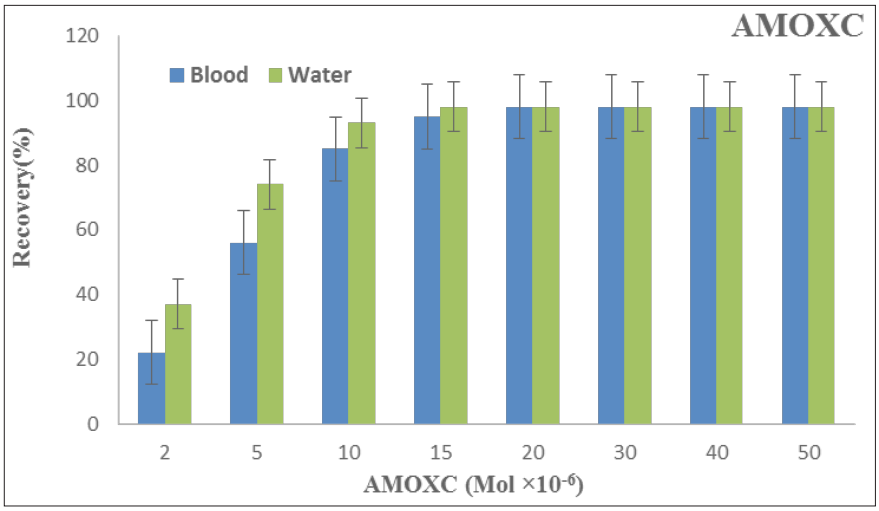

Fig. 5. The effect of AMOXC concentration by USA-DC-LLME procedure

of ions in different pH. So, in optimized pH many ions had no effect on extraction process, but some of them may be done. Therefore the effect of important ions which was bonding with amino acids or proteins was studied. The recovery of copper extraction based on AMOXC in presence of different concentration of 1-4 mg L^{-1} of cations and anions was evaluated by USA-DC-LLME procedure. As selectivity of determination of F-AAS, the concentration of other ions can't reported. So, the recovery was checked as effect of interference ions. The results showed, the interference ions had no effect on complexation processes of copper – AMOXV by USA-DC-LLME procedure (Table 1).

3.6. Validation procedure

The methodology of copper extraction must be validated by different technologies. By spiking of blood, serum, urine, plasma samples, the favorite recovery more than 95% was achieved for LLOQ and ULOQ range. So, the USA-DC-LLME procedure was validated for copper complexation based on AMOXC (Table 2). In addition, ET-AAS coupled with microwave digestion was used for evaluation of purposed procedure after dilution samples up to 100 mL(1:10) (Table 3). As intra-day and inter-day studies, the mean copper concentration based on AMOXC in subjects and control groups (N=30, men, 30-55 age) was checked by USA-DC-LLME procedure. The results showed no significance difference between subjects and control groups with favorite *p*-value (Table 4). The mean concentration of copper in control groups were a little higher than Cu blood subjects. The regression analysis and t-test were achieved between Cu in subject and control groups. There were a correlation (0.45< r <0.5) between blood of subject and control groups. (*p*-value < 0.001).

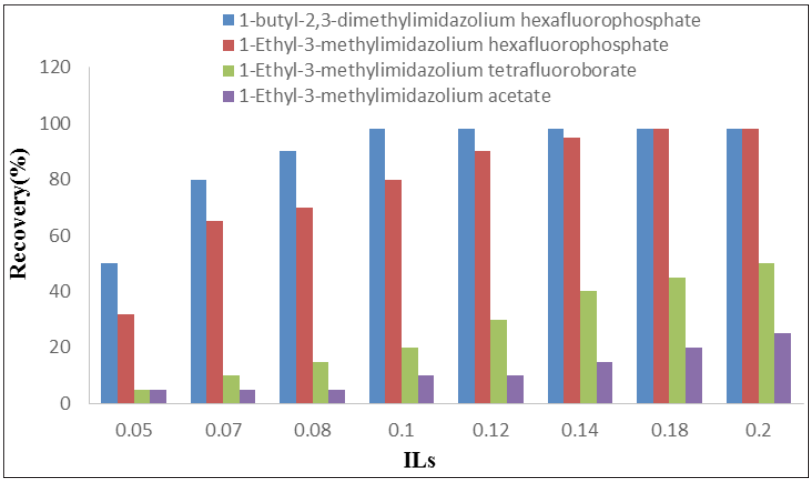

Fig. 6. The effect of different ILs on copper separation based on AMOXC by USA-DC-LLME procedure

Table 1. Effect of interfering ions on the extraction recovery of Cu (II) ions by USA-DC-LLME procedure

	Concentration ratio ($C_{interferent\ ion}/C_{Cu2+}$)		Recovery (%)	
Foreign Ions	**Standard**	**Blood**	**Standard**	**Blood**
K^+, Na^+, Li^+, Cl^-, F^-. Mg^{2+},Ca^{2+}	1200	1000	97.5	96.8
Co^{2+}, Ni^{2+}	900	700	98.2	97.3
Pb^{2+}, Ag^+	600	500	97.6	97.9
Zn^{2+}, Mn^{2+}	700	600	95.5	98.4
Fe^{2+}, V^{3+}, As^{3+}, Mo^{3+}	850	800	97.0	96.8
Cd^{2+}, Al^{3+}	800	550	98.2	97.3
Hg^{2+}	1000	900	96.5	95.7
CO_3^{2-}, SO_3^{2-}	950	600	99.1	98.5

4. Conclusions

A simple Pharmacology and biology method based on USA-DC-LLME was used for evaluating of AMOXC for copper extraction in human blood samples. The results demonstrated that AMOXC can decreased copper concentration in blood samples in efficient time. On the other hands amino acids and proteins was also complexed with copper and caused to decrease copper extraction by AMOXC. So, the AMOXC competed with amino acids and proteins for extraction copper and other metals at pH 7.2. In addition, *the antibiotics such as AMOXC* can treat the bacterial infections but they can decrease essential metals (Cu) in biological matrixes and cause disease in humans. By purposed procedure, the copper extracted with AMOXC at pH=7 and determined by F-AAS. The 1-butyl-2,3-dimethylimidazolium hexafluorophosphate ([BDMIM][PF_6] as hydrophobic IL was used for separation of Cu from liquid phase. In optimized conditions, the low LOD and RSD% values as well as good working ranges (0.02-2.58 mg L^{-1}) and high recoveries caused to consider as a recent innovative procedure.

5. Acknowledgements

The authors thank Azad University of Medical Sciences for supporting this work.
The Ethical Committee of Azad University confirmed the human sample method (SN.IAU.SRB.940522664).

6. References

[1] G.F. Nordberg, B.A. Fowler, M. Nordberg, Handbook on the Toxicology of Metals, (Fourth ed.), Academic Press, 2014.
[2] H.P. Roeser, G.R. Lee, S. Nacht, G.E. Cartwright, The role of caeruloplasmin in iron metabolism, J. Clin. Invest., 49 (1970) 2408-2417.
[3] S. Catalani, M. Paganelli, M. Enrica Gilberti, L. Rozzini, F. Lanfranchi, A. Padovani, P. Apostol, Free copper in serum: An analytical challenge and its possible applications, J. Trace Elem.Med. Biol., 45 (2018)176-180.

Table 2. Spiking of human samples based on AMOXC for copper extraction by USA-DC-LLME coupled to F-AAS

Sample	Added(mg L^{-1})	*Found(mg L^{-1})	Recovery (%)
Blood	--------	0.884 ±0.043	--------
	0.8	1.675±0.072	98.8
Serum	--------	1.226±0.058	--------
	1.2	2.384±0.094	96.5
Urine	--------	0.431± 0.022	--------
	0.4	0.838±0.039	101.7
Plasma	--------	0.362±0.024	--------
	0.3	0.657±0.028	98.3

Table 3. Comparing of ETAAS/digestion with USA-DC-LLME procedure coupled to F-AAS

Sample	Added	ET-AAS Microwave	USA-DC-LLME F-AAS	Recovery (%) ET-AAS	Recovery (%) F-AAS
Blood	--------	1.002±0.055	0.985±0.048	--------	--------
	1.0	1.977±0.112	1.981±0.094	97.5	99.6
Serum	--------	1.212±0.063	1.197±0.053	--------	--------
	1.2	2.423±0.124	2.376±0.103	100.9	98.3

Table 4. The mean copper concentration based on AMOXC in subjects and control groups (N=30) by USA-DC-LLME procedure

Sample	Control group (30n)		Patient group (30n)		r
	Intra-day	Inter-day	Intra- day	Inter day	
Blood	1.34±0.05	1.27±0.06	1.16±0.04	1.19±0.05	0.58
Serum	1.41±0.06	1.46±0.07	1.25±0.05	1.26±0.06	0.61

[4] R. Squitti, Copper in Alzheimer's disease: a meta-analysis of serum plasma, and cerebrospinal fluid studies, J. Alzheimers Dis., 24 (2011) 175-185.

[5] B.S. Choi, W. Zheng, Copper transport to the brain by the blood-brain barrier and blood-CSF barrier, Brain Res., 1248 (2009) 14-21.

[6] Y.U. Fengxiang, P. Gong, Z. Hu, Y. Qiu, Y. Cui, X. Gao, H. Chen, J. Li, Cu(II) enhances the effect of Alzheimer's amyloid-β peptide on microglial activation, J. Neuroinflamm., 12 (2015)122.

[7] S. Bolognin, L. Messori, D. Drago, C. Gabbiani, L. Cendron, P. Zatta, Aluminum, copper, iron and zinc differentially alter amyloid-Aβ1-42 aggregation and toxicity, Int. J. Biochem. Cell Biol., 43 (2011) 877–85.

[8] X.Y. Choo, L. Alukaidey, A.R. White, A. Grubman, Neuroinflammation and copper in Alzheimer's disease, Int. J. Alzheimers Dis., 2013 (2013) 145345.

[9] LM Gaetke, copper: toxicological relevance and mechanisms, Arch. Toxicol., 88 (2014) 1929-1938

[10] S. Radi, S. Tighadouini, M. Bacquet, S. Degoutin, Y. Garcia, New hybrid material based on a silicaimmobilised conjugated β-ketoenol-bipyridine receptor and its excellent Cu (II) adsorption capacity, Anal. Method., 8 (2016) 6923–6931.

[11] S. Tighadouini, S. Radi, M. Bacquet, S. Degoutin, M. Zaghrioui, S. Jodeh, I Warad, Removal efficiency of Pb (II), Zn (II), Cd (II) and Cu (II) from aqueous solution and natural water by ketoenol–pyrazole receptor functionalized silica hybrid adsorbent, Sep. Sci. Technol., 52 (2017) 608–621.

[12] A. Prkić, I. Mitar , J. Giljanović, V. Sokol, P. Bošković, I. Dolanc, T. Vukušić, Comparison of Potentiometric and ETAAS Determination of Copper and Iron in Herbal Samples, Int. J. Electrochem. Sci., 13 (2018) 9551 – 9560.

[13] S. Catarino, A. S. Curvelo-Garcia, Determination of copper in wine by ETAAS using conventional and fast thermal programs: Validation of analytical method, Atom. Spect. Norwalk Connecticut, 26 (2005) 73-78.

[14] E. A. Al-Harbi, M. S. El-Shahawi, Square wave-anodic stripping voltammetric determination of copper at a bismuth film/glassy carbon electrode using 3-[(2-Mercapto-Vinyl)-Hydrazono]- 1,3-dihydro-indol, Electroanal., 30 (2018) 1583-1885.

[15] J. F. Ayala-Cabrera, M. J. Trujillo-Rodríguez, V. Pino, Ó. M. Hernández-Torres, A. M. Afonso, J. Sirieix-Plénet, Ionic liquids versus ionic liquidbased surfactants in dispersive liquid–liquid microextraction for determining copper in water by flame atomic absorption spectrometry, Inter. J. Environ. Anal. Chem., 96 (2016) 101–118.

[16] N. Bader, H. Hasan, A. EL-Denali, Determination of Cu, Co, and Pb in selected frozen fish tissues collected from Benghazi markets in Libya, Chem. Methodol., 2 (2018) 56-63

[17] M. Soylak, O. Ercan, Selective separation and preconcentration of copper (II) in environmental samples by the solid phase extraction on multiwalled carbon nanotubes, J. Hazard. Mater., 168 (2009) 1527-1531.

[18] C. Duran, A. Gundogdu, V. N. Bulut, M. Soylak, L. Elci, H. B. Sentürk, M. Tüfekci, Solid-phase extraction of Mn (II), Co (II), Ni (II), Cu (II), Cd (II) and Pb (II) ions from environmental samples by flame atomic absorption spectrometry (FAAS), J. Hazard. Mater., 146 (2007) 347-355.

[19] Y. M. Hao, C. Man, Z. B. Hu, Effective removal of Cu2+ ions from aqueous solution by aminofunctionalized magnetic nanoparticles, J. Hazard. Mater., 184 (2014) 392–399.

[20] Y. T. Zhou, H. L. Nie, C. B. White, Removal of Cu2+ from aqueous solution by chitosan-coated magnetic nanoparticles modified with αketoglutaric acid, J. Colloid Interf. Sci., 330 (2009) 29–37.

[21] S. Golkhah, H. Zavvar Mousavi, H. Shirkhanloo, A. Khaligh, Removal of Pb(II) and Cu(II) Ions from Aqueous Solutions by Cadmium Sulfide Nanoparticles, Int. J. Nanosci. Nanotechnol., 13 (2017) 105-117.

[22] A. Sarı, M. Tuzen, D. Cıtak, M. Soylak, Adsorption characteristics of Cu (II) and Pb (II) onto expanded perlite fromaqueoussolution, J. Hazard. Mater., 148 (2007) 387-394.

[23] S. A. Arain, T. G. Kazi, H. I. Afridi, M. Shahzadi Arain, A. H. Panhwar, N. Khan, J. A. Baig, F. Shah, A new dispersive liquid–liquid microextraction using ionic liquid based microemulsion coupled with cloud point extraction for determination of copper in serum and water samples, Ecotoxicol. Environ. Safe., 126 (2016) 186–192.

[24] A.T. Bisgin, Surfactant-Assisted Emulsification and Surfactant-Based Dispersive Liquid-Liquid Microextraction Method for Determination of Cu(II) in Food and Water Samples by Flame Atomic Absorption Spectrometry, J. AOAC Inter., 102 (2019) 1516-1522.

Anal. Method Environ. Chem. J. 3 (1) (2020) 63-71

Research Article, Issue 1
Analytical Methods in Environmental Chemistry Journal
Journal home page: www.amecj.com/ir

AMECJ

Cloud point-dispersive liquid-liquid microextraction for preconcentration and separation of mercury in wastewater samples by methylsulfanyl thiophenol material

Azwan Morni[a] and Seyed Mojtaba Mostafavi[b,*]

[a] *Department of Chemometrics, International Institute of Theoretical and Computational Chemistry, India*
[b,*] *Department of Chemistry, Iranian-Australian Community of Science, Hobart, Tasmania, Australia*

ARTICLE INFO:
Received 14 Dec 2019
Revised 12 Feb 2020
Accepted 4 Mar 2020
Available online 30 Mar 2020

Keywords:
Mercury,
Wastewaters,
Methylsulfanyl thiophenol,
Ionic liquid,
Cloud point dispersive liquid-liquid microextraction

ABSTRACT
A efficient method based on 4-methylsulfanyl thiophenol (MSTP, $C_7H_8S_2$) and ionic liquid ([BMIM][PF_6]) was used for mercury (Hg) separation and preconcentration from wastewater of petrochemical industries. The 0.01 mile molar of MSTP, 80 mg of [BMIM][PF_6] was diluted with 0.2 mL of ethanol (Et 98%). The mixture was injected to 10 mL of wastewater samples, shacked by ultrasonic bath for 5.0 min and cloudy solution was achieved by ionic liquid micelles at pH=7.0. The mercury ions was complexed with MSTP and extracted on micelles (IL/Et) by cloud point dispersive liquid-liquid microextraction (CP-DLLME) at 50°C before determined by cold vapor atomic absorption spectrometry (CV-AAS). The favorite extraction for mercury with low LOD (15 ng L^{-1}) and good linear rages (0.05- 6.2 µg L^{-1}) was achieved (RSD<5%). The main parameters such as, pH, sample volumes, amount of MSTP, amount of IL and ultra-sonic time were optimized. The method validated by spiking samples and certified reference material (CRM, NIST) in water sample.

1. Introduction

Mercury compounds (Hg, R-Hg) as toxic pollutants enter to environment from wastewater factories and cause different disease in humans. There are three forms of Hg (Hg^0, Hg (II), R-Hg) which was used in different industries [1]. The high exposure of inorganic mercury damaged the human organs such as renal, liver and CNS [2]. Although the exposure to organic mercury or fish food can be created an main problem in blood brain barrier (BBB) and cortex of brain but is weaker than inorganic compounds [3]. The hazardous defect in humans organs such as, CNS, respiratory, cells, renal and liver caused to different diseases, hypertension, chromosomal aberrations, tremor and MS [4]. So, as high toxicity, mercury determination in wastewaters is very important as industries samples. The mercury concentration in water is less than 6 µg L^{-1} [5] and in blood is less than 1-2 µg dL^{-1} [6]. So, the reliable, accurate and fast analytical methods must be used for wastewater samples. Among different analytical methods cold vapor atomic absorption spectrometry (CV-AFS) has been widely used for mercury determination in water samples due to simple, lower LOD and good sensitivity [7]. But,

*Corresponding Author: Seyed Mojtaba Mostafavi
E-mail: mojtabamostafavi@gmail.com
https://doi.org/10.24200/amecj.v3.i01.97

as low concentration of Hg and high interferences ions in wastewaters, the preconcentration and extraction processes must be done [8,9]. Recently, different extraction or microextraction mechanisms were used for this purpose. The micro-solid phase extraction (μ-SPE) [10]. CPE [11], LLME based on ionic liquids [12], The DLLME and LLME are a strategy promotes the complexation processes between metal and ligand [13]. CP-DLLME technique can be assisted by ultrasonic accessory [14]. Solidified floating organic drop DLLME (SFO-DLLME) was developed by Kocurov et al and many other techniques introduced by liquid extraction procedure [15-22]. The cloud point extraction (CPE) caused to two phases for solution by temperature. The surfactants such as T-X100 were used for metal separation by clouding phenomena (S-CPE). The S-CPE has many advantages as compared to traditional extraction. The two components, salt and surfactant solutions separate into immiscible phases [23]. The metal mineral can analysis by different methods such as electrochemistry, ionic liquids and nano sorbents [24]. In the presence of salt, ionic liquids and surfactants self assemble in liquid phase at special temperature change to micelles [25-28]. Many metals interacted to micelles and so preconcentrated into the surfactant-rich phase. The aim of this study is to develop a new analytical method for rapid preconcentration and determination of trace mercury in wastewater samples based on the combination of CP-DLLME technique coupled to CV-AAS. Ionic liquid of [BMIM][PF_6] dispersed in ethanol was used as trapping solvent for separation of MSTP from liquid phase. All factors which were affected on mercury extraction were studied and performance of the proposed method was validated.

Table 1. The CV-AAS conditions for mercury analysis

Features	Value
Linear range, μg L^{-1}	1-62
Wavelength, nm	253.7
Lamp current, mA	3.0
Slit, nm	0.5
Mode	Peak Area
HCl carrier solution 37%, mol L^{-1}	3.0
$NaBH_4$ reducing agent, % (m/v)	0.5(in 0.5% w/v NaOH)
Argon flow rate, mL min^{-1}	10-15
Sample flow rate, mL min^{-1}	3-5
Reagent flow rate, mL min^{-1}	4-6

2. Experimental

2.1. Apparatus and Reagents

Mercury was determined by atomic absorption spectrometer with a cold vapor accessory (GBC 932, CV-AAS, AUS), deuterium-lamp (UV), Hg HCL, and a unit of circulating cooling. The conditions of CV-AAS were shown in Table 1. The pH values of the solutions were measured by a digital pH meter Metrohm (744, Swiss). A Hettich centrifuge (Germany) and an ultra sonic accessory (Tecno-GAZ, Germany) were used. All reagents with high purity and analytical grade were purchased from Merck (Germany). All standard solutions were prepared with deionized water (DW) from Millipore (USA). The Hg (II) standard stock solution (1000 ppm in 1% HNO_3) was prepared from Sigma Aldrich, Switzerland. The experimental standard mercury were prepared daily by diluting of DW. The standards from 0.05- 6.2 ppb were freshly prepared and stored in a fridge (4 °C). A 0.5% (w/v) sodium borohydride ($NaBH_4$) was prepared daily by dissolving an appropriate amount of $NaBH_4$ in 0.5% (w/v) of NaOH and used for hydration of mercury (HgH_2). 1-Benzyl-3-methylimidazolium hexafluorophosphate ≥97.0% ([BMIM][PF_6]; CASN: 39447), 1-Butyl-2,3-dimethylimidazolium hexafluorophosphate (CASN: 70869), 1,3-Diethoxyimidazolium hexafluorophosphate ≥ 97% (CASN: 688649), 1,3-Dimethoxyimidazolium hexafluorophosphate 98% (CASN: 690821) were purchased from Sigma–Aldrich ,Germany. The 4-methylsulfanyl thiophenol (CAS N: 1122-97-0, 96%, MSTP, $C_7H_8S_2$) was purchased from Sigma Aldrich, Germany. The pH adjusted to 6.5 by using sodium phosphate (Na_2HPO_4/NaH_2PO_4,) as pH of 5.8-8.2. All the laboratory glasses were cleaned and washed by nitric acid and DW.

2.2. Sampling

Samples of wastewater (paint factory, Tehran, Iran), wastewater (industrial factories, Jajrood, Iran), oil company wastewater (Tehran, Iran) and chemical factory wastewater (Tehran, Iran) collected and filtered (0.45 µm) with polyethylene tubes and cellulose membrane (CMF), respectively before we used. The pH was tuned up to 7.0 with phosphate buffer solution. Then, the cloud point dispersive liquid-liquid microextraction (CP-DLLME) procedure was used for mercury extraction and determination in wastewater samples. The standard reference materials NIST NIST-SRM 1641e (total mercury in water) from the National Institute of Standard and Technology (NIST, Gaithersburg, USA) were also analyzed in a similar manner according to the general procedure.

2.3. CPE procedure

A simple procedure based on MSTP was used for separation of mercury ions from wastewater samples by cloud point dispersive liquid-liquid microextraction (CP-DLLME) at 50°C. The 10 $\times 10^{-6}$ mol L^{-1} of MSTP solution, 80 mg of [BMIM][PF_6] and 0.2 mL of ethanol was injected to 10 mL of wastewater samples. The samples were shacked by ultrasonic bath for 10 min and cloudy solution was achieved by ionic liquid/ethanol micelles at pH=7.0. The pH of sample adjusted with 1 mL of buffer solution up to 7.0 which was added to 10 mL of wastewater samples. Based on ionic liquid/ethanol micelles, the cloud point extraction (CPE) for Hg(II) ions was obtained by adding, 0.08 g (120 µL) of [BMIM][PF_6] and 0.2 mL of ethanol as a dispersive solvent in wastewater samples. For optimizing and recovery, 10 mL of 0.02, 0.1, 0.5. 1.0, 3.0 and 6.0 µg L^{-1} Hg(II) as working standard solution was prepared and used by CP-DLLME procedure. The cloudy solution was shaken for 5.0 min by ultrasonic shaking at 50 °C. In order to separate the phases, the turbid solution was centrifuged for 5.0 min at 4500 rpm and the liquid phase was removed with an auto-sampler of 10 mL. Hg(II) ions back-extracted from [BMIM][PF_6] with 0.5 mL of nitric acid (1.5 M) and after dilution with DW up to 1 mL determined by CV-AAS (Fig.1). The blank solutions proceeded the same way and are used for the preparation of the calibration solutions and for measurement of the blanks. The extraction mercury based on MSTP-CP-DILLME method was shown in Table 2.

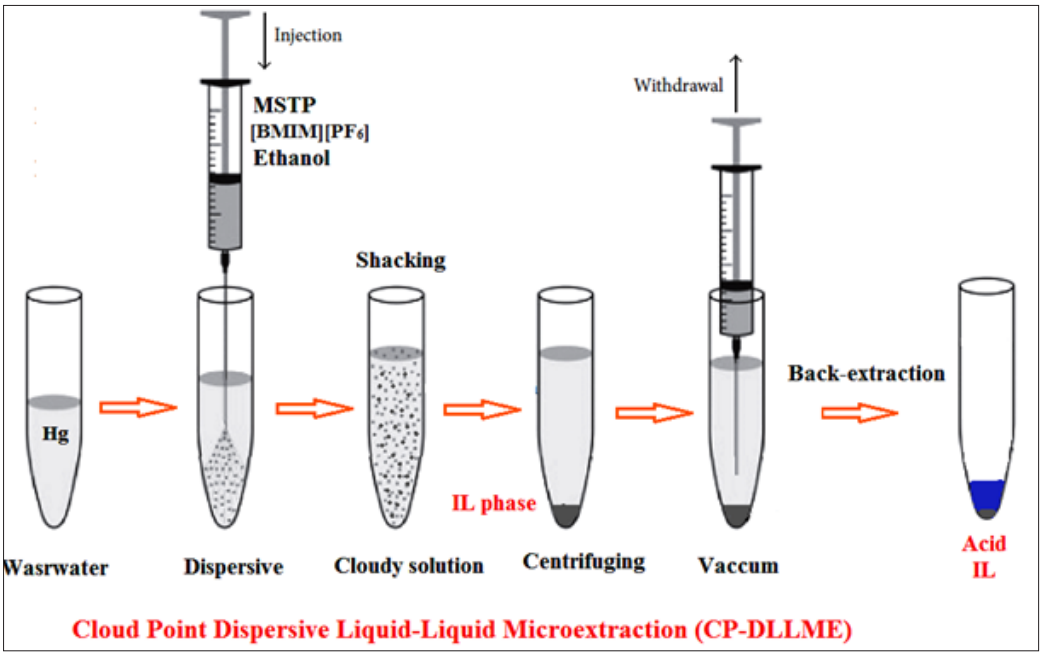

Fig. 1. The mercury extraction based on MSTP by cloud point dispersive liquid-liquid microextraction (CP-DLLME)

Table 2 The characteristics of the developed MSTP-CP-DILLME method for mercury extraction in wastewater samples (10 mL, pH=6.5, 0.02-6.2 µg L^{-1})

Parameter (Inter-day)	Wastewater sample	Standard sample
PF[a]	9.8	10.2
LOD[b] (n=10, ng L^{-1})	15.8	15.2
LOQ (n=10, μg L^{-1})	0.053	0.048
RSD[c] (n=6, %)	2.4	2.2
Linear range (μg L^{-1})	0.05– 6.3	0.05-6.1
Working Range (μg L^{-1})	0.05-14.5	0.05-14.2
Correlation coefficient	0.9993	0.9997

[a] Preconcentration factor, [b] Limit of detection , [c] Relative standard deviation.

3. Results and discussion

3.1. Optimization of pH

The effect of pH on complexation of mercury ions based on MSTP was investigated in different pH from 2 to 10 for 0.05 µg L^{-1} , 0.5 µg L^{-1} , 6.2 µg L^{-1} Hg(II) as a LLOQ, MLOQ and ULOQ ranges. The complexation was strongly depended on the pH sample and subsequently caused to increase the extraction efficiency of mercury in wastewater samples. Based on results, the maximum extraction efficiency for mercury was obtained at pH=7.0 and the recovery were below 5% in acidic or basic pH. Therefore, the pH=6-8 was selected as optimum pH for mercury extraction from wastewater samples by the developed MSTP-CP-DILLME method with high recovery (Fig. 2). In pH=6-10, the sulfur (-) has negative charge but mercury based on positive charge (+) can be complexed with sulfur in pH more of 6 and less than 8. The results showed the maximum extraction was achieved at pH=7 for mercury by coordinating covalent bond of sulfur (Hg^{2+}---: S^{2-}).

3.2. Optimization of ionic liquid

By procedure, the wastewater samples were shaked by ultrasonic bath for 10 min and cloudy solution was achieved by ionic liquid/ethanol micelles at pH=7.0. So the kind and amount of ionic liquid has critical role as generation micelles in liquid phase and extraction process by MSTP-CP-DILLME method. For this purpose, different ILs such as, 1-Benzyl-3-methylimidazolium hexafluorophosphate, 1-Butyl-2,3-dimethylimidazolium hexafluorophosphate, 1,3-Diethoxyimidazolium hexafluorophosphate, 1,3-Dimethoxyimidazolium hexafluorophosphate were selected and used for mercury extraction in optimized conditions. Based on results, the extraction efficiency was remarkably affected by amount ionic liquid amount, so it was examined within the range of 20-200 mg. Quantitative extraction was achieved more than 60 mg of

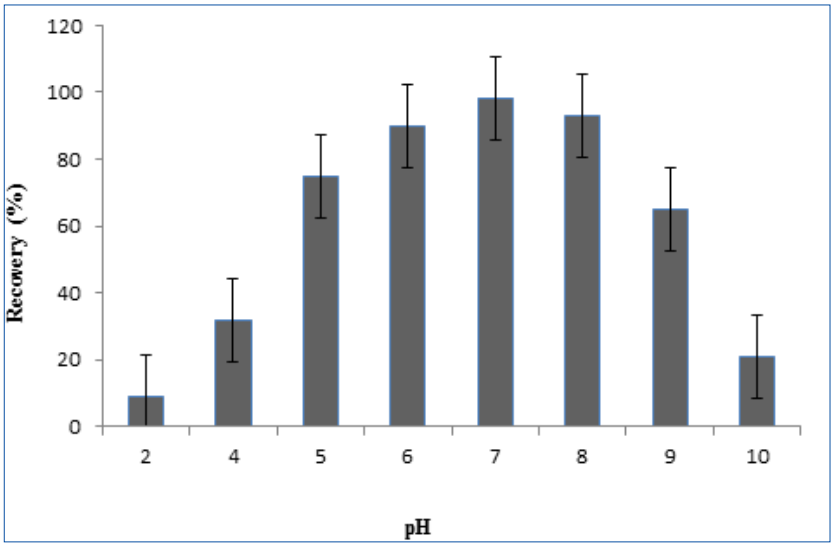

Fig. 2. The effect of pH on mercury extraction in wastewater samples by MSTP-CP-DILLME method

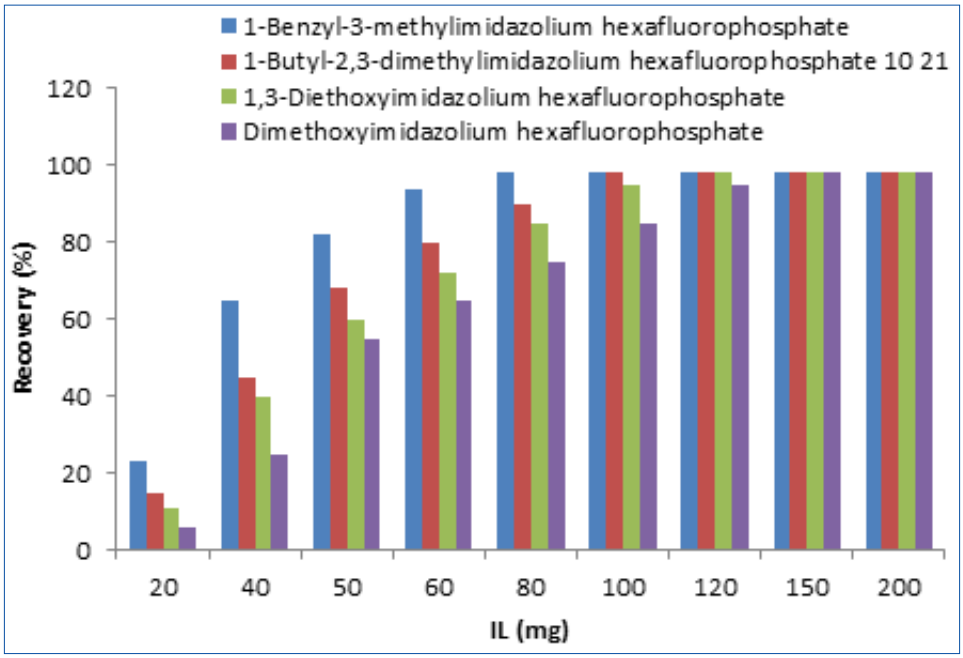

Fig. 3. The effect of different ionic liquids on mercury extraction by MSTP-CP-DILLME method

[BMIM][PF_6]. Therefore, 80 mg (120 µL) of [BMIM][PF_6] was chosen as optimum leading to a final IL (Fig. 3).

3.3. Optimization of amount of MSTP

The amount of methylsulfanyl thiophenol (MSTP, $C_7H_8S_2$) was evaluated by CP-DLLME. By procedure, The concentration of MSTP between 1.0×10^{-6} - 50.0×10^{-6} mol L^{-1} was prepared and optimized for maximum extraction mercury in wastewater samples in pH=7.0. The results showed the recovery has high extraction more than 5.7×10^{-6} and then no effected on mercury extraction by increasing MSTP. In fact, the 5.7×10^{-6} mol L^{-1} of MSTP was the minimum concentration which was necessary for high recovery for mercury extraction from wastewater samples. So, the 10×10^{-6} mol L^{-1} of MSTP was selected as optimum concentration as interference ions in wastewater and more than the signal remained constant (Fig. 4).

3.4. Optimization of acids

The ionic liquids cannot directly use by CV-AAS, because of high viscosity and low interaction with redacting reagents such as NaBH4. By MSTP-CP-DILLME procedure, the Hg-MSTP loaded on

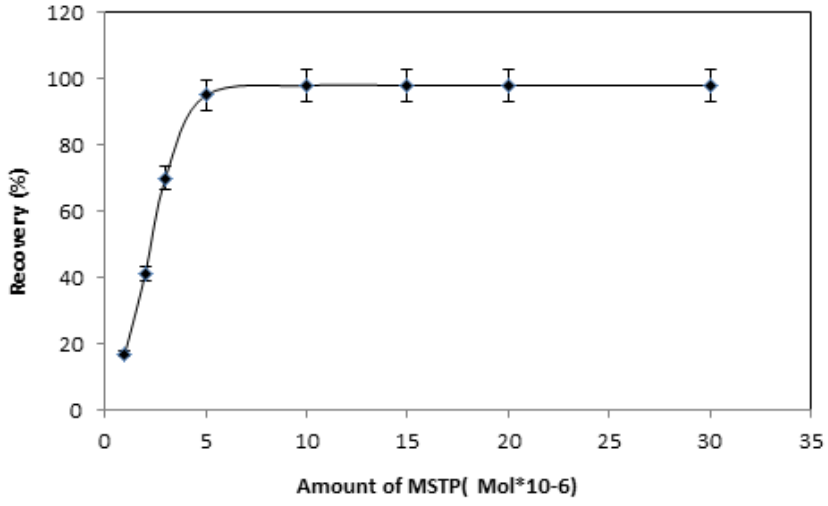

Fig. 4. The effect of MSTP ligand on mercury extraction in wastewater samples by MSTP-CP-DILLME method

[BMIM][PF6] was back-extraction by the mineral acidic/basic solution. By changing of pH, the covalence bond between sulfur and mercury leads to dissociation and mercury ions release to liquid phase of acid. Different concentration of mineral reagents from 0.1-3 mol L^{-1} (HCl, HNO3, CH3-COOH, NaOH) were used for back-extraction mercury from IL. The results showed that 1.5 mol L^{-1} of HNO_3 can back-extracted of Hg(II) from the IL phase. Then, different of volume of reagents between 0.1-1.0 mL was studied and optimized. The results showed, 0.5 mL, 1.5 M of HNO_3 had maximum back-extraction mercury in wastewater samples (Fig. 5).

3.5. Optimization of sample volume

The different sample volume for extraction mercury was studied. The effect of sample volume was evaluated between 5.0 to 35 mL of wastewater/ standard samples for 0.0.5 µg L^{-1} and 6.0 µg L^{-1} of Hg(II). Quantitative extraction was achieved less than 15 mL. In addition, the higher sample volumes caused to trace soluble the ionic liquid in liquid phase and lead to non-accurate results. So, a sample volume of 10 mL was selected for further work by CP-DLLME procedure **(**Fig. 6**).**

3.6. Interferences Ions

For analytical application of the CP-DLLME procedure, the effect of interference of coexisting

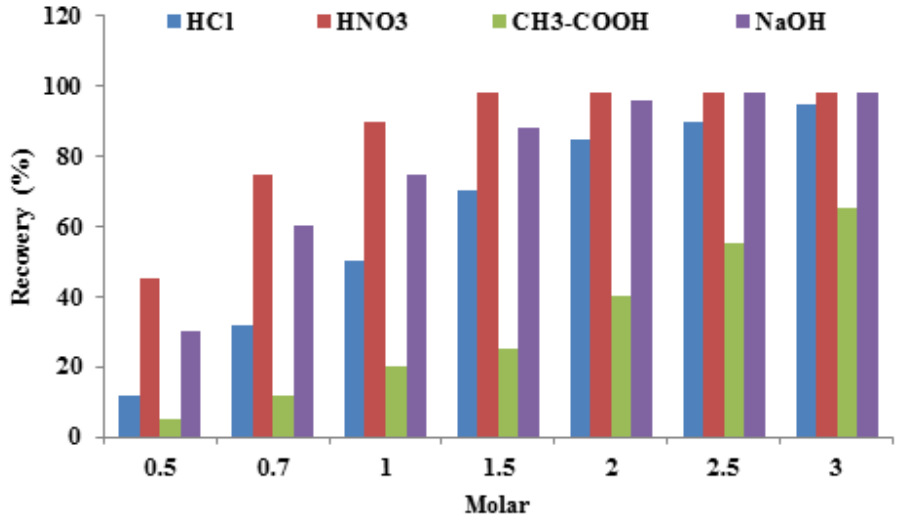

Fig. 5. The effect of different reagents for back-extraction of mercury from MSTP by CP-DILLME method

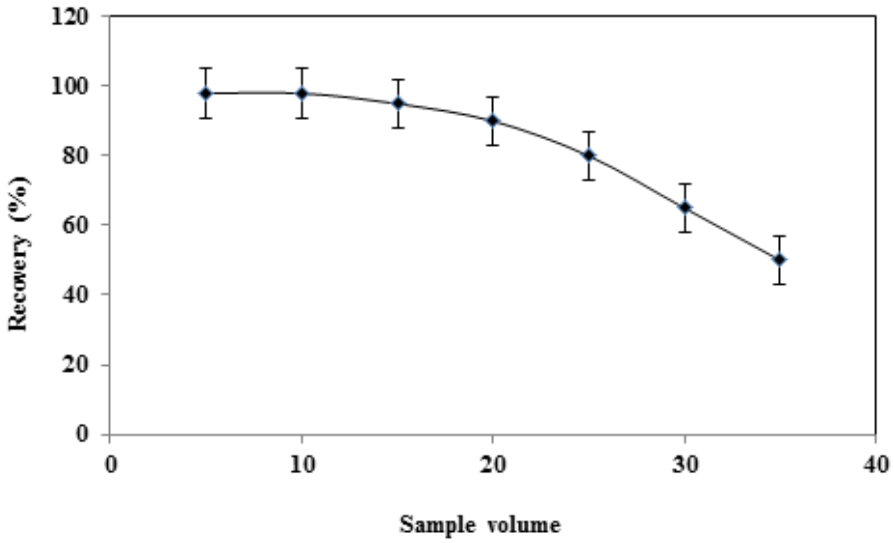

Fig. 6. The effect of sample volume on mercury extraction by MSTP-CP-DILLME method

Table 3. Effect of interfering ions on the recovery of Hg (II) ions by CP-DLLME procedure

Interfering ions C_M	Concentration ratio (C_M/C_{Hg}^{2+})	Recovery (%)
Co^{2+}, Ni^{2+}, Pb^{2+}, Mn^{2+}, Cd^{2+}	750	98.3
PO_4^{3-}, CO_3^{2}, NO_3^{-},	1000	97.7
Na^{+}, K^{+}, Ca^{2+}, Mg^{2+}	900	98.4
Ag^{+}, Au^{3+}	40	96.5
Cu^{2+}, Zn^{2+}	300	97.2
Cr^{3+}, As^{3+}, Fe^{3+}, Al^{3+}	500	99.3
F-, Cl-, Br-, I-	1100	98.8

ions for mercury extraction in wastewater samples was studied. The various amounts of the interfering ions were added to 10 mL of wastewater sample containing 6.2 µg L^{-1} of Hg (II). As Table 3, the most of the probable concomitant ions have no considerable effect on the recovery efficiencies of Hg (II) ions under optimized conditions.

3.7. Real sample analysis

The developed CP-DLLME procedure was used for mercury determination in wastewater samples. The results showed the three separate determinations mercury in water samples. The results was verified by spiking of samples with standard concentration of Hg mercury. Table 4 showed, high recovery (more than 95%) between the added and found of mercury amount by procedure which confirms the accuracy of the procedure. The recoveries of spiked samples for mercury were ranged from 96% to 105%, which demonstrated satisfactory of mercury results. In order to validate the method described, the certified standard reference materials, NIST-SRM 1641e (total mercury in water), was analyzed and the results were given in Table 5. The results of the SRM were satisfactorily in agreement with the certified values.

4. Conclusions

A simple, fast and sensitive method based on MSTP was used for preconcentration and speciation of mercury in wastewater samples by CP-DILLME procedure. After extraction , the mercury concentration was determined by CV-AAS. The [BMIM][PF6] as ionic liquid was used as trapping agent of MSTP-Hg for rapid separation in short time. Utilizing ionic liquid micelles and MSTP together introduced a CPE procedure based on environmentally friendly for mercury extraction

Table 4. Validation of methodology based on MSTP for mercury analysis by CP-DILLME

Sample	Added (µgL^{-1})	*Found (µgL^{-1})	Recovery(%)
[a]Wastewater Factory	--------	0.86 ± 0.04	--------
	0.8	1.64 ± 0.62	97.5
Wastewater oil	--------	1.01 ± 0.05	--------
	1.0	1.98 ± 0.09	97.0
[a]Wastewater paint	--------	1.76 ± 0.09	--------
	1.5	3. 28 ± 0.16	101.3
[a]Wastewater Chemical	--------	1.12 ± 0.06	--------
	1.0	2.10 ± 0.11	98.0
Well water	--------	0.15 ± 0.01	--------
	0.2	0.36 ± 0.01	105.0

* Mean of three determinations ± confidence interval (P = 0.95, n =5).

[a] Dilution (1:10)

Table 5. Validation of developed CP-DILLME method by standard reference material

Sample	Certified (µg L^{-1})	Added(µg L^{-1})	Found [a] (µg L^{-1})	Recovery (%)
CRM	1.016 ± 0.017	--------	0.986 ± 0.057	--------
		0.5	1.475 ± 0.057	97.8
		1.0	1.971 ± 0.069	98.5

[a] Mean of three determinations ± confidence interval (P = 0.95, n =5).
[b] NIST, SRM 1641e, total mercury in water (p=0.95).

from wastewaters. This procedure provides low LOD values as well as good RSD with quantitative recoveries more than 95% in optimized conditions. The CP-DILLME procedure based on MSTP and [BMIM][PF6] can be considered as effective sample preparation for mercury extraction from wastewater samples.

5. References

[1] M. Tariq, Toxicity of mercury in human: a review, J. Clin. Toxicol., 9 (2019) 9-5.

[2] V.A. Dixit, A simple model to solve a complex drug toxicity problem, Toxicol. Res., 8 (2018) 157-171.

[3] R.A. Bernhoft, Mercury toxicity and treatment: a review of the literature, J. Environ. Public Health, 2012 (2012) 460508.

[4] A.M. Attar, A. Kharkhaneh, M. Etemadifar, K. Keyhanian, V. Davoudi, M. Saadatnia, Serum mercury level and multiple sclerosis, Biol. Trace Elem. Res., 146 (2012) 150-153.

[5] A. M. Al-Ghouti, D. Da'ana, M. Abu-Dieyeh, M. Khraisheh, Adsorptive removal of mercury from water by adsorbents derived from date pits. Sci. Reports, 9 (2019) 15327.

[6] S.E. Schober, T.H. Sinks, R.L. Jones, P.M. Bolger, M. McDowell, J. Osterloh, E.S. Garrett, R.A. Canady, C.F. Dillon, Y. Sun, Blood mercury levels in US children and women of childbearing age, JAMA, 289 (2003) 1667-1674.

[7] S. Santana Lins, C. Francisco Virgens, W. Nei Lopes dos Santos, I. Helena Santos Estev, On-line solid phase extraction system using an ion imprinted polymer based on dithizone chelating for selective preconcentration and determination of mercury in natural waters by CV AFS, Microchem. J., 150 (2019) 104075.

[8] Y. Hui, Y. Liu, W C. Tang, Determination of mercury(II) on a centrifugal microfluidic device using ionic liquid dispersive liquid−liquid microextraction, Micromachin., 10 (2019) 523.

[9] Y.M. Liu, F.P. Zhang, B.Y. Jiao, J.Y. Rao, G. Leng, Automated dispersive liquid-liquid microextraction coupled to high performance liquid chromatography-cold vapor atomic fluorescence spectroscopy for the determination of mercury species in natural water samples, J. Chromatogr., A 1493(2017) 1–9.

[10] M. Mei, X. Huang, X. Yang, Q. Luo, Effective extraction of triazines from environmental water samples using magnetismenhanced monolith-based in-tube solid phase microextraction, Anal. Chim. Acta, 937(2016) 69–79.

[11] I. López-García, Y. Vicente-Martínez, M. Hernández-Córdoba,Non-chromatographic speciation of chromium at sub-ppb levels using cloud point extraction in the presence of unmodified silver nanoparticles, Talanta, 132 (2015) 23-28.

[12] M. Sajid, Dispersive liquid-liquid microextraction coupled with derivatization: A review of different modes, applications, and green aspects. TrAC Trends Anal. Chem., 106 (2018) 169–182.

[13] M. Tuzen, O. Z. Pekiner, Ultrasound-assisted ionic liquid dispersive liquid-liquid microextraction combined with graphite furnace atomic absorption spectrometric for selenium speciation in foods and beverages, Food Chem., 188 (2015) 619–624.

[14] H. Shirkhanloo, M. Ghazaghi, M. M. Eskandari, Cloud point assisted dispersive ionic liquid -liquid microextraction for chromium speciation in human blood samples based on isopropyl 2-[(isopropoxycarbothiolyl)disulfanyl] ethane thioate, Anal. Chem. Res., 10 (2016) 18-27.

[15] L. Kocurov, I. S. Balogh, J. Sandrejov, V. Andruch, Recent advances in dispersive liquid-liquid microextraction using organic solvents lighter than water, A review, Microchem. J., 102 (2012) 11–17.

[16] S.P.M. Ventura, F.A. E Silva, M.V. Quental, D. Mondal, M.G. Freire, J.A.P. Coutinho, Ionic-liquid-mediated extraction and separation processes for

bioactive compounds: past, present, and future trends, Chem. Rev., 117 (2017) 6984–7052.

[17] S. M. Mostafavi, M. Adibi, F. Pashaee, M. Piryaei, Modification of glassy carbon electrode by a simple, inexpensive and fast method using an ionic liquid based on immidazolium as working electrode in electrochemical determination of some biological compounds, Asian J. Chem., 23 (2011) 5247-5252.

[18] S. M. Mostafavi, M. Adibi, F. Pashaee, M. Piryaei, Electrochemical Investigation of Thiophene on Glassy Carbon Electrode and Quantitative Determination of it in Simulated Oil Solution by Differential Pulse Voltammetry and Amperometry Techniques. Asian J. Chem., 23 (2011) 5356-5360.

[19] H. Zheng, J. Hong, X. Luo, S. Li, M. Wang, Combination of sequential cloud point extraction and hydride generation atomic fluorescence spectrometry for preconcentration and determination of inorganic and methyl mercury in water samples, Microchem. J. 145 (2019) 806-812.

[20] S.L.C. Ferreira,V.A. Lemos, L.O.B. Silva, A.F.S. Queiroz, A.S. Souza, E.G.P. da Silva, W.N.L. dos Santos, C.F. das Virgens, Analytical strategies of sample preparation for the determination of mercury in food matrices,A review, Microchem. J., 121 (2015) 227–236.

[21] A. Badamchi Shabestari, M. Shekarchi, S. M. Mostafavi, Development of environmental analysis for determination of total mercury in fish oil pearls by microwave closed vessels digestion coupled with ICP-OES, Ekoloji, 27 (2018) 1935-1943.

[22] S.M. Mostafavi, Mercury determination in work place air and human biological samples based on dispersive liquid-liquid micro-extraction coupled with cold vapor atomic absorption spectrometry, Anal. Method. Environ. Chem. J., 2 (2019) 49-58.

[23] K. Seebunrueng, Y. Santaladchaiyakit, S. Srijaranai, Vortex-assisted low density solvent liquid-liquid microextraction and salt-induced demulsification coupled to high performance liquid chromatography for the determination of five organophosphorus pesticide residues in fruits, Talanta, 132 (2015) 769–774.

[24] S. M. Mostafavi, A. A. Miranbeigi, Handbook of mineral analysis. Mani publication, Ltd, 2012.

[25] G. D'Orazio, M. Asensio-Ramos, J. Hernandez-Borges, M. A. Rodrıguez-Delgado, S. Fanali, Evaluation of the combination of a dispersive liquid-liquid microextraction method with micellar electrokinetic chromatography coupled to mass spectrometry for the determination of estrogenic compounds in milk and yogurt, Electrophoresis, 36 (2015) 615–625.

[26] K.D. Danov, P.A. Kralchevsky, K.P. Ananthapadmanabhan, Micelle-monomer equilibria in solutions of ionic surfactants and in ionic-nonionic mixtures: A generalized phase separation model, Adv. Colloid Interfac. Sci., 206 (2014) 17-45.

[27] T.P. Nguyen, P. Hesemann, T.M.L. Tran, J.J.E. Moreau, Nanostructured polysilsesquioxanes bearing amine and ammonium groups by micelle templating using anionic surfactants, J. Mater. Chem. 20 (2010) 3910-3917.

[28] JYuan, A. Li, T. Chen, J. Du, J. Pan, Micelle dominated distribution strategy for non-matrix matched calibration without an internal standard, Anal. Chim. Acta, 1102 (2019) 24-35.